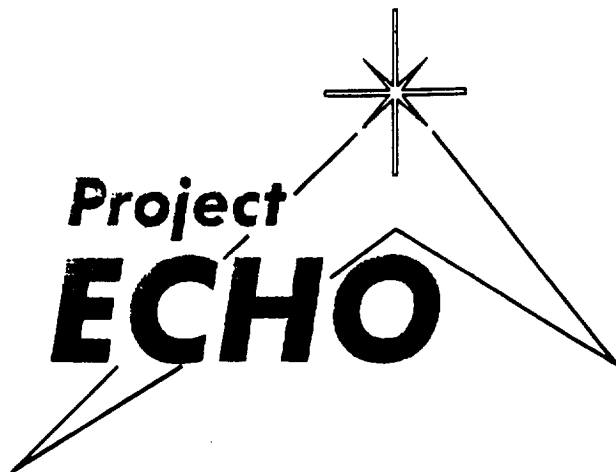


*IN 32-CA  
20162  
p. 157*



# Electronic Communications from Halo Orbit

Aerospace Engineering 401A & 401B  
The Pennsylvania State University

1993-94

Sponsored by:

NASA/Universities Space Research Association  
Advance Design Program

N95-12644

Unclas

G3/32 0026162

(NASA-CR-197190) PROJECT ECHO:  
ELECTRONIC COMMUNICATIONS FROM HALO  
ORBIT (Pennsylvania State Univ.)  
157 p

# List of Contributors

## Systems Integration

Jason Borrelli  
Bryan Cooley  
Marcy Debole  
Lance Hrivnak  
Kenneth Nielsen  
Gary Sangmeister  
Matthew Wolfe

## Command and Data Handling

Adam Lash  
Gary Sangmeister  
Shane Wilcox  
Michael Witt

## Communications

David Davis  
Christopher Frye  
Elana Hammond  
Kenneth Nielsen  
Geoffrey Uy

## Guidance, Navigation, and Control

Sheri Coates  
Bryan Cooley  
Jamie Copeland  
William Scheetz  
Andy Staugler

## Power

John Freeman  
Lance Hrivnak  
Jonathan Rader  
Patrick Tamburri  
Grant Waltz

## Propulsion

Jason Borrelli  
John Nagy  
Brent Paul  
Richard Saylor  
Alfred Sullivan

## Structures/Launch Vehicle

Matthew Hykes  
Justin Knavel  
Brian Shaw  
Frank Shelby  
Matthew Wolfe

## Thermal Control

Marcy Debole  
Gary Mego  
Tracie Tepke  
John Vantuno

## Instructors

Dr. Robert G. Melton  
Dr. Roger C. Thompson

## Teaching Assistant

Thomas F. Starchville Jr.

## NASA Mentor

Kurt Hack, NASA Lewis

# Project ECHO: Electronic Communications from Halo Orbit

## EXECUTIVE SUMMARY

The Pennsylvania State University  
Department of Aerospace Engineering  
University Park, Pennsylvania

Dr. Robert G. Melton and Dr. Roger C. Thompson  
Thomas F. Starchville Jr., Teaching Assistant

Jason Borrelli, Bryan Cooley, Marcy Debole, Lance Hrivnak,  
Ken Nielsen, Gary Sangmeister, Matt Wolfe

---

### Abstract

The design of a communications relay to provide constant access between the Earth and the far side of the Moon is presented. Placement of the relay in a halo orbit about the  $L_2$  Earth-Moon Lagrange point allows the satellite to maintain constant simultaneous communication between Earth and scientific payloads on the far side of the Moon. The requirements of NASA's Discovery-class missions adopted and modified for this design are: total project cost should not exceed \$150 million excluding launch costs, launch must be provided by Delta-class vehicle, and the satellite should maintain an operational lifetime of 10 to 15 years.

The spacecraft will follow a transfer trajectory to the  $L_2$  point, after launch by a Delta II 7925 vehicle in 1999. Low-level thrust is used for injection into a stationkeeping-free halo orbit once the spacecraft reaches the  $L_2$  point. The shape of this halo orbit is highly elliptical with the maximum excursion from the  $L_2$  point being 35000 km.

A spun section and despun section connected through a bearing and power transfer assembly (BAPTA) compose the structure of the spacecraft. Communications equipment is placed on the despun section to provide for a stationary dual parabolic offset-feed array antenna system. The dual system is necessary to provide communications coverage during portions of maximum excursion on the halo orbit. Transmissions to the NASA Deep Space Network 34 m antenna include six channels (color video, two voice, scientific data from lunar payloads, satellite housekeeping and telemetry, and uplinked commands) using the S- and X-bands. Four radioisotope thermoelectric generators (RTG's) provide a total of 1360 W to power onboard systems and any two of the four Hughes 13 cm ion thrusters at once. Output of the ion thrusters is approximately 17.8 mN each with xenon as the propellant. Presence of torques generated by solar pressure on the antenna

dish require the addition of a "skirt" extending from the spun section of the satellite for balance. Total mass of the satellite is approximately 900 kg at a cost of \$130 million FY99.

### Mission Objective

The objective of Project ECHO (Electronic Communications from Halo Orbit) is to provide a continuous communications link between Earth and the far side of the Moon. The spacecraft will provide real-time or delayed transfer of information, telemetry, and voice/video data.

### Background

This satellite will provide the link necessary to communicate with the Moon's far side. The project will allow for the exploration and utilization of the far side of the Moon by establishing a communications link to scientific outposts, mining operations, lunar rovers, or exploration probes. The spacecraft will be in halo orbit about the Earth-Moon Lagrange point  $L_2$  (located on the Earth-Moon line approximately 64,500 km beyond the Moon's center) and will maintain an uninterrupted line-of-sight with both the Earth and the Moon. Development of Project ECHO is restricted by modified NASA Discovery-class mission parameters: 1) total cost must not exceed \$150 million (excluding launch vehicle), 2) launch must be achieved by a Delta-class vehicle, and 3) the design lifetime must be greater than 10 years.

### Mission Scenario

Launch will occur at Cape Canaveral, Florida in 1999 via a Delta II 7925. This vehicle contains three stages with a payload assist module (PAM) comprising the third stage. After final separation, the satellite is placed on a transfer trajectory to the  $L_2$  point and the entire spacecraft will have a spin rate of

45 rpm. Deployment of the RTG's will take place 60 minutes after launch and will reduce the spacecraft's spin rate to 9.4 rpm. Despinning of the despun section will then take place and raise the spun section's rate to 9.7 rpm. Stabilization of the satellite once in the halo orbit is obtained by using thrusters to increase the spun section's spin rate to 35 rpm.

The parabolic antenna will also be deployed during the transfer trajectory, however, twin dipole antennas will provide communications while in

transit to avoid problems in pointing the parabolic dish. After arrival at the L<sub>2</sub> point, the spacecraft continues toward injection into a halo orbit using a low-thrust spiral. A non-optimal, zero-thrust transfer trajectory from Earth to L<sub>2</sub> was found. The spacecraft's ion thrusters are required for the patched trajectory from L<sub>2</sub> to Halo. This event sequence is illustrated in Figure 1.

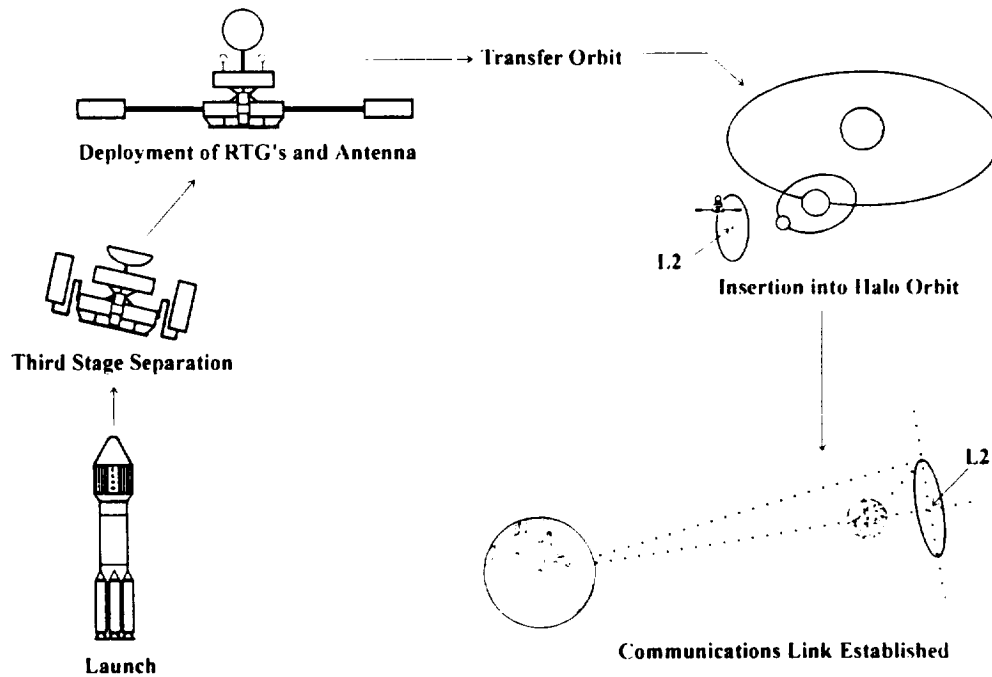


Figure 1 Project ECHO Mission Scenario.

### Structures and Launch Vehicle

The structure of the satellite will be composed of a despun and a spun section connected through a Bearing and Power Transfer Assembly (BAPTA). Figure 2 shows the overall configuration of Project ECHO. The spun section, shown in Figure 3, is a combination of a truss and semi-monocoque structure. The truss members will be made from Al 7075-T6, and will carry the axial and lateral loads. All axial loads induced during launch will be transferred through the Payload Attach Fitting (PAF) into the third stage of the launch vehicle. The skin,

made of Al 6061-T6, will help to carry torsional loads and act as a micrometeoroid shield for the sensitive components.

As required by the mission parameters, a Delta II 7925 launch vehicle will be used. The 2.9 m diameter fairing will be used since its mass is less than the 3.0 m diameter fairing and therefore allows for a greater spacecraft mass. For a maximum mass of 1200 kg, ECHO will utilize the 3712C PAF to interface the satellite to the launch vehicle, which contains the control systems for the third stage of the launch vehicle.

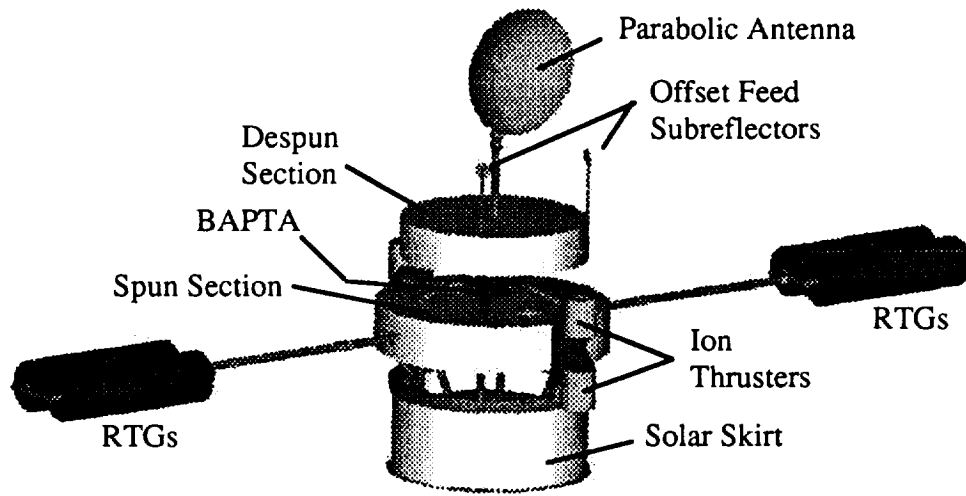


Figure 2 Isotropic view of the ECHO spacecraft.

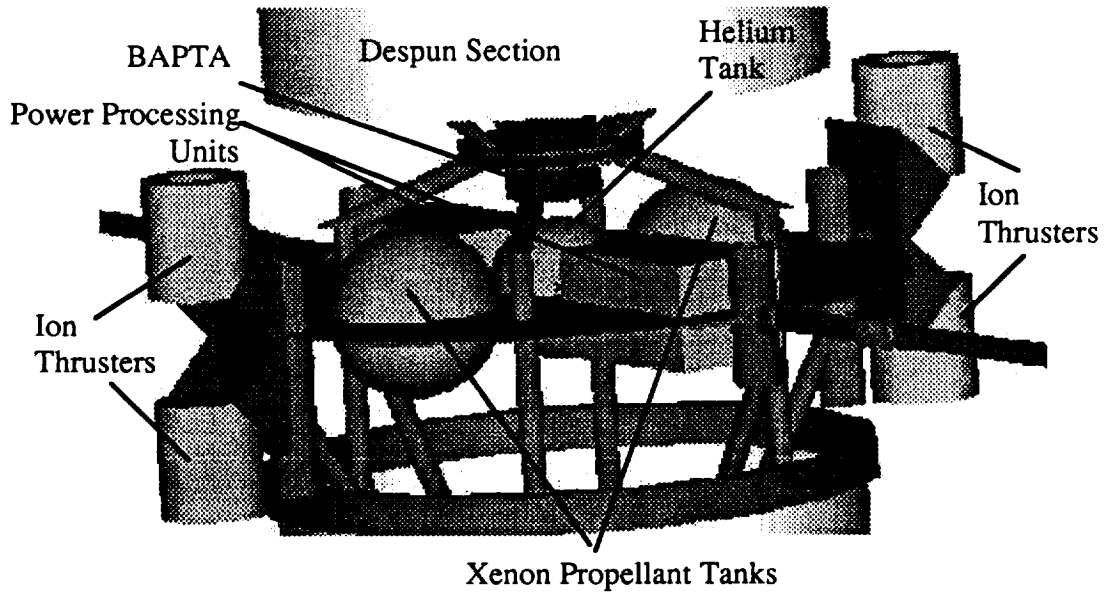


Figure 3 Cut-away view of the spun section.

## Power

The electrical power system (EPS) design was driven by the following requirements: the EPS must generate, distribute, and regulate all electrical power within the ECHO spacecraft and provide enough power for 2 ion thrusters in addition to the other components.

ECHO's electrical power system has several main components. First, a radioisotope thermoelectric generator (RTG) will be used to generate the 1280 Watts necessary to power the spacecraft during maximum steady-state power consumption. The General Electric MOD-RTG has been selected for this purpose. Power distribution will be via a standard 28 V-dc power bus located in the spacecraft's spun section, with electromechanical switches providing circuit isolation for unused components. A decentralized regulation scheme will be utilized on the bus, and power transmission from the RTG to the bus will be through a direct energy transfer system relying on shunt resistors to dissipate unused power. The specific power regulation will be accomplished with the Arnold Magnetics EL-2000 series of DC-DC power converters.

## Thermal

The requirement of the thermal subsystem is to maintain all of the components of the spacecraft within their operational temperature ranges: 0 °C to 40 °C for the despun section and 10 °C to 30 °C for the spun section. Because ECHO is powered by RTGs, a high thermal flux will impinge on the satellite. This heat, along with that radiated from the Sun, Earth, and internal components provide minimum and maximum temperature ranges experienced by the spacecraft in the halo orbit of -31 °C to 31 °C for the despun section and -44 °C to 25 °C for the spun section. The worst case cold temperatures are well below the lower limits allowed for the operation of the components.

Though a completely passive system had been the ultimate goal for this system, it will not be possible for ECHO. The components necessary to bring the temperatures into the required ranges will be silverized Teflon thermal coating on the top of the despun section and bottom of the spun section and heaters in both sections. The activation and deactivation of the heaters will be regulated by the command and data handling subsystem using readings from temperature sensors placed throughout the spacecraft.

In addition to the system that regulates the thermal environment of ECHO in the halo and transfer orbits, some additional control is necessary while the spacecraft is inside the fairing during launch. This system will consist of a shield including

steel plates and multilayer insulation (MLI) placed between the RTG's and the satellite in the stowed position in the Delta rocket. For the five minutes between loss of air conditioning and separation from the fairing, this shield will absorb and reflect approximately 14 kW of heat radiated by the RTG's.

## Propulsion

The propulsion system for Project ECHO must be capable of completing the translunar orbit, injecting the satellite into the halo orbit, and providing for routine stationkeeping and attitude control maneuvers. Based on a trade study of electric, or low-thrust, propulsion systems, the Hughes Research Lab 13 cm ion propulsion system (IPS) was chosen for Project ECHO. Each of the four thrusters is capable of delivering 17.8 mN of thrust at a peak input power of 439 W. Three power processor units (PPU's), each requiring 500 W of input power and operating at 88% efficiency, are used to transfer power to the thrusters. The two thruster pairs are mounted to a turntable capable of rotating 360°, and in addition, each thruster is connected to two PPU's simultaneously through a technique termed cross-strapping. This system configuration on the spun section allows for a single level of redundancy for the thrusters and PPU's. Xenon was selected as the propellant to be used in conjunction with the ion thrusters. Employing a stationkeeping-free orbit about the L<sub>2</sub> point will drastically reduce the amount of propellant needed. Therefore, 70 kg of propellant would be adequate for a 10 year mission. The xenon will be housed in two tanks constructed of Al 5456, each having a diameter of 0.358 m and a thickness of 4.39 mm. The xenon tanks will be maintained at a constant 7.6 MPa using a helium pressurization system. Three kilograms of helium, stored at 10 MPa, will be housed in another aluminum 5456 tank with a diameter of 0.295 m and thickness of 4.74 mm.

## Guidance Navigation & Control

The guidance, navigation, and control subsystem will be a fully autonomous system incorporating dual spin stabilization and low-level thrust. A computer code was written to integrate the restricted three-body equations in order to determine the transfer trajectory. The integration was performed backward in time starting at the L<sub>2</sub> point. Velocity of the spacecraft at the L<sub>2</sub> point was assumed to be zero. A non-optimal, zero-thrust transfer trajectory was found (see Figure 4). At the L<sub>2</sub> point, the spacecraft will perform another transfer trajectory to place it into a stationkeeping-free orbit (see Figure 5).

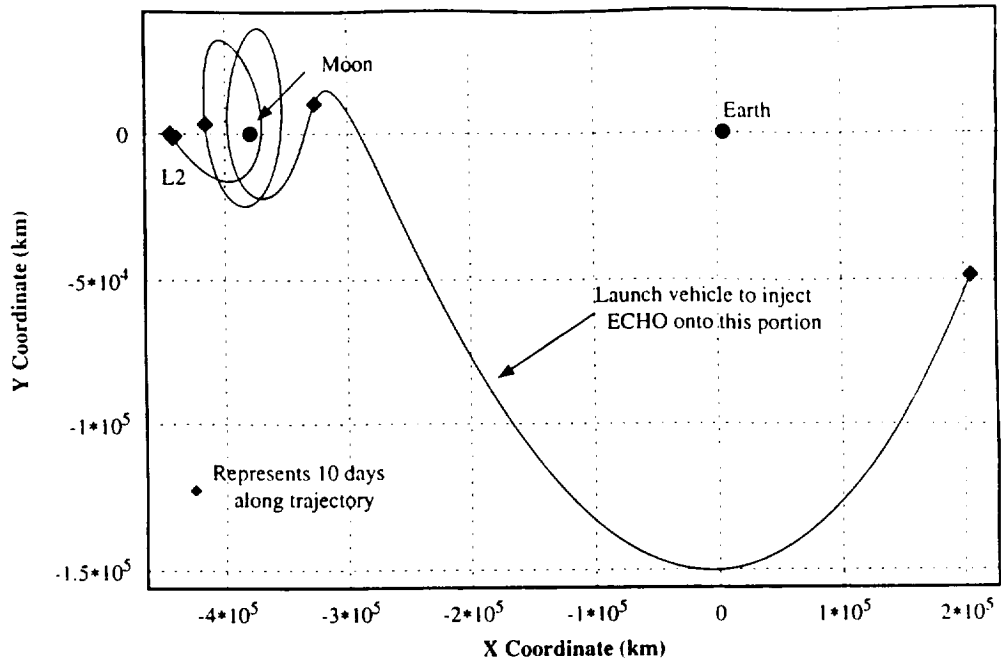


Figure 4 Transfer trajectory from Earth to L<sub>2</sub> point.

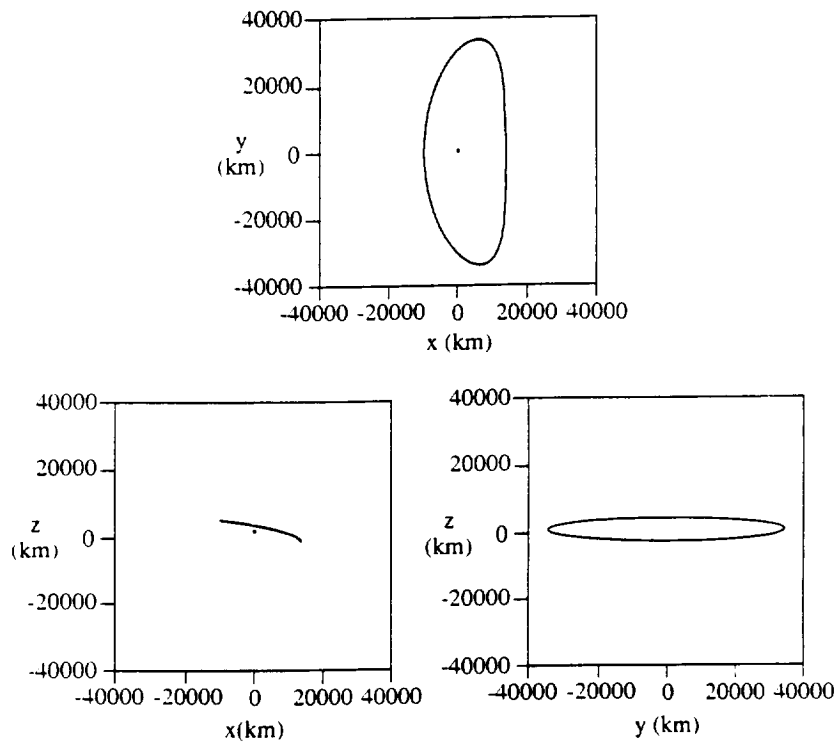


Figure 5 Station-keeping free halo orbit.

Upon separation from the third stage of the Delta, the satellite is rotating uniformly at 45 rpm. The RTGs are then deployed which slows the craft to 9.4 rpm. This slower spin rate allows the satellite to be easily maneuvered during the transfer orbit. Once the craft is inserted into the halo orbit, the thrusters are used to accelerate the spun section and the BAPTA to decelerate the despun section. The resulting spin rates are 0.5°/hr and 35 rpm for the despun and spun sections respectively. The spin rate for the despun section allows the antenna to remain pointed at the Earth and the Moon. The spin rate for the spun section along with a 1.0 m long skirt attached at the bottom stabilizes the craft against disturbance torques for approximately two years.

The Microcosm Autonomous Navigation System (MANS) will be used as the navigation system. It will have to be modified slightly for this specific orbit since it has not been tested outside of LEO/GEO. The MANS sensors are unique to this navigation system because they incorporate dual horizon scanners along with silicon light detectors in each sensor. Two sensors are sufficient to triangulate the spacecraft's position using the Moon, Sun and Earth.

### Command & Data Handling

The command and data handling subsystem of the communications satellite must be able to successfully process and relay data to and from the Moon and Earth. The C&DH subsystem is also used to distribute commands and accumulate, store, and format data from the spacecraft and payload. In its general form, the C&DH subsystem includes a central processor, data buses, remote interface units, and data storage units. For Project ECHO, the factors that determine the complexity and capability of the C&DH subsystem include communications, data storage, and guidance and navigation requirements.

The subsystem consists of two on-board central processors, one payload processor, two hardware controllers, two sensor rings, two digital multiplexers, one data switch, and a digital radio link between the spun and despun platforms for data transfer. Figure 6 illustrates the command architecture. The digital radio link consists of digital multiplexing equipment, transceivers, and receivers. The components are linked by a bus architecture and the central processors to be used on-board the satellite are two CDC 444's that will provide 3.906 Mbytes of RAM each. The payload processor will be a Honeywell ASC/PAM.

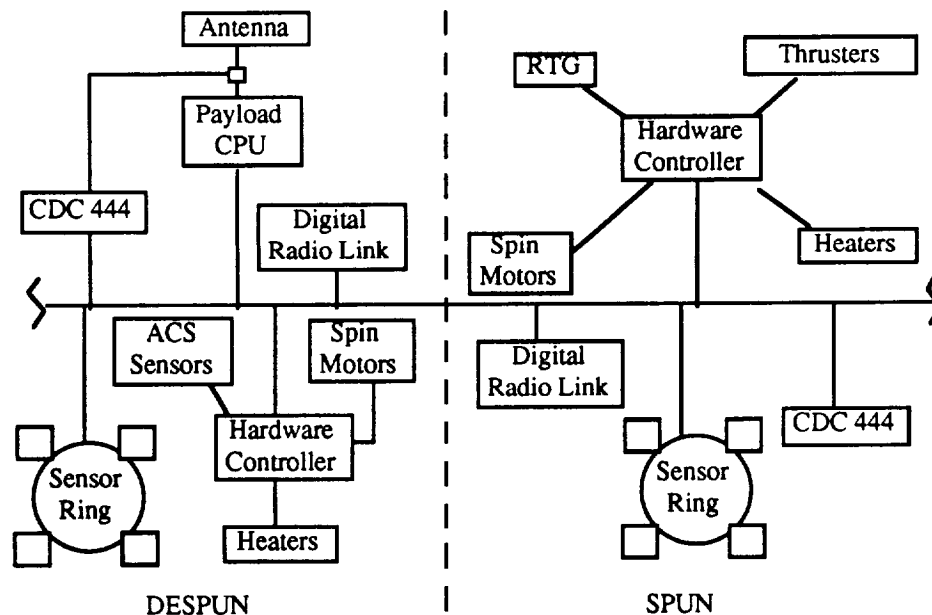


Figure 6 Command architecture design.



## Communications

The communications subsystem of the ECHO satellite will transmit 6 channels on the NASA Deep Space Network (NASA DSN) using the X- and S-bands. All transmissions will be received by the 34 m parabolic dish antenna provided by the NASA DSN. The specified channels are one color video, two voice, one for scientific data from lunar payloads, one satellite housekeeping and telemetry, and one for uplinked commands. Data rates for the communication channels are listed in Table 1. Quadruphased Phase Shift Keying (QPSK) plus R-1/2, K=7, Viterbi soft decoding is the modulation and coding scheme to be used for all transmissions. The system will contain two dipole antennas for transmission during the transfer orbit and a fixed, 0.83 m, parabolic, dual offset feed antenna for transmissions from the halo orbit. The system will also contain an Frequency Division Multiple Access

(FDMA) multiplexer, two solid-state amplifiers, two diplexers, and two transponders.

## Mass, Power & Cost Budgets

The completed mass, power, and cost budgets for this mission are as shown in Table 2. As indicated, the total estimated cost of \$125.2M is \$24.8M under the \$150M allowed. This total is in FY99 dollars and will allow for unforeseen contingencies. The power budget total of 1280 W is under the allowable 1360 W by 80 W. These power budget estimates take into account losses due to wiring and the power subsystem itself (hence the zero power requirement for the power subsystem.) Maximum payload mass of the Delta II for this mission is 1200 kg. After setting a 20% contingency factor, the total allowable mass is 960 kg. The present design configuration of ECHO has a mass of 855.1 kg.

**Table 1 Communication channel data rates.**

Communications Channel	Data rate
Color Video	44 Mbps
Voice	64 kbps
Scientific (low)	75 kbps
Scientific (high)	40 Mbps
Telemetry/housekeeping	1000 bps
Uplinked commands	1000 bps

**Table 2 Mass, Power & Cost Budgets.**

Subsystem	Mass (kg)	Power (W)	Cost (MSFY99)
Communications	22.2	85.0	13.1
Thermal Control	89.6	100.0	6.1
GNC	9.0	22.0	13.9
Power	321.0	0.0	60.0
Structures	201.6	5.0	14.0
Propulsion	197.0	1000.0	4.0
CDH	14.7	58.2	14.1
<b>TOTAL</b>	<b>855.1</b>	<b>1270.2</b>	<b>125.2</b>

## Conclusion

A preliminary mission design that provides continuous communications services between the far side of the Moon and the Earth has been completed. The design fulfills the modified Discovery-class criteria: 1) total cost must not exceed \$150 million (excluding launch vehicle), 2) launch must be achieved by a Delta-class vehicle, and 3) the design lifetime must exceed 10 years.

There are some design issues that still need to be addressed. First, the thermal effects in the launch shroud due to the four RTG's are a major concern. A detailed thermal analysis is required to determine if the heat shield will provide adequate protection during the time interval between loss of ground-support air conditioning and ejection of the the shroud. A reduction in the number of RTG modules may be possible with refinements to the L<sub>2</sub>-Halo transfer trajectory. At this time, the thrust history required to inject ECHO into the halo orbit has not been determined. If the ion thrusters do not need to operate at full power, it would be possible to reduce the number of RTG modules. Lastly, the communications system for the data relay between the Earth and the far side of the Moon is general in design. Once the types of missions to be sent to the Moon's far side are defined, the communications system design could become more specialized.

## Table of Contents

List of Figures.....	xv
List of Tables.....	xvi
<b>1.0 Introduction .....</b>	<b>1</b>
1.1 Mission Objective .....	1
1.2 Background .....	1
<b>2.0 Mission Scenario.....</b>	<b>3</b>
<b>3.0 Structures and Launch Vehicle.....</b>	<b>5</b>
3.1 Introduction .....	5
3.2 Configuration .....	5
3.2.1 Despun Platform.....	7
3.2.2 Spun Section.....	7
3.3 Material Selection .....	12
3.3.1 Material Selection for the Skin.....	14
3.3.2 Material Selection for the Columns .....	15
3.3.3 Material Selection for Fasteners.....	15
3.3.4 Material Selection for the RTG Booms.....	16
3.3.5 Material Selection for the Antenna Boom.....	16
3.3.6 Material Requirements for Micrometeoroid Shielding .....	16
3.4 Dual-Spin Linkage .....	17
3.5 Launch Vehicle .....	18
3.5.1 Payload Fairing .....	19
3.5.2 Payload Attach Fittings .....	19
3.6 Budgets.....	23
3.6.1 Cost Budget.....	23
3.6.2 Mass Budget.....	26
3.6.3 Power Budget.....	26
3.7 Conclusion.....	26
3.8 References .....	28
<b>4.0 Power Subsystem.....</b>	<b>29</b>
4.1 Introduction .....	29

4.2	Power Source.....	29
4.2.1	Power Requirements .....	30
4.2.2	RTG Design.....	30
4.3	Power Distribution .....	32
4.3.1	Power Bus-Bar .....	32
4.3.2	Power Harness.....	33
4.3.3	Power Control Circuits.....	35
4.3.4	Power Auxiliary Circuits.....	37
4.4	Power Regulation .....	37
4.4.1	Bus Input Regulation.....	37
4.4.2	Component Regulation.....	38
4.4.3	Power Regulation Hardware .....	38
4.5	Budget Summary.....	39
4.6	Conclusion.....	40
4.7	References .....	41
<b>5.0</b>	<b>Thermal Control Subsystem .....</b>	<b>42</b>
5.1	Introduction .....	42
5.2	Theory .....	43
5.3	Launch Cooling.....	45
5.4	Spun Platform.....	47
5.4.1	Thermal Coatings.....	48
5.4.2	Truss.....	49
5.4.3	RTG Thermal Concerns .....	49
5.5	Despun Section.....	50
5.6	Budgets.....	51
5.7	Conclusion.....	52
5.8	References .....	52
<b>6.0</b>	<b>Propulsion Subsystem.....</b>	<b>54</b>
6.1	Introduction .....	54
6.2	Propulsion System Design Overview.....	55
6.2.1	Propulsion System Determination.....	55
6.2.2	Thruster Positioning .....	57

6.2.3	Propellant Selection.....	59
6.2.4	Propellant Tank Design.....	61
6.2.5	Pressurization System .....	63
6.2.6	Interactive Effects of Propulsion System.....	64
6.2.7	Completion of Duties with Present Design .....	69
6.2.8	Mass, Power, and Cost Budgets.....	69
6.3	Conclusion.....	70
6.4	References .....	71
<b>7.0</b>	<b>Guidance, Navigation, and Control Subsystem.....</b>	<b>73</b>
7.1	Introduction .....	73
7.2	Trajectory and Halo Orbit .....	73
7.2.1	Trajectory .....	73
7.2.2	Halo Orbit.....	77
7.3	Spacecraft Stabilization.....	80
7.3.1	Spin Down.....	80
7.3.2	Disturbance Torques .....	81
7.4	MANS System.....	83
7.4.1	Background .....	83
7.4.2	The MANS Sensor .....	83
7.5	Budget .....	84
7.6	Conclusion.....	85
7.7	References .....	85
<b>8.0</b>	<b>Command and Data Handling Subsystem.....</b>	<b>87</b>
8.1	Introduction .....	87
8.2	Architecture.....	88
8.3	Software Sizing .....	88
8.3.1	Customized System Estimate .....	90
8.3.2	MANS Estimate .....	90
8.3.3	Comparison .....	92
8.3.4	Payload Software.....	93
8.4	Hardware Selection .....	93
8.4.1	CPU Selection .....	94
8.4.2	Payload Processor Selection.....	96
8.4.3	Hardware Controllers .....	98

8.5	Data Transfer Across the Spin Linkage .....	98
8.5.1	Slip Ring.....	99
8.5.2	Digital Radio Link.....	100
8.5.3	Data Transfer System Trade Study .....	101
8.6	Operational Lifetime .....	102
8.7	Channel Sizing .....	103
8.8	Budgets.....	104
8.8.1	Mass Budget.....	104
8.8.2	Power Budget.....	105
8.8.3	Cost Budget.....	105
8.9	Conclusion.....	106
8.10	References .....	107
<b>9.0</b>	<b>Communication Subsystem .....</b>	<b>108</b>
9.1	Introduction .....	108
9.2	Ground Support.....	108
9.2.1	NASA DSN.....	109
9.2.2	Frequency Ranges .....	109
9.2.3	Ground Segment and Operations Cost.....	110
9.3	Channels .....	112
9.3.1	Data Rates .....	112
9.3.2	Channel Design .....	112
9.4	Modulation and Coding.....	113
9.5	Link Design for ECHO .....	115
9.5.1	Satellite Downlinks .....	115
9.5.2	Satellite Uplinks.....	117
9.6	Antenna .....	119
9.6.1	Antenna for Communications in Halo Orbit.....	119
9.6.2	Beam Coverage .....	120
9.6.3	Antenna Usage for Halo Orbit Insertion .....	120
9.7	Multiplexer .....	122
9.8	Amplifiers.....	123
9.9	Budgets.....	125

9.9.1	Components.....	125
9.9.2	Component Mass and Power.....	125
9.9.3	Component Costs .....	126
9.10	Conclusion.....	126
9.11	References .....	127
<b>10.0</b>	<b>Conclusion.....</b>	<b>129</b>
<b>Appendix - Guidance, Navigation, and Control.....</b>		<b>130</b>
A.1	Computer Source Code for Computing Low-Thrust Trajectory.....	130
A.2	Input Parameters for Trajectory Calculation.....	136
A.3	Calculations for Spin Rates .....	136
A.4	Calculation of Solar Skirt Size .....	137

## List of Figures

Figure 2.1	Project ECHO Mission Scenario.....	4
Figure 3.1	Overall Configuration of the ECHO Spacecraft .....	6
Figure 3.2	Four-view of the Despun Platform.....	8
Figure 3.3a	Spun Section - Front View .....	9
Figure 3.3b	Spun Section - Side View.....	10
Figure 3.3c	Spun Section with Solar Skirt and Skin Removed.....	11
Figure 3.4	Spacecraft Envelope, Star 48B Configuration with 3712 PAF.....	20
Figure 3.5	ECHO in its Stowed Configuration.....	21
Figure 3.6	ECHO within the Delta II Payload Fairing .....	22
Figure 3.7	3712C PAF Interface Flange.....	24
Figure 3.8	3712C PAF Assembly .....	25
Figure 4.1	Overall Configuration of the ECHO Spacecraft .....	31
Figure 4.2	Power Harness .....	34
Figure 5.1	Heat Shield Schematic .....	46
Figure 5.2	Satellite Temperature Ranges.....	49
Figure 6.1	Propulsion Components Configuration .....	58
Figure 6.2	Ion Plume Impingement on Antenna and Solar Skirt .....	67
Figure 6.3	Ion Plume Impingement on RTG Modules .....	68
Figure 7.1	Overall Configuration of the ECHO Spacecraft .....	74
Figure 7.2	Transfer Trajectory from near-Earth Vicinity to L <sub>2</sub> Point .....	76
Figure 7.3	Orbital Energy w.r.t. Earth for Earth-L <sub>2</sub> Transfer.....	78
Figure 7.4	Stationkeeping-free Halo Orbit .....	79
Figure 8.1	Command and Data Handling Architecture .....	89
Figure 8.2	Slip Ring Data Transfer: (a) internal view, (b) cross-sectional view.....	100
Figure 8.3	Generalized Digital Radio Link System.....	101
Figure 9.1	Side View of Beam Coverage for Moon and Earth Links .....	121
Figure 9.2	Top View of Beam Coverage for Moon and Earth Links.....	121
Figure 9.3	Satellite Transmitter Power and Mass Versus rf Power Output.....	124



## List of Tables

Table 3.1	Characteristics of Possible Spacecraft Materials .....	13
Table 3.2	Material Property Ratings for Trade Study of Material Selection .....	13
Table 3.3	Trade Study Values for Skin, Columns, Fasteners, and RTG Booms .....	14
Table 3.4	Sample Despun Platform Drive Specifications.....	18
Table 3.5	Structures/Launch Vehicle Cost Budget.....	23
Table 3.6	Structures/Launch Vehicle Mass Budget.....	26
Table 4.1	MOD-RTG Design Summary.....	32
Table 4.2	Trade Study Comparing CRA and DRA Systems .....	33
Table 4.3	Trade Study Comparing Electromechanical and Solid-state Relays .....	36
Table 4.4	Trade Study Comparing FCH and HC Electromechanical Relays .....	36
Table 4.5	Some Specifications for Arnold Magnetics EL-2000 Series Power Regulators.....	38
Table 4.6	Final Subsystem Design Budget Estimates.....	39
Table 4.7	Subsystem Power Requirements.....	40
Table 5.1	Thermal Control Trade Study .....	47
Table 5.2	Thermal System Budget.....	51
Table 6.1	Trade Study on Electrical Propulsion Systems.....	56
Table 6.2	Specification of Possible Propellants.....	59
Table 6.3	Tank Mass and Size for Prospective Propellants.....	59
Table 6.4	Trade Study of Ion Thruster Propellants.....	60
Table 6.5	Trade Study of Propellant Tank Materials.....	62
Table 6.6	System Monitoring Channel Breakdown.....	66
Table 6.7	Mass, Power, and Cost Budgets for Propulsion Subsystem .....	70
Table 7.1	Spin Rates .....	80
Table 7.2	GNC Budgets.....	84
Table 8.1	Software Requirements for ECHO .....	91
Table 8.2	Software Requirements for MANS System.....	92
Table 8.3	MANS versus Customized System.....	93
Table 8.4	Payload Software Requirements.....	94
Table 8.5	Space Qualified Computers .....	95
Table 8.6	CPU Trade Study .....	96
Table 8.7	Space Qualified Computer for Role of Payload Processor.....	97
Table 8.8	Payload Processor Trade Study .....	98
Table 8.9	Data Transfer System Trade Study.....	102

Table 8.10	Mass Budget for C&DH .....	105
Table 8.11	Power Budget for C&DH.....	105
Table 8.12	Cost Budget for C&DH .....	106
Table 9.1	Ground Segment and Operations Costs (M\$,FY99).....	111
Table 9.2	Trade Study on Modulation and Coding.....	114
Table 9.3	Downlink Budgets for ECHO.....	116
Table 9.4	Uplink Budgets for ECHO.....	118
Table 9.5	Antenna Trade Study for High-Gain Communication between ECHO and Earth .....	119
Table 9.6	Trade Study for Low-Gain Antenna Communications during the Transer Orbit.....	122
Table 9.7	Multiplexer Trade Study.....	123
Table 9.8	Trade Study of Amplifiers .....	124
Table 9.9	Parameters for Communications Subsystem. ....	126

## 1.0 Introduction

The Advanced Design Project completed this academic year at The Pennsylvania State University was a communications relay satellite to provide continuous communication services between the Earth and the far side of the Moon. At the beginning of the Fall '93 semester the students were organized into six groups (five or six students per group) and each was given the task of developing a conceptual-level design of the spacecraft and its mission. These designs were then evaluated at the end of the Fall semester and components of the six different missions were assembled into one complete mission. To facilitate the work required for the now single mission design, the class was reorganized in the Spring '94 semester by matching the students (taking into account particular interests and specializations from the previous semester) with a subsystem of the spacecraft. A systems integration team consisting of one student from each of the major subsystems was formed so that communication and transfer of information would be easier among the subsystem groups.

### 1.1 Mission Objective

The objective of Project ECHO (Electronic Communications from Halo Orbit) is to provide a continuous communications link between Earth and the far side of the Moon. The spacecraft will provide real-time or delayed transfer of information, telemetry, and voice/video data.

### 1.2 Background

This satellite will provide the link necessary to communicate with the Moon's far side. The project will allow for the exploration and utilization of the far side of the Moon by establishing a communications link to scientific outposts, mining operations, lunar rovers, or exploration probes. The spacecraft will be in a halo orbit about the Earth-Moon Lagrange point  $L_2$  (located 64,500 km beyond the Moon's center) and will maintain an uninterrupted

line-of-sight with both the Earth and the Moon. Development of Project ECHO was restricted by modified NASA Discovery-class mission parameters: 1) total cost must not exceed \$150 million (excluding launch vehicle), 2) launch must be achieved by a Delta-class vehicle, and 3) the design lifetime must be greater than 10 years.

In order to meet the requirements (especially w.r.t. cost) posed by the Discovery-class missions, current or off-the-shelf technology must be used extensively. In the case of the ECHO spacecraft, key components are either current technologies or those that will be available in time for launch in 1999.

## 2.0 Mission Scenario

The mission scenario of Project ECHO is presented in Figure 2.1 showing the events from launch on a Delta II 7925 to its nominal operational state.

Since the ECHO spacecraft relies solely on the use of RTG's for electrical power, ground-support air conditioning must be used to help regulate the harsh thermal environment that the spacecraft will experience while enclosed in the payload fairing. A few moments before launch, all ground-support services on the launch pad will be disconnected from the vehicle. Launch of ECHO will occur in 1999 from Cape Canaveral. The Delta II 7925 vehicle contains three stages with a payload assist module (PAM) comprising the third stage.

After separation from the payload fairing, ECHO is injected on a transfer trajectory to the L<sub>2</sub> point and the entire spacecraft will have a spin rate of 45 rpm. Deployment of the RTG's will take place 60 minutes after launch and will reduce the ECHO's spin rate to 9.4 rpm. Also deployed during the transfer is the parabolic antenna system, however, twin dipole antennas will provide communications while in transit to the halo orbit to avoid problems in pointing the main antenna. The transfer trajectory from the launch vehicle injection point to the L<sub>2</sub> point requires zero additional thrust from ECHO, but mid-course corrections but propellant reserves will allow for mid-course corrections. Total time for this transfer is approximately 40-50 days. A second transfer trajectory allows ECHO to be injected into a stationkeeping-free halo orbit from the L<sub>2</sub> point. Since the main propulsion of ECHO is electric (low-thrust), this trajectory is a slow (14 days) spiral to the injection point.

Once in halo orbit, the despun section will be slowed by the bearing and power transfer assembly (BAPTA) to a rate of 0.5°/hr. Stabilization of ECHO once in the halo orbit is maintained by using the ion thrusters to increase the spun section's spin rate to 35 rpm. Even though ECHO is on a stationkeeping-free orbit, some corrections may be required and can be adequately provided by the ion thrusters. Before normal communication services begin, systems will be tested and evaluated.

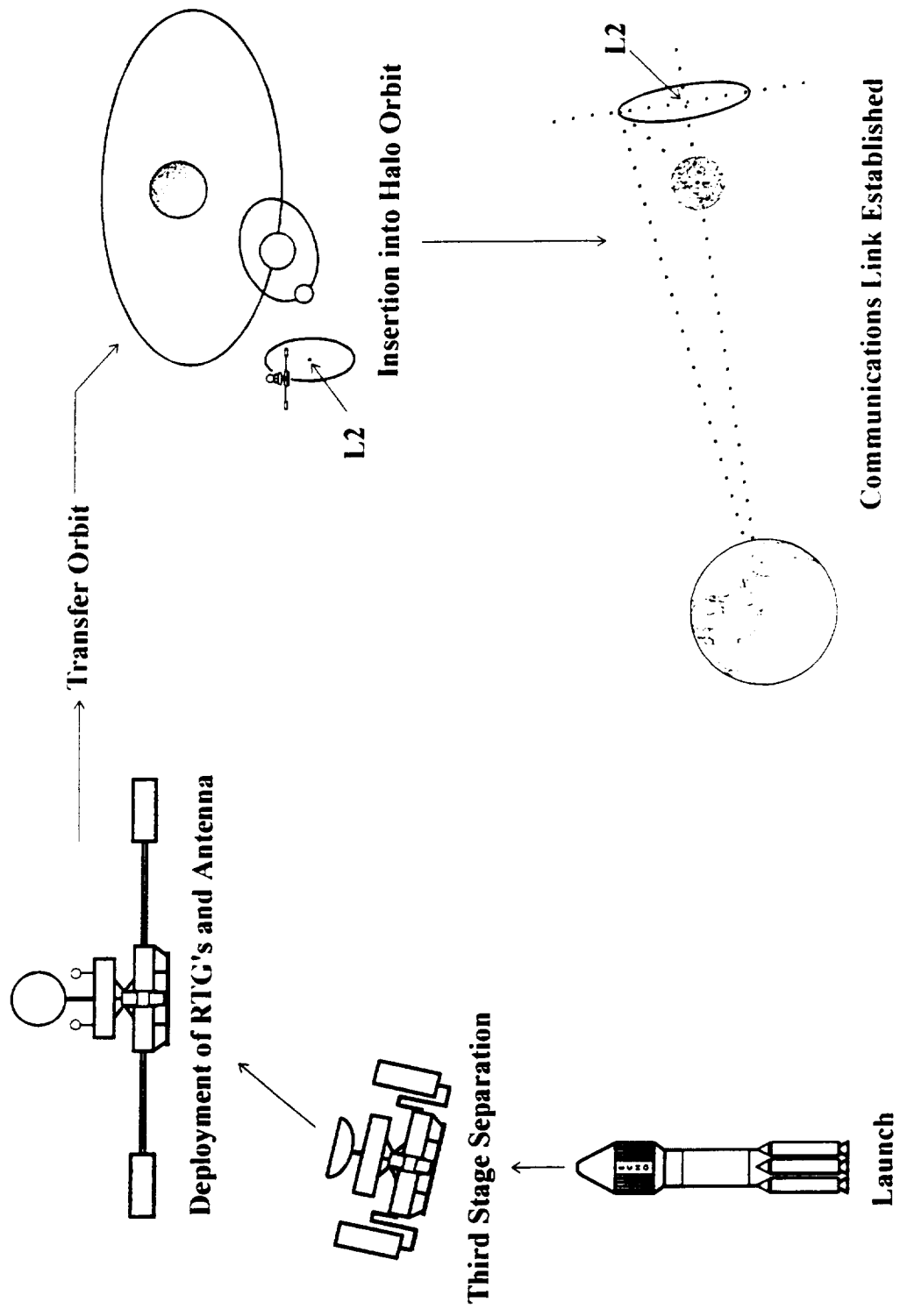


Figure 2.1 Project ECHO Mission Scenario.

## **3.0 Structures and Launch Vehicle**

### **3.1 Introduction**

The structures/launch vehicle subsystem must integrate the design with the other subsystem designs. This involves incorporating other subsystems' components, providing structural support to a propulsive system, and other interactions which are detailed throughout this section. The interaction with the other subsystems was accomplished through an integration team which consisted of subsystem representatives.

The structures and launch vehicle subsystem is responsible for: the satellite's configuration, material selection, a micrometeoroid protection scheme, a dual-spin linkage development, and the launch vehicle interface. The satellite configuration is documented using the software program I-DEAS. The materials used to construct the spacecraft must be selected for different parts of the satellite. The combination of satellite configuration and material selection should also provide an adequate micrometeoroid protection scheme. A dual-spin linkage must be developed to last throughout the expected 10-15 year lifetime of the satellite. A payload attach fitting must be chosen from among those available with the Delta II class launch vehicles. The entire satellite must be launched by a Delta II-class launch vehicle, and the type of launch vehicle and fairing must be chosen.

### **3.2 Configuration**

As dictated by the mission requirements, the satellite configuration will consist of a despun platform and a spun section, linked together through a BAPTA (bearing and power transfer assembly). The results from structural ground testing may reveal the necessity for additional structure to aid the BAPTA during launch. The overall configuration is shown in Figure 3.1.

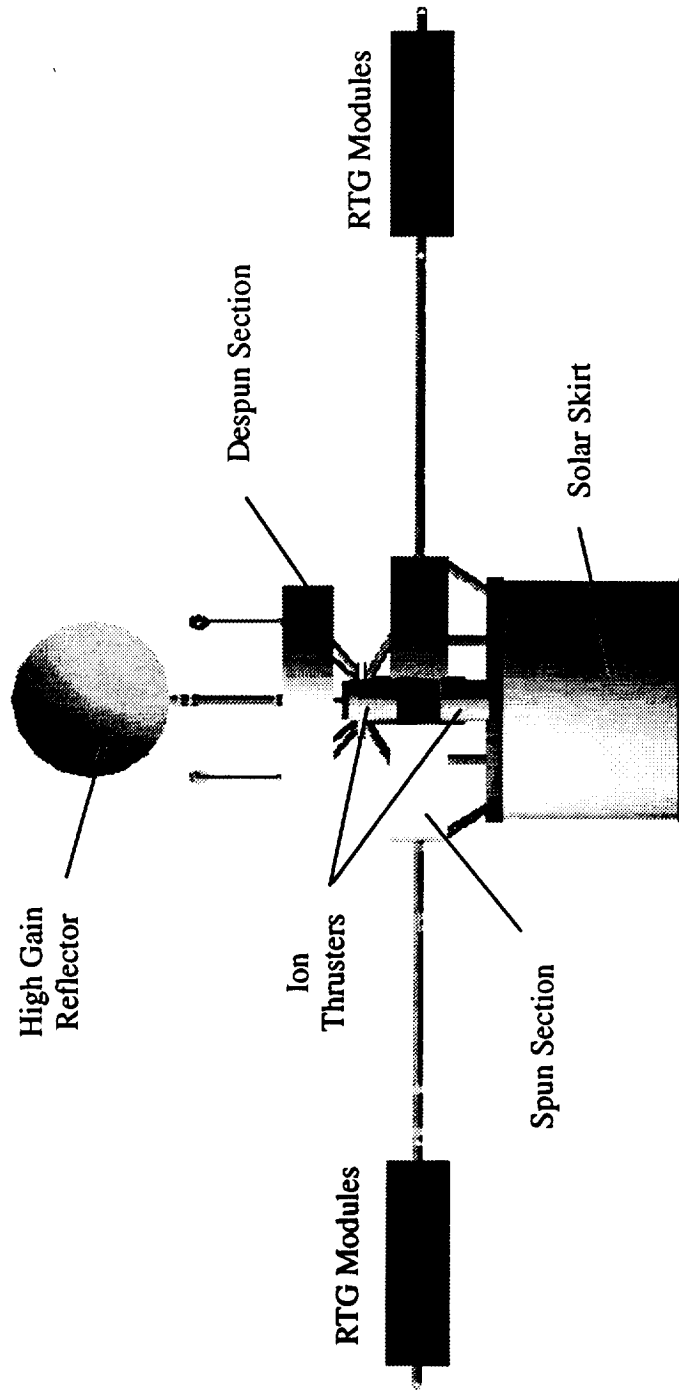


Figure 3.1 Overall Configuration of the ECHO Spacecraft.



### 3.2.1 Despun Platform

The despun platform will house the majority of the electronics of the satellite. The cylindrical platform is 1.2 m in diameter and 0.25 m in height. The high-gain antenna will be located on a 1.0 m long boom extending from the top of the platform, as seen in Figure 3.2, with a support running down through the center of the platform to support the weight of the antenna during launch. The rest of the platform will be a semimonocoque structure, with the components resting on a reinforced shelf.

### 3.2.2 Spun Section

The spun section will be 1.0 m in height, and will have a maximum diameter of 1.5 m. This section will be a combination of a truss and semimonocoque structure. Figure 3.3a shows the despun platform with the RTG booms and the solar skirt visible. Figure 3.3b shows the spun section rotated 90 degrees from Figure 3.3a, this shows the thruster modules mounted on the sides of the spun section. The taper of the spun section that allows for a reduction in mass is shown in Figure 3.3c. This shows the structure of the spun section without the solar skirt deployed. The entire axial load that the satellite will encounter during launch will be transferred through the structure, through the payload attach fitting, and into the structure of the launch vehicle. All of the spun section will be open with the exception of the platform where electronics will be located. All electronics will be housed within a 1 mm thick skin of Al 6061-T6 to provide protection from possible micrometeoroid impacts. This skin will also be part of the semimonocoque structure to help provide reinforcement against torsional loads.

The spun section will account for the majority of the mass of the satellite structure. The entire propulsion system will be placed on a modular platform. This will allow the thrusters and propellant tanks to be located about the center of mass to enable the thrusters to act through the center of mass as much as possible, and to limit the shifting of the center of mass due to propellant usage.

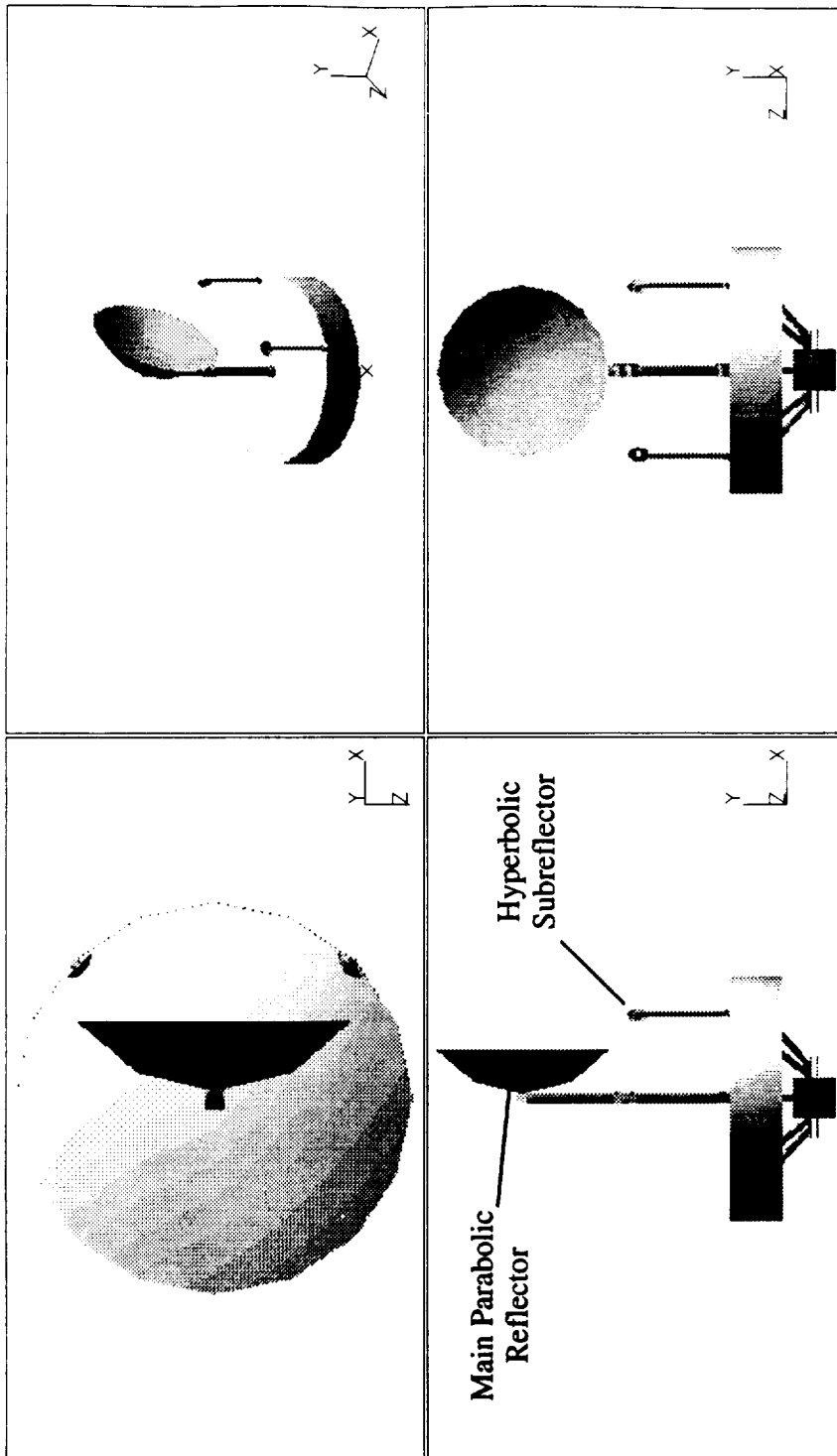


**Figure 3.2 Four-view of the Despun Platform.**

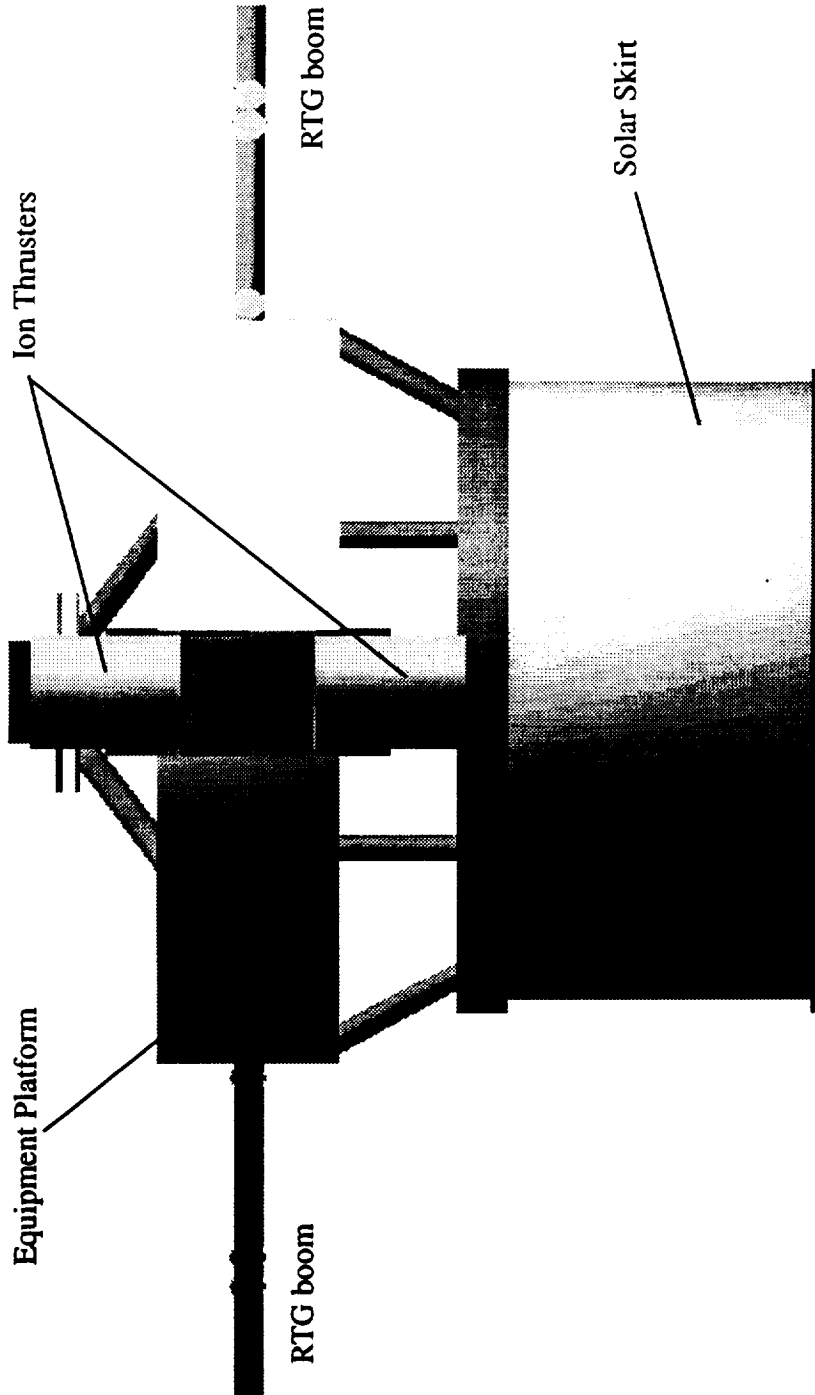


Figure 3.3a Spun Section - Front View.

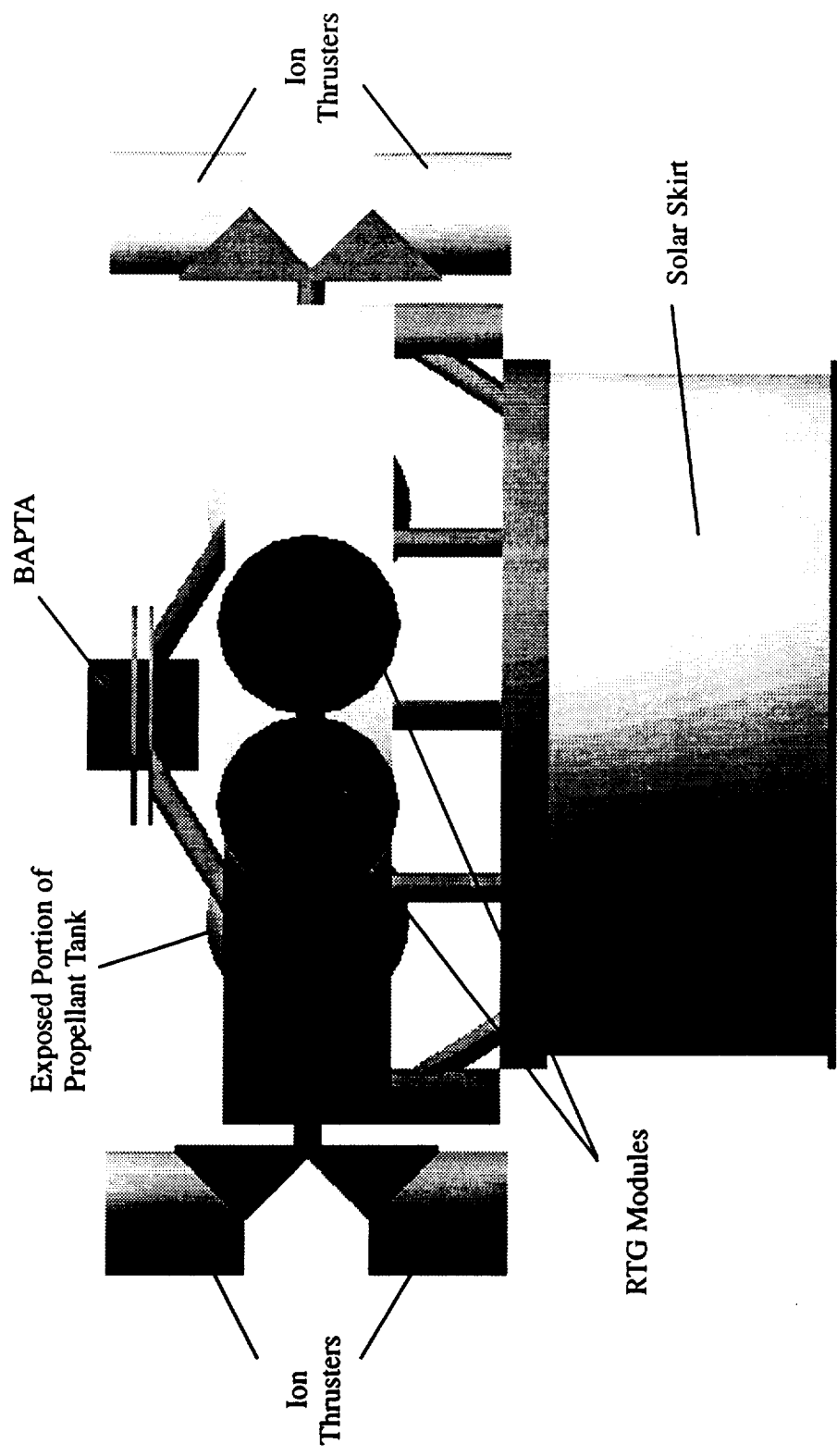


Figure 3.3b Spun Section - Side View.

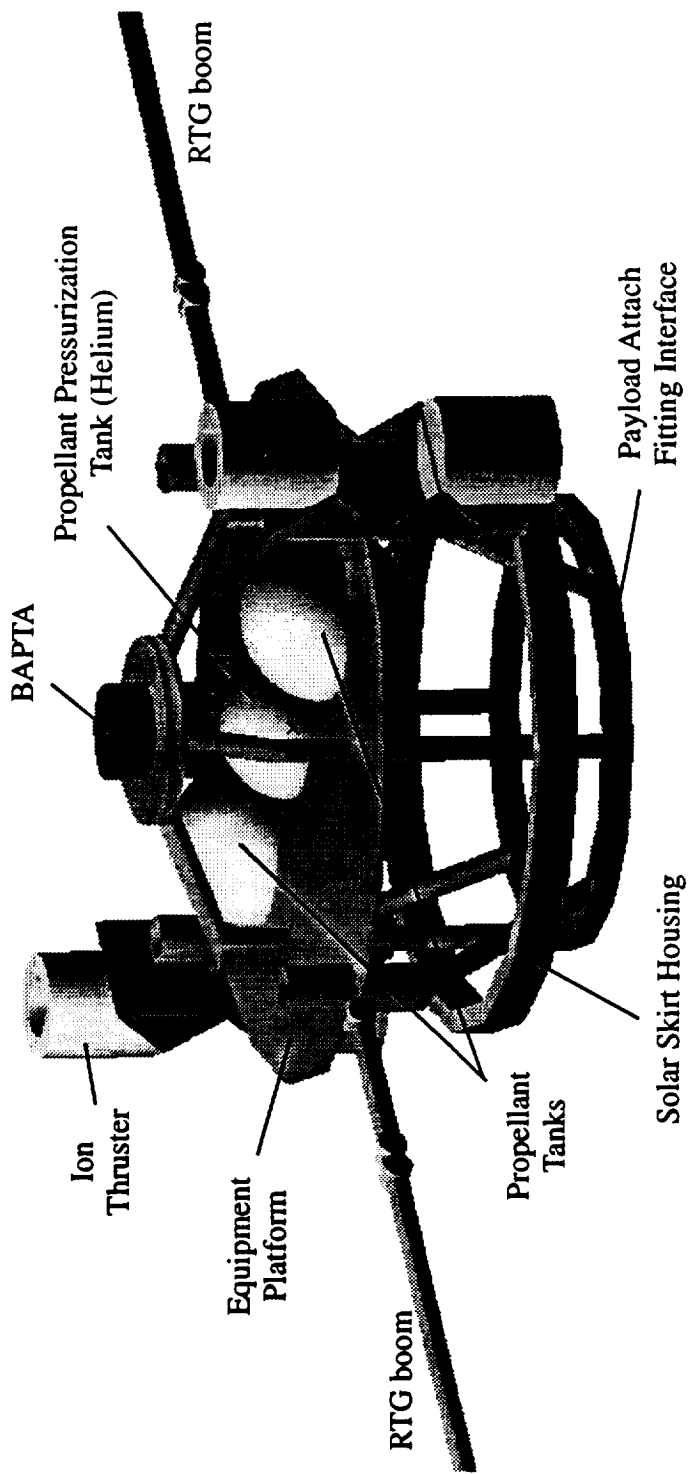


Figure 3.3c: Spun Section with Solar Skirt and Skin Removed.

The RTG power generators will be located on two booms extending radially outward from the spun section. The booms will be offset 90 degrees from the thruster modules, and will place the RTG's 1.6 m away from the satellite as dictated by thermal subsystem requirements. Since the power subsystem requires four separate RTG modules, two will be located on each boom for stability. Given that each RTG module is 42.4 kg, each boom will be designed to carry a mass of 84.8 kg through any type of loading situation that may be encountered. The booms will have an outside diameter of 5 cm and an inside diameter of 1.67 cm. Pyrotechnic latches will release the booms from their stowed positions. Once released a spring-damper system will be used to deploy the booms. Each boom will split into two segments at 1.5 m and will extend radially 0.165 m, then will continue away from the satellite for another 0.1 m. These dimensions have been verified using an elementary finite element analysis. Each boom was divided into 3 elements out to a length of 1.5 m then each segment of the boom was modeled as an element. The maximum stress in each boom will occur during its deployment. There will be a transverse force on each boom when the RTG reaches its deployed configuration and comes to a stop, and a radial force resulting from the spin-down of the satellite when the RTG is moved away from the center of mass. The maximum stress in the booms did not exceed 75% of the yield tensile stress of the material being used (see Section 3.3.4).

### 3.3 Material Selection

At this stage in the design, the selection of materials must be differentiated for several applications. These applications can be split into five main categories: skin, columns, fasteners, RTG booms, and antenna boom. The skin for the spacecraft bus needs to be ductile for easy machining, low weight, and low cost. High specific stiffness to resist buckling is needed for the columns. The fasteners need to have a high specific strength to withstand heavy point loading. To resist the combination of forces due to angular

acceleration and angular velocity, the RTG booms need to have a large tensile yield strength. The antenna boom has a limitation of very low thermal expansion, and is analyzed separately. The characteristics of several materials are compiled in Table 3.1.

**Table 3.1 Characteristics of Possible Spacecraft Materials.** (Metals Reference Book, American Society for Metals, 1981 and Metals Handbook, American Society for Metals, 9th ed. Vol. 2, 1990)

Material	Density g/cm <sup>3</sup>	Yield Strength (MPa)	Young's Modulus (GPa)	Specific Strength (Y.S./density)	Specific Stiffness (E/density)
Aluminum					
6061-T6	2.71	275	68	101.5	25.1
7075-T6	2.8	505	71	180.4	25.4
2014-T6	2.8	415	72	148.2	25.7
Titanium					
6Al-4V	4.43	900	110	203.2	24.8
13V-11Cr-3Al	4.46	1170	101	262.3	22.6

Table 3.2 contains the ratings of the physical properties of several materials. These ratings are used in trade studies to select a material for the skin, columns, fasteners, and RTG booms. Each material is rated from 1 (lowest) to 5 (highest).

**Table 3.2 Material Property Ratings for Trade Study of Material Selection.**

Material	Weight	Specific Strength	Specific Stiffness	Cost	Machine- ability
Aluminum					
6061-T6	2	2	3	1	5
7075-T6	2	3	3	2	4
2014-T6	2	2	3	2	4
Titanium					
6Al-4V	4	4	3	4	3
13V-11Cr-3Al	4	5	2	4	3

Table 3.3 contains the trade study values of different materials for the application to the skin, columns, fasteners, and the RTG booms. The best performance index, J, corresponds to the highest value. The material selection of each application along with its respective trade study equations is explained in further detail in Section 3.3.1 through Section 3.3.4.

**Table 3.3 Trade Study Values for Skin, Columns, Fasteners, and RTG Booms.**

Material	J skin	J columns	J fasteners	J RTG booms
Aluminum				
6061-T6	0.5	1.5	2.2	1.4
7075-T6	0.2	1.6	2.45	1.65
2014-T6	0.1	1.3	1.9	1.15
Titanium				
6Al-4V	-1.1	1.2	2.5	1.3
13V-11Cr-3Al	-1.1	1.2	2.95	1.55

### 3.3.1 Material Selection for the Skin

The skin only needs to transfer torsional loads and serve as a micrometeoroid shield. The torsional loading is proportional to skin thickness to the fourth power. Therefore, the most important aspect of the skin is to be very low in mass. The skin also needs to be ductile for easy machining. This will reduce manufacturing cost and risk.

The performance index, J, for the skin is calculated using:

$$J = -0.4 (\text{Weight}) + 0.1 (\text{Spec. Strength}) + 0.1 (\text{Spec. Stiffness}) - 0.2 (\text{Cost}) + 0.2 (\text{Machinability}) \quad (3.1)$$



Table 3.2 shows that Al 6061-T6 has the best trade value for the skin application. This material satisfies the micrometeoroid shielding requirements which are detailed in Section 3.3.6.

### 3.3.2 Material Selection for the Columns

The main concern for the columns is that they resist buckling. The critical buckling loads are directly proportional to the stiffness and the area moment of inertia. Therefore, high specific stiffness with low weight is crucial to columns in compression. All of the materials in the trade study have about the same specific stiffness. This makes it difficult to choose the coefficients in the trade study. The performance index for the columns is calculated using:

$$J = - 0.2 (\text{Weight}) + 0.3 (\text{Spec. Strength}) + 0.3 (\text{Spec. Stiffness}) \\ - 0.1 (\text{Cost}) + 0.1 (\text{Machinability}) \quad (3.2)$$

Aluminum 7075-T6 has the best trade study value. This material is manufactured as drawn tubing, so the proven manufacturability lowers the risk for the column application.

### 3.3.3 Material Selection for Fasteners

The fasteners require high specific strength and accurate machining to withstand heavy point loading. The performance index for the fasteners is calculated using:

$$J = - 0.05 (\text{Weight}) + 0.55 (\text{Spec. Strength}) + 0.1 (\text{Spec. Stiffness}) \\ - 0.1 (\text{Cost}) + 0.2 (\text{Machinability}) \quad (3.3)$$

Titanium 13V-11Cr-3Al had the best trade study values of the materials being investigated for selection. Titanium is commonplace among fasteners for aerospace applications, so proven technology will reduce risk.

### 3.3.4 Material Selection for the RTG Booms

The main concern for the RTG booms is that they resist large tensile forces. These tensile forces result from the combination of angular accelerations and centrifugal forces. The specific stiffness is also a consideration, because if the booms allow large tip deflections the spacecraft could suffer stability problems. The booms are designed as tubular beams, so machinability will not be a major concern. The equation to determine the material with the highest performance index is given by:

$$J = - 0.2 (\text{Weight}) + 0.5 (\text{Spec. Strength}) + 0.25 (\text{Spec. Stiffness}) \\ - 0.2 (\text{Cost}) + 0.05 (\text{Machinability}) \quad (3.4)$$

Aluminum 7075-T6 had the highest performance index using Equation 3.4. The other values shown in Table 3.3 are within a close proximity to the performance index of aluminum 7075-T6. Titanium 13V-11Cr-3Al will be used if structural ground testing reveals it to be necessary.

### 3.3.5 Material Selection of the Antenna Boom

The major constraint on the boom for the antenna is that it has a very small coefficient of thermal expansion. This can be accomplished using a composite of epoxy resin with a combination of PAN-based and pitch-based graphite fibers. The booms must withstand extreme temperature ranges and high radiation energies. This environment may cause serious loss of physical properties in most composite materials, but has only a moderate effect on epoxy/graphite composites and even less on toughened epoxy/graphite composites [3.4].

### 3.3.6 Material Requirements for Micrometeoroid Shielding

The spacecraft will need some micrometeoroid shielding to protect the wiring, computers, and other essential components. The majority of the micrometeoroids

encountered on this mission will have a diameter of 0.01 mm or less. A small number of micrometeoroids with a diameter of 0.1 mm may also impact the spacecraft. In 1990, the LDEF (Long Duration Exposure Facility) was recovered after six years in space. The LDEF used an aluminum test plate to study the effects of micrometeoroids. The study showed the crater depth ranged from one-half to one-third of the diameter of the micrometeoroid [3.5]. Therefore, even the larger micrometeoroids encountered by the spacecraft will leave craters only 0.05 mm deep. With an aluminum skin thickness of 1 mm, ECHO should not have difficulty with micrometeoroids. With the 1 mm skin thickness, some problems may occur if larger micrometeoroids impact near the same location, but this is not very likely.

### 3.4 Dual-Spin Linkage

Since the satellite is composed of two sections, a spun section and a despun section, a linkage between the two sections that will transfer power and data from one section to the other is required. Every linkage used in a satellite to date has been designed for the specific satellite; therefore, no off-the-shelf linkage technology is readily available. Current information has been taken into account to estimate the specifications needed.

The available information is for a despun platform that contains only antennas and experiments that need accurate pointing. The mass of this platform is most likely much lower than the mass of the despun platform of ECHO because the despun platform will contain most of the needed computers. The specifications of this platform can be found in Table 3.4.

**Table 3.4 Sample Despun Platform Drive Specifications.** (Chetty, P. R. K., Satellite Technology and its Applications, 2nd edition, TAB Professional and Reference Books, 1991, pp. 328, 333-334.)

Weight	9.75 kg
Speed Range	0-120 rpm
Power consumption	<9 watts
Torque Available	1.27 Nm
Power Circuits	27 @ 3 amps each
Signal Circuits	58 @ .1 amps
Grounding Circuits	5

ECHO will contain a spin linkage that has similar capabilities to the one discussed above. The mass of the linkage is projected to be less than 20 kg. The angular rotation rate for this satellite is under 35 revolutions per minute, but the mass it will be supporting is higher, approximately 100 kg in the despun section. There will be three power channels required in the slip ring of the linkage, but six will be provided for redundancy.

The linkage, which has a shape similar to a long cylinder, will be supported by four beams attached to the equipment platform of the spun section. The length of the spin linkage will be 220 mm with a diameter of 120 mm. The beams will carry the axial load of the linkage and the despun section down to the payload attach fitting through the equipment platform of the spun section. The housing of the linkage must be made of a very strong material in order to support the mass of the despun section during launch. A titanium alloy will be used for this purpose. A small motor will be used to overcome the internal friction of the linkage. This will consist of a redundant wound brushless motor that will require 5 watts to operate. This motor will also be used to rotate the despun section so the antenna can track the Earth and Moon.

### 3.5 Launch Vehicle

The launch must be achieved via a Delta-class launch vehicle. The three stage Delta II 7925 model was chosen since it is the only three stage Delta-class vehicle currently being

produced. The payload fairing and the payload attach fitting were chosen based on the mass, volume, and trajectory specifications of the satellite as detailed in Sections 3.5.1 and 3.5.2. The satellite should be positioned in the usable payload envelope above the separation plane shown in Figure 3.4. Otherwise, the critical clearances would need to be analyzed.

### 3.5.1 Payload Fairing

The payload fairing (PLF) will shield the spacecraft from buffeting and aerodynamic heating while in the lower atmosphere. The fairing will then be jettisoned during the second stage of the flight at an altitude no less than 125 km. The 2.9 m diameter payload fairing will be used because it is the only fairing size that permits the Delta 7925 to place a 1200 kg spacecraft into a translunar trajectory. Since this fairing allows for an increased payload of 50 kg, the spacecraft's mass can be increased which will allow for any necessary contingencies. The 2.9 m diameter fairing also has a lighter structural mass which saves 159 kg [3.7].

The separation plane is the space around the payload attach fitting, which is connected to the PAM-D motor. See Figure 3.4 for the PLF dimensions. The stowed configuration of the satellite is shown in Figure 3.5. The stowed satellite and the PLF are shown in Figure 3.6. It can be seen that the satellite will not enter any restricted areas in the PLF.

### 3.5.2 Payload Attach Fittings

The payload attach fitting (PAF) is the interface between the spacecraft and the third stage of the Delta II 7925 model. The PAF supports the clamp assembly which attaches the spacecraft to the third stage and allows the spacecraft to be released on separation. The PAF that is used with the three-stage Delta rocket is the 3712 model PAF. This fitting is available in three configurations depending on the specifications of each satellite to meet the spacecraft's mass and center of gravity requirements. The 3712C PAF was chosen for Project

Note: 1. All Station Numbers Are in Inches  
 2. Station Numbers With an Asterisk (\*) Indicate Outside Stations

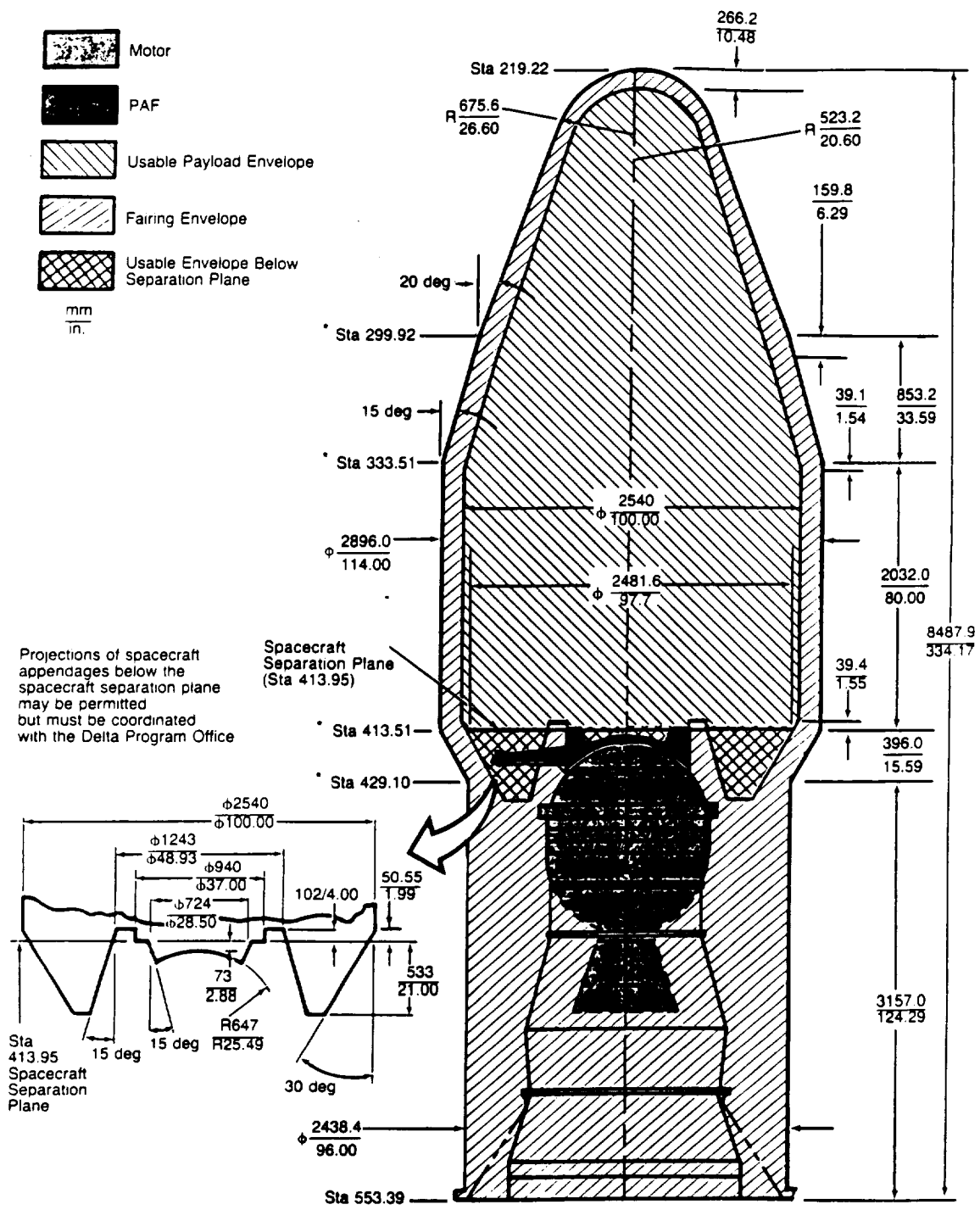


Figure 3.4 Spacecraft Envelope, Star 48B Configuration with 3712 PAF.  
 (Commercial Delta II Payload Planner's Guide, McDonnell Douglas Commercial Delta, Inc.,  
 Huntington Beach, California, 1990, p. 3-5.)

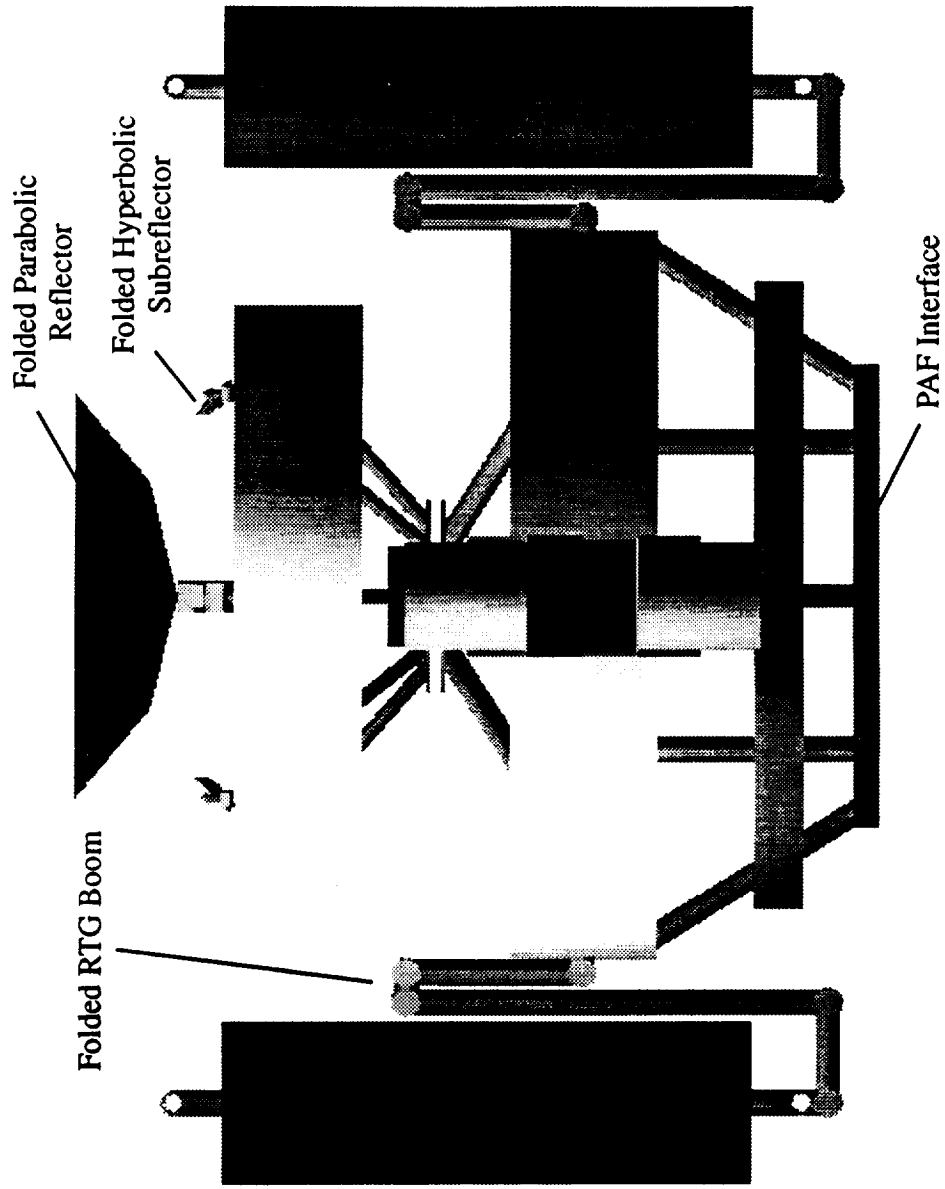
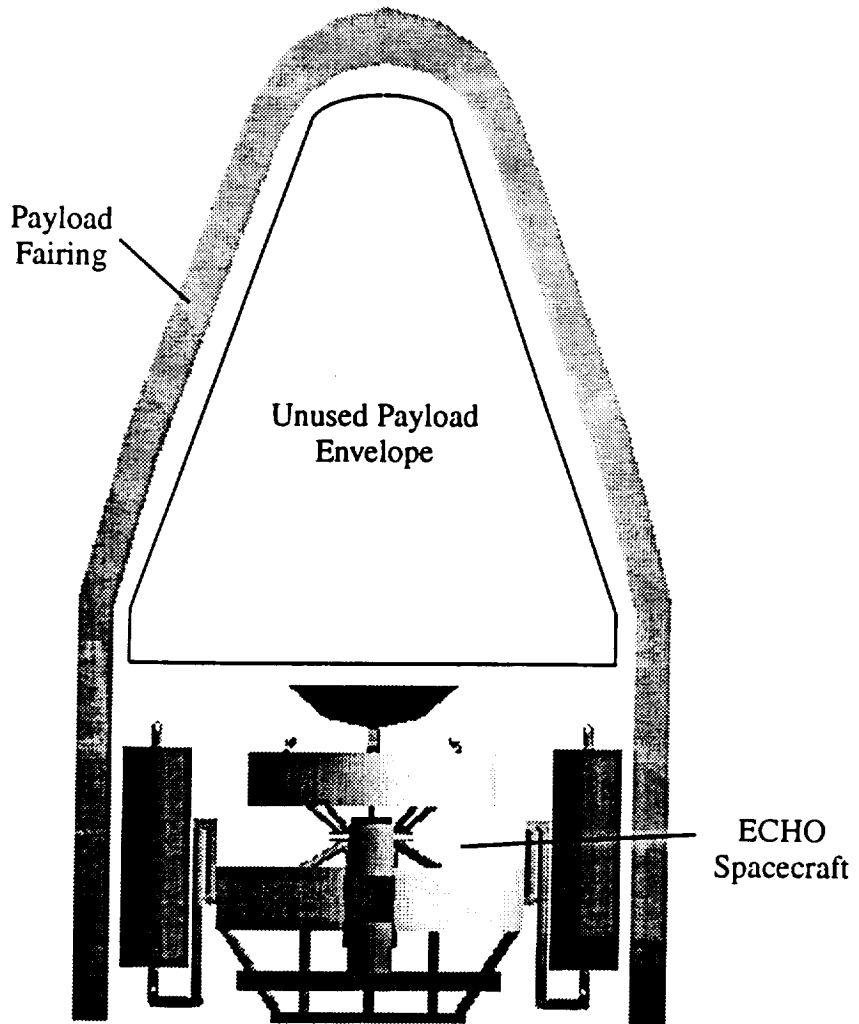


Figure 3.5 ECHO in its Stowed Configuration.



**Figure 3.6 ECHO within the Delta II Payload Fairing.**



ECHO because of the spacecraft's mass (1200 kg) being less than the maximum limit of model C at 1361 kg [3.8]. The flange requirements and PAF configurations are shown in Figures 3.7 and 3.8. From the dimensions in these diagrams, the satellite interface conforms to these specifications in order to attach the spacecraft to the PAF. As the configuration of the satellite was determined, the fittings and clamps were designed to meet these specifications.

### 3.6 Budgets


#### 3.6.1 Cost Budget

The launch vehicle and structures design group was allotted \$15 million for the cost budget. The cost of the launch vehicle is not included in this project's budget. The distribution of the \$15 million is shown in Table 3.5.

**Table 3.5 Structures/Launch Vehicle Cost Budget.**

Item	Cost (millions of dollars, FY99)
Aluminum	0.2
Titanium	0.3
Manufacturing and Testing	10.5
20 % Contingency	3.0
<b>TOTAL</b>	<b>14.0</b>

The cost of purchasing the material is very small compared to the manufacturing and testing of the structure. These values include manufacturing three identical satellites. One satellite will be used for failure testing, another for non-destructive evaluation, and the third will be launched into orbit.

For Section Marked   
 Area = 269 mm<sup>2</sup>/0.417 in.<sup>2</sup> ± 15%  
 I = 11,654 mm<sup>4</sup>/0.028 in.<sup>4</sup> ± 15%  
 Applicable Length, L = 25.4 mm/1.0 in.

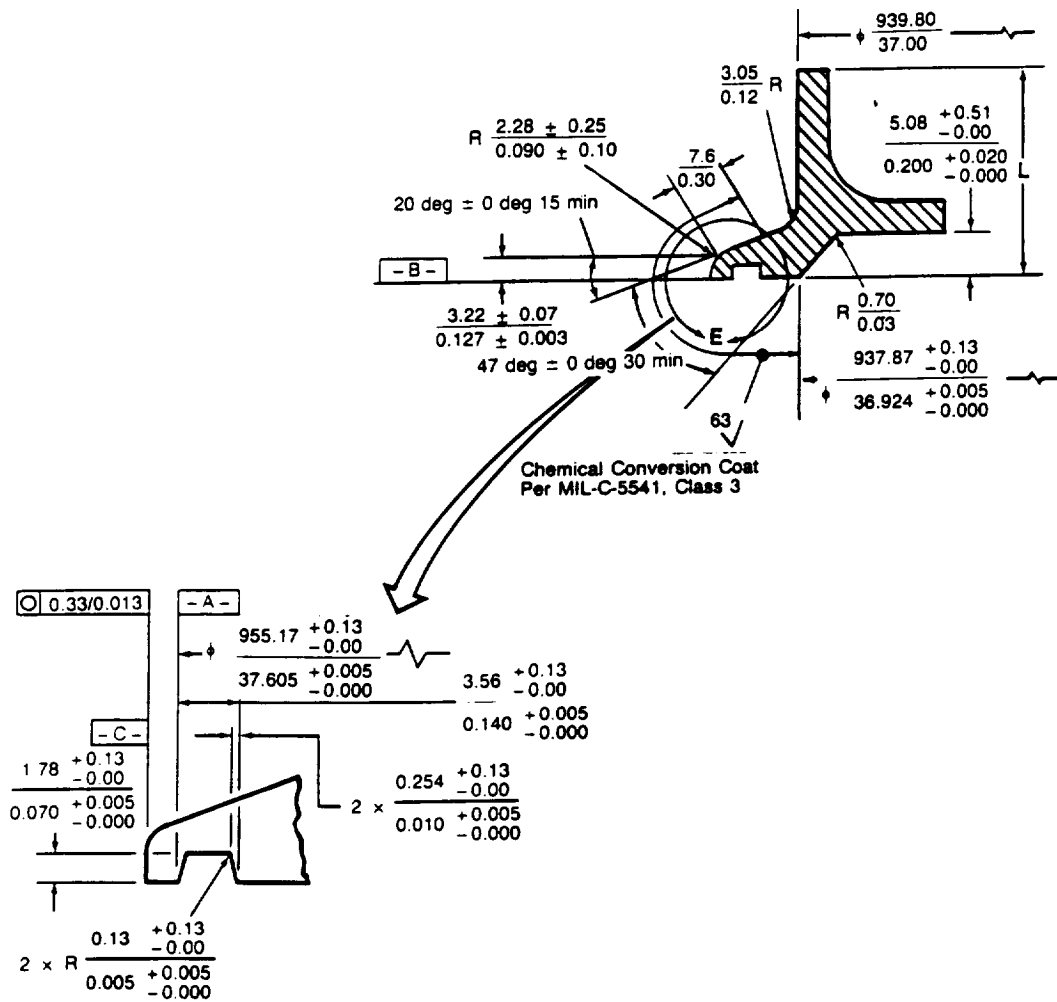


**Figure 3.7 3712C PAF Interface Flange.** (Commercial Delta II Payload Planner's Guide, McDonnell Douglas Commercial Delta, Inc., Huntington Beach, California, 1990, p. 5-11.)

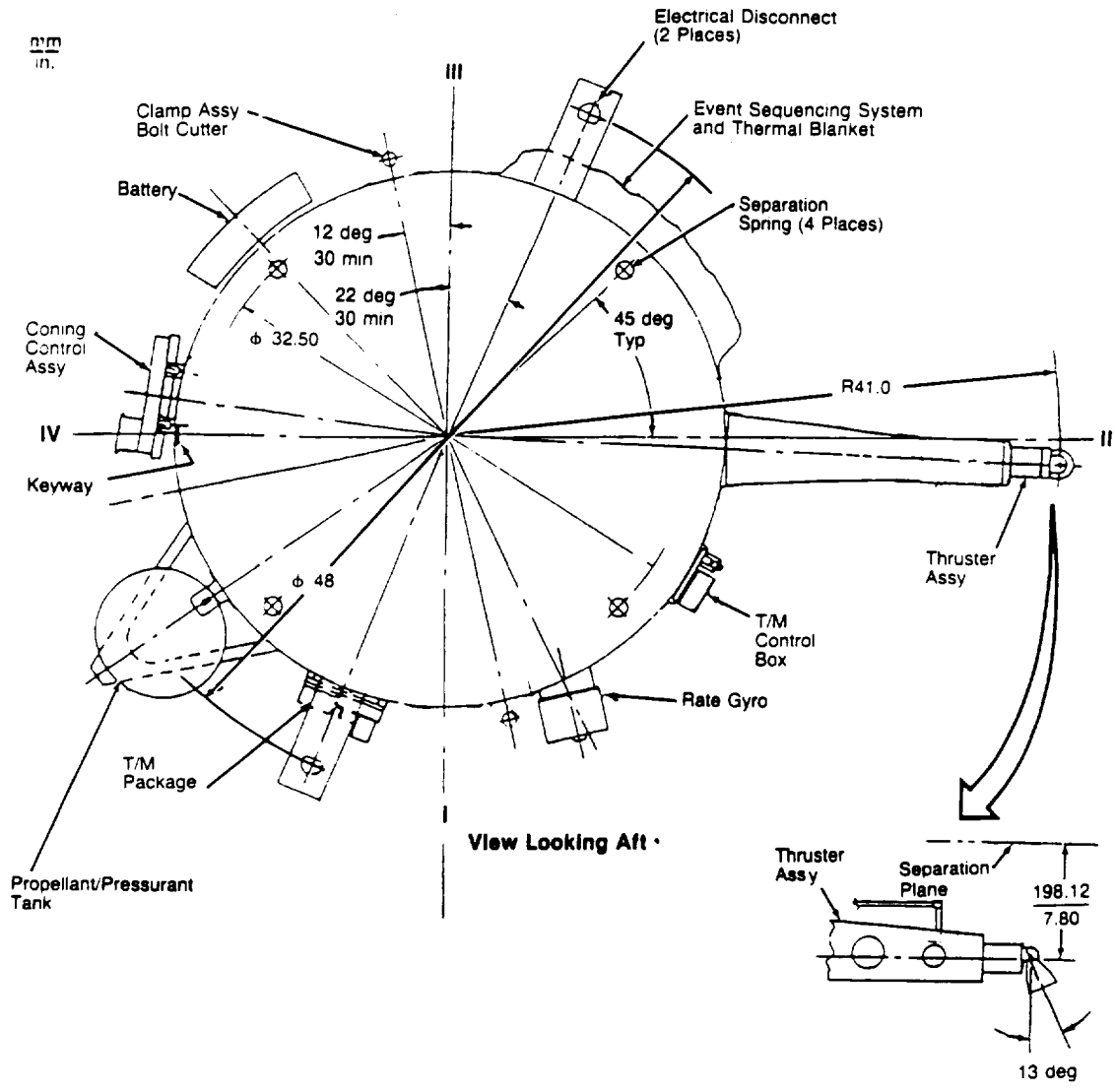


**Figure 3.8 3712C PAF Assembly.** (Commercial Delta II Payload Planner's Guide, McDonnell Douglas Commercial Delta, Inc., Huntington Beach, California, 1990, p. 5-5.)

### 3.6.2 Mass Budget

The structures and launch vehicle group was allotted 300 kg. The budget includes the spin linkage and all of the structural material on the satellite. The mass of the PAF is not included in the budgets because it is considered part of the launch vehicle.

The spun section will have a total structural mass of 135.6 kg, and the despun section will have a structural mass of 45.5 kg. Table 3.6 contains the distribution of masses.

**Table 3.6 Structures/Launch Vehicle Mass Budget.**

Item	Mass (kg)
Spun Section	
Plate	38.0
Frame	84.9
Skin	12.7
Despun Section	
Frame	10.6
Skin	35.4
Spin Linkage	20.0
<b>TOTAL</b>	<b>201.6</b>

### 3.6.3 Power Budget

The power budget is very small for this subsystem. The only component that will require power is the spin linkage, which will consume five watts of power. A small amount of power will be used to release the latches that hold the RTG booms and the antenna booms in place during launch. This estimated power is less than one watt and will be necessary only once during the mission.

### 3.7 Conclusion

The structural configuration is designed to incorporate the various components of the satellite, and is also designed to interface with the launch vehicle. With the integration of the

components, the configuration consists of a despun section and a spun section connected by a spin linkage.

The despun platform contains the electronics and the antenna and is designed as a semimonocoque structure. The spun section will consist of a combination of semimonocoque and truss structure and will house the majority of the components. The spun section includes the propellant tanks, thrusters, and the RTG booms. The propellant tanks are mounted as close to the center of mass as possible. Two thrusters are positioned on each side of the satellite with the RTG located on booms offset from the thrusters by 90 degrees. The spin linkage has a cylindrical shape and will connect the two sections together.

Using trade studies, the material for five different applications within the spacecraft was chosen. The columns and RTG booms both will be made of Al 7075-T6. The skin will be constructed of Al 6061-T6 and the fasteners will be made from Ti 13V-11Cr-3Al. The skin will also serve as a micrometeoroid shield. A material which will not expand under temperature changes is required for the antenna boom. This is accomplished by using a toughened graphite/epoxy composite boom with an almost zero coefficient of thermal expansion.

With the mass and volume of the satellite, it was found that the 2.9 m diameter payload fairing and the 3712C payload attach fitting will be used to affix the satellite to the third stage of the launch vehicle. This satellite will be launched on the three-stage Delta II 7925 model.

The cost budget of the structures/launch vehicle subsystem is \$14 million dollars (FY99). This does not include the cost of the launch vehicle, which is not considered part of the overall \$150 million budget. The structural mass of the satellite is approximately 202 kg, and the only power required is five watts for the BAPTA.

### 3.8 References

- [3.1] Aerospace 401A Project Description, The Pennsylvania State University, University Park, PA, Fall 1993.
- [3.2] Metals Reference Book, American Society for Metals, 1981.
- [3.3] Metals Handbook, American Society for Metals, 9th ed. Vol. 2, 1990
- [3.4] Strong, Dr. A. Brent, Fundamentals of Composites Manufacturing, Society of Manufacturing Engineers, Dearborn, Michigan, 1st ed., 1989, pp. 222-223.
- [3.5] Stella, Paul M., LEO Micrometeorite/Debris Impact Damage, California Institute of Technology, 1991.
- [3.6] Chetty, P. R. K., Satellite Technology and its Applications, 2nd. edition, TAB Professional and Reference Books, 1991, pp. 328, 333-334.
- [3.7] Isakowitz, Steven J., International Reference Guide to Space Launch Systems, American Institute of Aeronautics and Astronautics, Washington D.C., 1991, p. 205.
- [3.8] Commercial Delta II Payload Planner's Guide, McDonnell Commercial Delta, Inc., Huntington Beach, CA, 1990, p. 5-2.
- [3.9] Commercial Delta II Payload Planner's Guide, p. 3-5.
- [3.10] Commercial Delta II Payload Planner's Guide, p. 5-11
- [3.11] Commercial Delta II Payload Planner's Guide, P. 5-5

## **4.0 Power Subsystem**

### **4.1 Introduction**

This section details the design of the electrical power subsystem (EPS) for Project ECHO. Several parameters guided the design of the EPS. Project ECHO is a modified NASA Discovery-class mission subject to the following criteria: 1) the total mission cost must not exceed \$150 million, 2) launch must be achieved by a Delta class launch vehicle, and 3) the operational lifetime of the spacecraft must be ten to fifteen years, subject to the first two requirements. The propulsion system will utilize ion thrusters which will require a large amount of power in relation to the other satellite components as a whole. The peak power for ECHO is 1180 W. However, since the thrusters will use a reduced amount of power after achieving the L<sub>2</sub> orbit, the period of maximum power consumption will be during the transfer orbit and will require 1095 W.

Several topics are covered: methods of power generation are discussed, along with the current architectures of the power distribution and regulation schemes. Rationale is given for all decisions and the overall system design is summarized.

### **4.2 Power Source**

Two types of main power sources have been considered for ECHO, photovoltaic and radioisotope thermoelectric generators (RTG). Initially, the photovoltaic system was to be used in order to minimize overall system cost. However, the solar arrays needed to generate the power for the spacecraft tended to shadow the communications subsystem antenna. In light of this fact, the project integration team, in conjunction with the power subsystem team has decided on the use of an RTG system.

#### 4.2.1 Power Requirements

The power source will need to provide enough power to operate all functioning subsystems at any given time during the mission. The period of maximum power consumption will be during the transfer orbit and will require a power output of 1095 Watts. Two ion thrusters will be firing during this time and the spacecraft subsystems will be operating at reduced power levels. Once the spacecraft is inserted into the halo orbit, all subsystems will be capable of full operation throughout the orbit (with some exceptions). Since the projected lifetime of this mission is ten years, the low degradation over time of the RTG system further illustrates its advantage over a photovoltaic system.

#### 4.2.2 RTG Design

The RTG unit to be used will be of a modular nature in order to maximize performance and minimize cost. The RTG will be a General Electric MOD-RTG unit which was to have been flight ready by late 1993 [4.1]. This type of RTG has a much higher performance over the previous style, the general purpose heat source (GPHS), and has the added benefit of being configured to the specific needs of the mission. The MOD-RTG consists of a set of 18 GPHS units housed in a single module capable of producing 340 Watts of power [4.2]. These modules can then be connected together to provide power levels suitable for a given mission. Given a 1095 Watt maximum consumption requirement, four such modules will provide a total power output of 1360 Watts at 30.8 volts that will be converted to the standard 28 volts within the regulation unit. This output provides approximately a 4% contingency margin over the end of life (EOL) requirement.

Each module is 1.08 meters in length by 0.33 meters in diameter and has a mass of 42.2 kg. This corresponds to a total unit mass of 168.8 kg to be divided among two 1.6 meter booms attached to the satellite rotor to reduce thermal radiation and maintain symmetry (Figure 4.1). Two modules will be placed side by side on each boom for a total mass of 84.4 kg. The total mass of the RTG group is 53.4% of the total subsystem mass. Assuming a



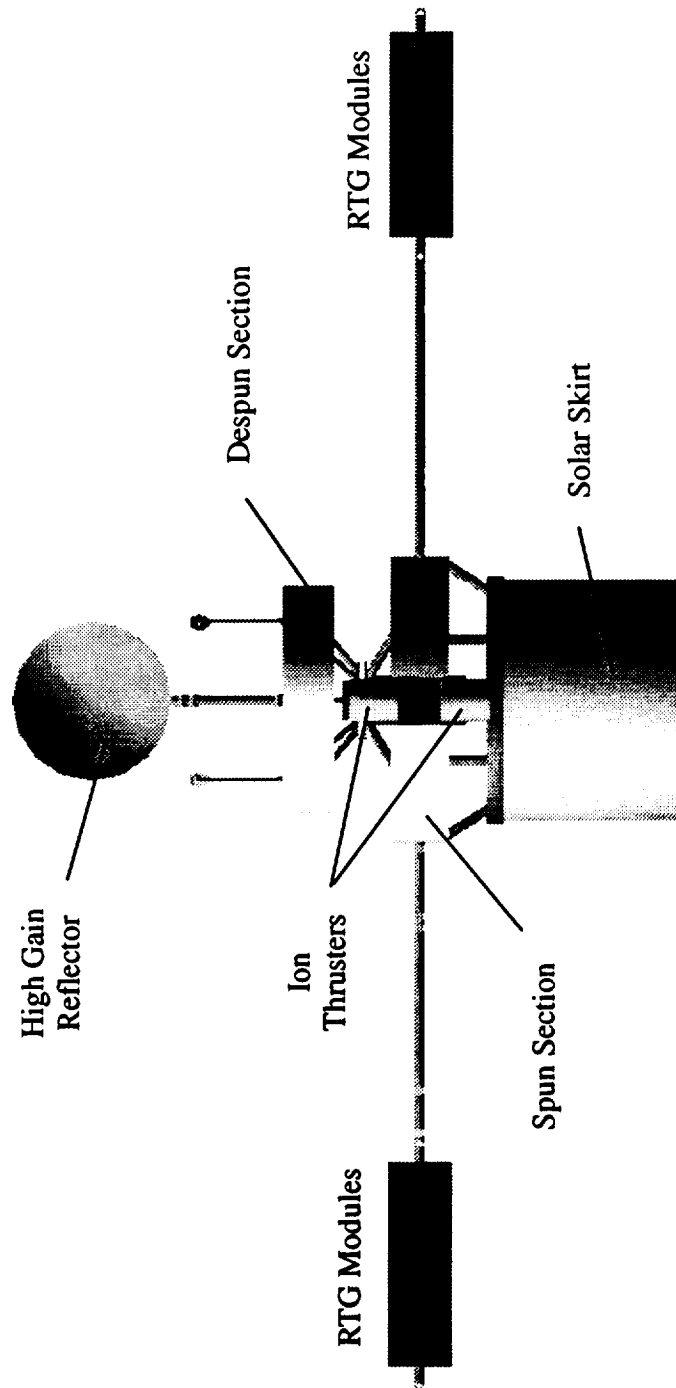


**Figure 4.1 Overall Configuration of the ECHO Spacecraft.**

specific cost of \$20,000 per Watt produced [4.3] the total cost for the RTG source itself will be \$33.5 Million FY99. Due to the high survivability of the MOD-RTG and low degradation rate, the power source is expected to operate at full capacity throughout the lifetime of the mission and possibly beyond. Table 4.1 shows the MOD-RTG design summary.

**Table 4.1 MOD-RTG Design Summary.**

Max Power Required (W)	1095
# of Modules	4
Total Power Output (Watts)	1360
Margin (% of Required)	+4
Module Mass (kg)	42.2
Length (m)	1.08
Diameter (m)	0.33
Total System Mass (kg)	168.8
Specific Cost (FY92)	\$20,000 / Watt
Total Cost (FY 99)*	\$33.5 Million

\* Accounting for 3%/year inflation

#### 4.3 Power Distribution

The power distribution system is unique to each satellite. It entails the spacecraft power bus, wiring or harness, power control circuits, and auxiliary control circuits. This apparatus is responsible for regulating the power supply to each component. The distribution system also has to isolate any faults in the satellite to prevent damaging any working parts.

##### 4.3.1 Power Bus-Bar

The satellite's power subsystem will regulate the power generated from the RTG into a standard voltage with which all the satellite's components are compatible. ECHO has a peak power requirement of 1180 Watts. The standard power bus-bar for a satellite this size is a 28 V-dc distribution bus. However, in the case that any number of components should require other than a 28 V-dc power regulation, the power bus will be able to further convert the supply. This regulation is accomplished in one of two ways: a centralized regulation approach (CRA) or a decentralized regulation approach (DRA). The centralized

approach places the power converters at each load end, separate from the main bus. The decentralized approach converts power within the bus-bar. A performance index, Equation 4.1, was assigned to choose the better method. Power dissipation, mass, and isolation are very important factors and have been weighted accordingly. Regulation compromise and cost have also been considered. The index values are: 1-lowest to 3-highest. Index values and results are shown in Table 4.2.

$$J = (.25)*\text{isolation} - (.20)*\text{mass} - (.20)*\text{pow. dis.} - (.20)*\text{comp.} - (.15)*\text{cost} \quad (4.1)$$

**Table 4.2 Trade Study Comparing CRA and DRA Systems.**

	Isolation	Mass	Pwr Dist.	Comp.	Cost	J
CRA	2	3	3	2	2	-1.4
DRA	2	1	1	1	1	-.25

This trade study shows that the decentralized regulation approach will best suit ECHO. Although both systems isolate faults equally, the CRA needs more electronics and parts. This results in a higher cost, mass, and power dissipation.

#### 4.3.2 Power Harness

The power generated by the RTG will be transferred throughout the satellite by means of the power harness. The geometry of the wiring is dependent upon the placement of the components within the satellite. The harness will pass through each of the symmetric booms upon which the RTG's are mounted. The harness will then run into the main power regulation unit, located in the spun section (Figure 4.2). The bus will then transfer the tailored loads to each component or through the bearing and power transfer assembly (BAPTA) into the despun section.

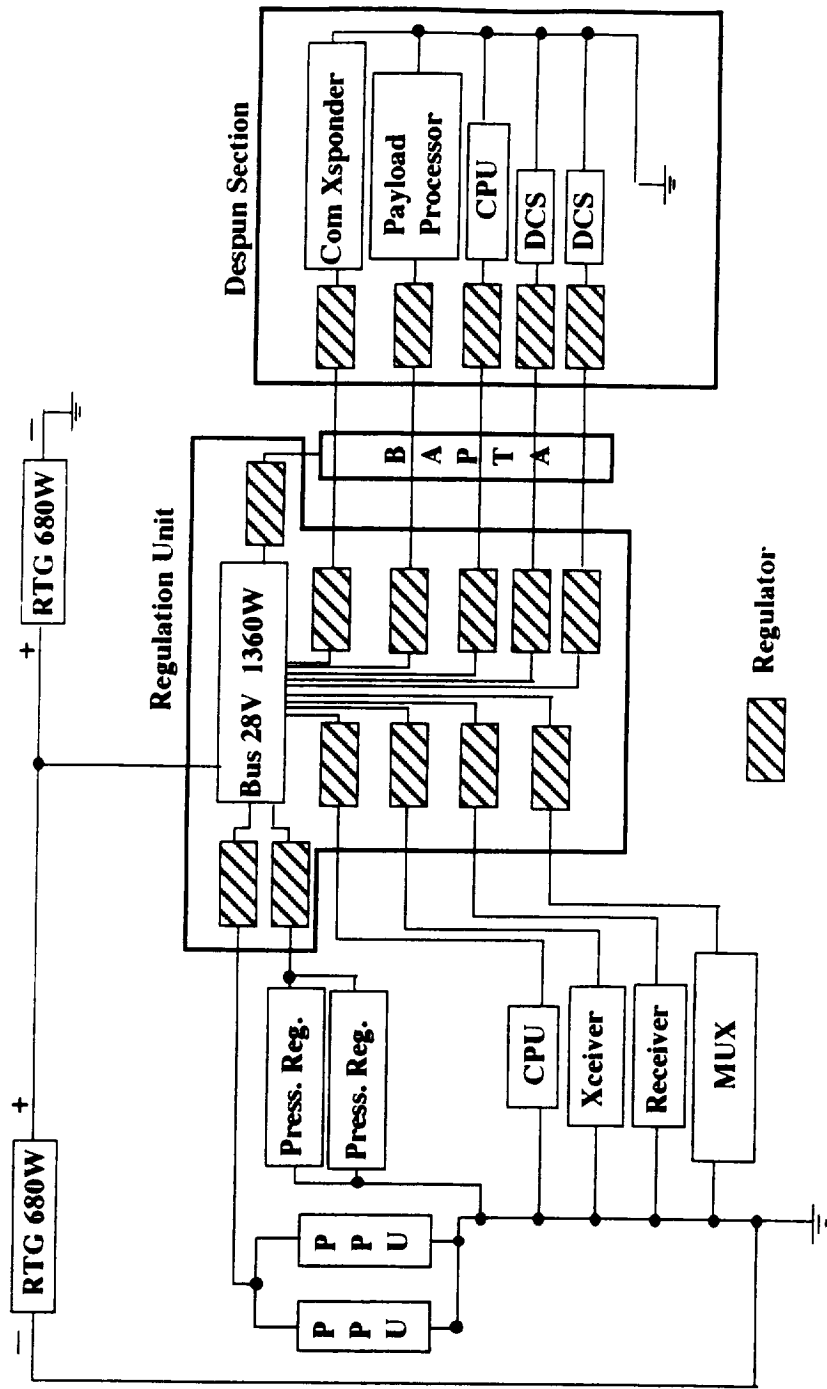


Figure 4.2 Power Harness.

Although electrical systems for spacecraft are similar to ground systems, there are certain constraints that must be observed. ECHO's power harness must be Teflon insulated as opposed to standard PVC because PVC is flammable, and the harness will be exposed to the heat generated by the RTG. It is also important to keep the harness as short as possible. This will reduce the voltage drop between the bus and the loads, thus reducing any electrical noise that may be generated. The shorter wiring also provides more accurate power regulation, as well as reduces the harness mass. The harness mass is taken as 20% of the subsystem's dry mass [4.4], or 47.8 kg. Line losses total 4% of the satellite's power, yielding a total loss of 47 W.

#### 4.3.3 Power Control Circuits

The power control circuits of the distribution system consist of on/off relays and fault protection. Their main function is to isolate active and non-active circuits from the rest of the EPS. For example, the ion thrusters will be switched off when orbital maintenance functions are not being carried out. Isolation is important because any transient behavior will create electrical noise which may interfere with the data links to the despun section or the BAPTA. There are two types of power relays from which to choose: electromechanical or solid-state. A performance index, Equation 4.2, was assigned to this study. Reliability, power dissipation, and cost were taken into consideration. The index values are: 1-lowest to 3-highest. Table 4.3 shows the indices and results of the trade study.

$$J = (.30)*\text{reliability} - (.30)*\text{power dissipation} - (.40)*\text{cost} \quad (4.2)$$

**Table 4.3 Trade Study Comparing Electromechanical and Solid-state Relays.**

	Reliability	Pwr Dist.	Cost	J
Electromech.	3	1	1	0.2
Solid-state	1	3	3	-1.8

From the trade equation, electromechanical relays better fit ECHO's design constraints. Power relays are a very common electrical device and there are many space proven types to choose from. The Potter & Brumfield electromechanical relays have a very high reliability and can withstand a 150g shock [4.5]. Of these relays, the Potter & Brumfield FCH and HC series are the best choice for ECHO's mission because they operate in a 28 V-dc power flow. A performance index, Equation 4.3, was assigned to choose the better isolation relay. Power dissipation, size, mass and reliability were taken into consideration. The index values are: 1-lowest to 3-highest. Index values and results are shown in Table 4.4. From the trade equation, the HC power relay better fits ECHO's design parameters.

$$J = (.20)*reliability - (.30)*size - (.30)*mass - (.20)*power\ dissipation \quad (4.3)$$

**Table 4.4 Trade Study Comparing FCH and HC Electromechanical Relays.**

	Reliability	Size	Mass	Pwr Dist.	J
FCH	3	3	3	1	-1.3
HC	3	1	1	1	-0.2

Fault protection in the power distribution system consists mainly of fuses connected in parallel with the power harness. In the event of a short circuit, the fuses will isolate the

load from the rest of the EPS. A failed load, if not properly isolated, can draw excess power, stress the cabling, or damage working parts in the satellite.

#### 4.3.4 Power Auxiliary Circuits

The power system auxiliary control circuits are mainly for monitoring the power flow and interface with the telemetry link to the ground control. The components of the auxiliary system consist of current and voltage sensors. These will monitor the power flow to each of the satellite's components. The auxiliary circuits also interface with the telemetry channel of the communications subsystem. This enables the satellite to transmit necessary information for monitoring the status of the power system. It also includes circuits to receive switching commands from the ground to operate the power relays. These monitoring circuits alert the ground station of power failures and regulation problems.

#### 4.4 Power Regulation

The power regulation hardware is responsible for providing the spacecraft's electronic components with clean electricity at a given voltage and current capacity. All regulation equipment will be installed with a single level of redundancy. The regulation hardware is estimated to have a mass of 36.6 kg; a cost of \$0.1 million FY99; and a volume of 0.019 m<sup>3</sup>. Losses due to regulator efficiencies total 206 W [4.6].

##### 4.4.1 Bus Input Regulation

Power generated by an RTG is generally stable in voltage and current output. Since the RTG provides 30.8 V-dc, a step down regulator within the bus will be used to provide the power bus-bar with the 28 V-dc input that it requires.

A Direct Energy Transfer (DET) scheme will be used to transmit the necessary power to the bus-bar. Unused power will be dispersed as heat through a bank of shunt resistors. The DET scheme is extremely efficient (greater than 80%). As a consequence of this high

efficiency, electrical noise and line losses will be minimized, thereby reducing the size and mass of the regulation equipment.

#### 4.4.2 Component Regulation

The ECHO power system will have a decentralized architecture - regulation for the loads (the spacecraft components) will, to the greatest extent possible, be performed at the bus itself. The primary advantage of this architecture is mass centralization and reduction within the spacecraft, which could be significant in maintaining the mass centroid of the satellite. Further regulation may be necessary at specific loads requiring highly conditioned electrical power, and a second non-redundant main regulator will be necessary in the despun section to correct for electrical noise generated across the BAPTA. The regulators themselves vary in nominal efficiency from 85% to 95% [4.7].

#### 4.4.3 Power Regulation Hardware

The power regulation hardware for Project ECHO will be the Arnold Magnetics EL-2000 series of DC-DC modular power supplies [4.7]. This series of power regulators was chosen because these regulators are space qualified and flight tested in LEO. Because of the Van Allen radiation belts, radiation effects are more intense in LEO than in deep space, where the Project ECHO satellite will operate; it is therefore assumed that the EL-2000 series will perform well in the L<sub>2</sub> orbit. Operating specifications are summarized in Table 4.5.

**Table 4.5 Some Specifications for Arnold Magnetics EL-2000 Series Power Regulators.** (*Electronics Engineers Master Catalog 93-94*, Vol. D, Hearst Business Communications, Inc., Garden City, NY, 1993, p. 1587.)

Operating Temperature (baseplate)	-40°C to +85°C
Storage Temperature	-65°C to +100°C
Acceleration Tolerance	Up to 14g
Vibration Tolerance	Up to 15g
Shock Tolerance	Up to 40g



More detailed information on the EL-2000 series may be found in *Electronic Engineers Master Catalog 93-94* [4.7]. The following options will be included in the hardware:

- EXTENDED INPUT VOLTAGE on bus bar input regulator (located between RTGs and power bus-bar).
- INPUT TRANSIENT PROTECTION for all components to prevent damage by transient power spikes at circuit closure.
- OVER-TEMPERATURE SHUTDOWN on all regulators to prevent damage to the regulators themselves.

#### 4.5 Budget Summary

The budgets of each major section of the EPS are shown in Table 4.6.

**Table 4.6 Final Subsystem Design Budget Estimates.**

Section	Mass (kg)	Cost (\$M,FY99)	Volume (m <sup>3</sup> )	Power (W)
RTG	169	32.9	0.37	0
Distribution*	47.8	0.1	0.02 to 0.05	47
Regulation	36.6	0.1	0.019	159
<b>Total</b>	<b>253.4</b>	<b>33.1</b>	<b>0.409 to 0.439</b>	<b>206</b>

\* - denotes estimated values

The power distribution to each subsystem is listed in Table 4.7. During the transfer orbit, propulsion and GNC will be at full power, while the rest of the subsystems will draw no power or will be at a reduced power level.

**Table 4.7 Subsystem Power Requirements.**

Subsystem	Power Requirement (W) (Transfer Orbit)	Power Requirement (W) (Normal Operations)
Communications	15.0	85.0
Thermal	90.0	42.0
GNC	22.0	22.0
Power	206.0	206.0
Structures	—	15.0
Propulsion	1000.0	0.0
C & DH		58.2
<b>TOTAL</b>		<b>428.2</b>

#### 4.6 Conclusion

ECHO's power system will consist of four General Electric MOD-RTG Radioisotope Thermoelectric Generator units providing a total power of 1360 Watts. These units will be divided between two 1.6 m booms extended from the spacecraft rotor. The distribution system will use a 28 V-dc power bus and will use electromechanical power control circuits to isolate those loads which are not drawing power.

Power regulation will be provided with a single level of redundancy. Since the power source will be an RTG, a Direct Energy Transfer scheme will transmit the necessary power to the bus-bar with unused energy being dispersed as heat through a shunt resistor bank. The regulation for each individual load will be performed at the bus itself with additional regulators located in the despun section to correct for electrical noise generated across the BAPTA.

The ECHO power system has been designed for a lifetime of fifteen years, however the actual operational lifetime is expected to exceed this period given the high survivability and low degradation rates of the subsystem's components.

## 4.7 References

- [4.1] Hartman, Robert F., "Modular RTG Technology Status," *IECEC Proceedings 1990*, Vol. 1, p. 237.
- [4.2] Hartman, p. 235.
- [4.3] Wertz, J.R. and W.J. Larsen, eds., Space Mission Analysis and Design, Second ed., Microcosm, Inc., Kluwer Academic Publishers, Norwell, MA, 1991, p. 393.
- [4.4] Wertz, p. 405.
- [4.5] *Potter & Brumfield General Stock Catalog*, Potter & Brumfield, A. Siemen Co., Princeton, IN, 1988, pp. 71-72.
- [4.6] Telephone conversation with Philip Kite, Sales representative, Arnold Magnetics Corporation, Camarillo, CA, 8-April-1994.
- [4.7] *Electronic Engineers Master Catalog, 93-94*, Vol. D, Hearst Business Communications, Inc., Garden City, NY, 1993, pp. 1587-1588.

## 5.0 Thermal Control Subsystem

### 5.1 Introduction

The thermal control of a spacecraft is driven by the particular mission and the design of the spacecraft. Thermal effects, as a result of the satellite's position in the space environment, are determined by the mission. Design of the spacecraft influences its thermal performance from the perspective of component placement, power dissipated, thermal coating, and structural material. For the purpose of designing ECHO's thermal subsystem, the design process has been divided into two sections. The goal of the spun and despun sections is to keep all components of the spacecraft operating in a temperature range of 0 °C to 40 °C by totally passive thermal control [5.1]. The results of the calculations show this is not possible. During the early part of the mission lifetime, some heating will be required to maintain thermal control of the satellite within the allowable temperature range. Heat transfer between the spun and despun sections has been neglected. The third design consideration concerns launch cooling. The use of RTG's as the power source for the spacecraft has necessitated the placement of a disposable heat shield between the satellite and the RTG's to protect the satellite while in the Delta fairing.

All of the satellite temperature calculations were accomplished by modeling the satellite as a flat plate. In the calculations, the projected area of a cylindrical section was used to determine the incident power and the total surface area of the satellite was used to determine the radiated power. Temperature contribution from the Moon is so small that it may be assumed negligible [5.2]. Thus, the IR flux from the Moon is not included in any calculations. Heat shield calculations also model the satellite and RTG's as plates.

## 5.2 Theory

Using the blackbody radiation equations for flat plates, the steady state temperature ranges for each section of the satellite were determined [5.3]. The equation used to find the worst case hot temperature was:

$$T_{max} = \sqrt[4]{\frac{G_s A_{proj} \alpha [1 + a_e K_a \sin^2 \rho_e + a_m K_a \sin^2 \rho_m] + q \epsilon A_{proj} \sin^2 \rho + Q + P_{inc}}{\sigma \epsilon A_{tot}}} \quad (5.1)$$

and the equation used for the worst case cold temperature was:

$$T_{min} = \sqrt[4]{\frac{q \epsilon A_{proj} \sin^2 \rho + Q + P_{inc}}{\sigma \epsilon A_{tot}}} \quad (5.2)$$

where	$G_s$	=	solar constant = 1363 W/m <sup>2</sup>
	$q$	=	Earth IR emission = 237 ± 21 W/m <sup>2</sup>
	$a_e$	=	Earth albedo = 0.3
	$a_m$	=	Moon albedo = 0.067
	$Q$	=	electrical power dissipation
	$P_{inc}$	=	incident power from each RTG
	$s$	=	Stefan-Boltzmann constant = 5.67x 10 <sup>-8</sup> W/m <sup>2</sup> K <sup>4</sup>
	$a$	=	solar absorptivity
	$e$	=	IR emissivity
	$r_e$	=	angular radius of the Earth = 0.014
	$r_m$	=	angular radius of the Moon = 0.0262
	$K_a$	=	accounts for reflection of collimated incoming solar energy off a spherical Earth = 0.664 + 0.521r - 0.203r <sup>2</sup>
	$A_{proj}$	=	projected area of the section
	$A_{tot}$	=	total surface area of the section

In the calculations, the projected area of the cylindrical section was used to determine incident power, while the total surface area of the section was used to determine the radiated power.

In order to determine the length of the RTG booms and the incident power on the satellite from the RTG's, the following equation was employed [5.2]:

$$P_{inc} = \alpha \sigma T^4 a \frac{A_{proj}}{4\pi D^2} \quad (5.3)$$

where  $T$  = surface temperature of RTG = 1000 K  
 $a$  = total surface area of RTG = 2.24 m<sup>2</sup>  
 $D$  = distance between RTG and spacecraft (boom length)

The average temperature of the satellite will increase because of the close confinement of the main body with the RTG's in the stowed position inside the fairing during launch. There will also be hot spots on the satellite adjacent to the RTG's. In order to find this increase in temperature the following equation was used [5.4]:

$$\Delta T = \frac{Q}{[\rho V c]_{sat}} \Delta t \quad (5.4)$$

where  $Q$  = 14000 W  
 $c$  = 875 J/kg·K  
 $\rho V$  = 1000 kg

The temperature of the hot spots was calculated using:

$$T_{sat} = \sqrt[4]{\frac{Q}{\epsilon \sigma} + T_{RTG}^4} \quad (5.5)$$

where  $T_{sat}$  = temperature of the hot spot  
 $T_{RTG}$  = surface temperature of each RTG

Heat shields and MLI are necessary to protect ECHO against the formation of these hot spots. In order to determine the number of layers necessary in the heat shield, the following equations were used [5.5]:

$$q = \sigma F_e [T_1^4 - T_0^4] \quad (5.6)$$

$$F_e = \frac{1}{\frac{1}{\epsilon_1} + \frac{A_1}{A_0} \left[ \frac{1}{\epsilon_0} - 1 \right]} \quad (5.7)$$

where

$q$	=	heat conducted between plates
$F_e$	=	emittance factor
$\epsilon_1$	=	emissivity of plate #1
$\epsilon_0$	=	emissivity of plate #0
$A_1$	=	area of plate #1
$A_0$	=	area of plate #0
$T_1$	=	temperature of plate #1
$T_0$	=	temperature of plate #0

By repeating these calculations for each additional plate, the desired value for  $q$  and the number of plates that are necessary can be obtained.

### 5.3 Launch Cooling

Using RTG's as the power source for ECHO presents a thermal control problem for the satellite while in the fairing. The Delta rocket has an integral cooling system which will keep the payload at a specified temperature while it is on the launch pad. This system is capable of maintaining an isothermal environment within the launch shroud at a temperature of 273 K [5.8]. However, the RTG's must be activated prior to launch. It has been assumed that each RTG module operates at an external temperature of 600 K. At this temperature, the spacecraft will receive approximately 34 kW/m<sup>2</sup> of incident power flux. This corresponds to the external temperature of the spacecraft hot spots of approximately 450 K. This temperature is clearly unacceptable. To solve this problem, a heat shield has been designed consisting of a series of five parallel plates. A Teflon coated MLI 40-layer blanket is attached to the shield closest to ECHO. Each RTG module will require its own heat shield.

The plates will consist of polished steel (AM 450) which has an emissivity ranging from 0.2 to 0.095, depending on the temperature of the plate [5.6]. Two posts will connect the plates of the shield together. These posts will be made of stainless steel coated with black paint to minimize conduction between plates and are attached to the RTG booms by spring loaded latches. Each plate has the same surface area as an RTG module,  $0.96 \text{ m}^2$ , and an average thickness of 5 mm. Plates closer to the RTG's will be thicker than those closer to ECHO to allow for more heat storage at higher temperatures. This spacing will also compensate for any material problems encountered at higher temperatures. The temperature drop across the thickness of the plates has been neglected, as well as any conduction between the plates. To compensate for any error that may be incurred by these assumptions, a 40-layer MLI blanket ( $e_{\text{eff}} = 0.015$ ) was added to the last plate [5.7]. With this configuration, the total heat transfer to ECHO is anticipated to be approximately  $1 \text{ W/m}^2$  at a satellite temperature of 300 K. This amount of heat being transferred should not appreciably increase the temperature of the satellite. The basic construction of the shield and the temperature drops from plate to plate are illustrated in Figure 5.1.

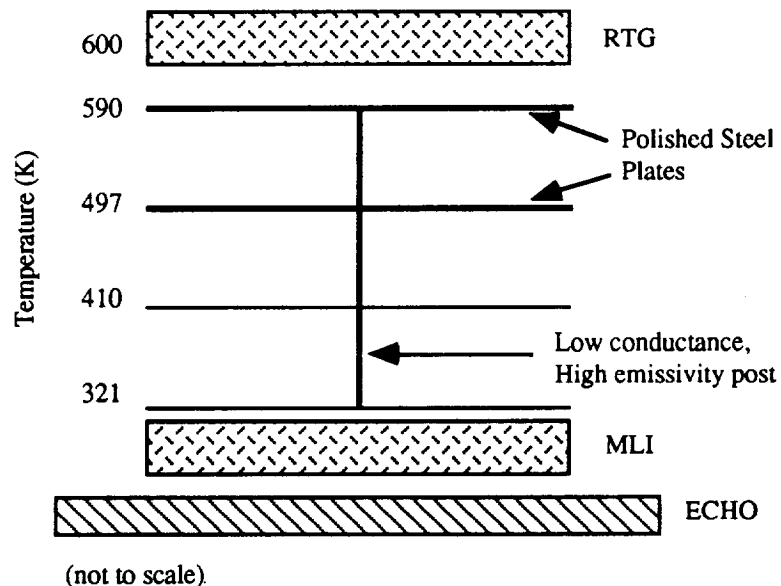


**Figure 5.1 Heat Shield Schematic.**



The heat shields are required only for the first five minutes during launch. The shield will be discarded by means of the spring loaded latches after the spacecraft emerges from the launch shroud and the RTG's are fully deployed.

#### 5.4 Spun Platform

The optimal temperature range for this section is 5° C to 25° C [5.8]. This is the prescribed temperature range with a 5° C safety margin. Components located in the spun section with their respective temperature ranges include thrusters and a power regulator (-65° C to 85° C), power processing units (0° C to 40° C), a computer (0° C to 40° C), propellant (-60° C to 30° C), and structures (-45° C to 65° C). An upper and lower temperature range for the entire section is limited by the propellant and electronics, respectively. An operating temperature range for the thrusters is unavailable at this time, but it is assumed they maintain their own proper range as they are mounted outside of the satellite.

Use of radiators and mechanical louvers was ruled out due to their added cost, weight, and complexity. ECHO will be thermally controlled with heaters installed beside critical components. These heaters will use the extra power produced by the RTG's. The following trade study shows the basis for choosing a type of thermal control system:

$$J = (0.2 * \text{Power}) + (0.2 * \text{Complexity}) + (0.4 * \text{Mass}) + (0.4 * \text{Cost}) \quad (5.8)$$

**Table 5.1 Thermal Control Trade Study.**

	Power	Complexity	Mass	Cost	J
Heaters (cold bias)	5	2	1	1	2.2
Radiators	1	3	2	2	2.4
Mechanical Louvers	2	4	3	2	3.2

Use of heaters has the lowest performance index, therefore, this choice best meets the criteria. Power was given a low weight value in the trade study because there is expected to be excess power produced by the RTG's. Mass and cost were given high weight values due to the stringent requirements in these budgets. Complexity was factored in to account for problems which may arise late in the mission and to account for a more complex system which has a greater likelihood of failure than a simple system.

#### 5.4.1 Thermal Coatings

Two different coatings, bare unpolished aluminum on the side and top, and silverized teflon on the bottom, were chosen for the outer coating of ECHO's spun section to provide the best environment for the internal components. An advantage of this coating scheme is that the thermal properties will not degrade appreciably over the life of ECHO to change the temperature ranges. As Figure 5.2 shows, the spun section is maintained at 24.6 °C with full solar flux and full power. This temperature drops to 6.5 °C when the thrusters are shut off, but is still within the prescribed temperature range. While ECHO is in eclipse, the temperature range, -44.5 °C to -14.4 °C, will be below the required limits. ECHO will be thermally controlled with heaters at this time.

The only components which will need to be heated are the computer and power processing unit (PPU). Each component can be maintained at a safe temperature while at full power if they are given the proper thermal coating. For example, the PPU, at full power, will be maintained at 25 °C if it is cased in a bare steel box or given a paint scheme with a total emissivity of 0.267. But, it will require heaters dissipating 90 watts of heat while it is shut off, such as during eclipse. This is a rare situation, but one that must be considered. The computer will always be operating at full power, so an appropriate thermal coating for safe temperatures is all that is needed. All of the other components can withstand the temperature drop to -44.5 °C.

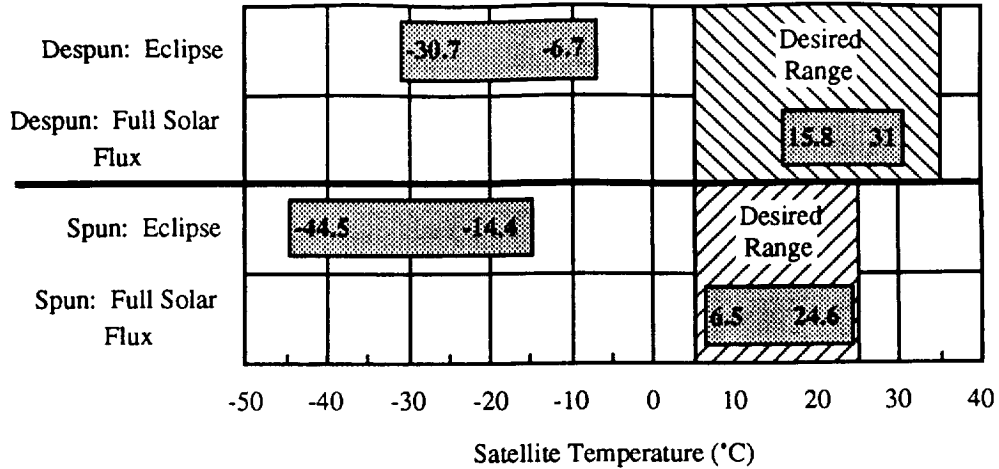


**Figure 5.2 Satellite Temperature Ranges.**

#### 5.4.2 Truss

Another component on the spun section is the payload attachment truss. The truss is made of aluminum, which suffers from large thermal expansion. If the truss is left uncoated, a temperature range of 32 K to 613 K would be experienced. Although the truss is not used after launch, its enormous expansions and contractions can prove troublesome to the remainder of the satellite. The truss would also absorb a great quantity of heat from the RTG during launch which could weaken it during the high-stress launch phase. To counter this problem economically, the truss will be painted with white epoxy. This will provide a temperature range of 32 K to 275 K. Although this is not an extremely narrow range, it is more reasonable and will minimize the expansions and contractions.

#### 5.4.3 RTG Thermal Concerns

Each of the four RTG units radiates 3500 W of power and the internal temperature of the RTG's is 1273 K [5.8]. If too much of this power is absorbed by the satellite, serious thermal problems can result. This heat can also be used to stabilize the temperature extremities during eclipse phases. An appropriate boom length had to be selected to keep the

RTG's far enough away from the satellite so it would not overheat. A boom length of 1.6 meters was determined to meet this criterion, as well as the requirements of the GNC and structures subsystems. A description of the theory used in the power impingement calculations is found in Section 5.2.

### 5.5 Despun Section

The despun section houses the communication, GNC and C&DH components. Because these components are electronics, a temperature range maintained between 0 °C to 40 °C is required in order to prevent problems or failures with these components [5.1]. Factoring in a safety margin, the desired temperature range became 3 °C to 35 °C. This temperature range is maintained using a silverized teflon and bare unpolished aluminum as thermal coating and heaters. The silverized teflon will be on the top of the despun section, and the bare unpolished aluminum is on the side and the bottom of the section.

Calculations, using thermal radiation theory, were made to find temperatures for the worst case hot and cold, and temperatures with maximum and minimum power experienced by the despun section at various times in the life of ECHO. For these calculations, the boom length was 1.6 meters, maximum power dissipated was 125 W, and minimum power dissipated was 55 W. Silverized teflon and unpolished aluminum were chosen as the thermal coatings for the despun section because they allowed for temperatures which were within the required range. Because most of the despun section is coated with unpolished aluminum, BOL and EOL temperatures are the same. The temperatures for eclipse could be maintained within the allowable range with the use of heaters. Worst case cold and hot temperatures were found to be 242.3 K and 304 K, respectively, and the minimum and maximum power temperatures were found to be 266.3 K and 288.8 K, respectively.

Since eclipse temperatures are not within the prescribed limits, heaters are needed to maintain the required temperature. Heaters will not be required at all other times since these temperatures are within the prescribed limits. The worst case cold temperature will be

experienced when ECHO is in eclipse and possibly in the transfer orbit, depending on the orientation of the spacecraft during this time. If the spun section is facing the Sun in the transfer orbit, the spun section will completely block the despun section from the Sun since the spun platform is larger than the despun platform. In eclipse at minimum power, the despun section requires 112 W of dissipated power to maintain a temperature within the allowable range. The maximum power with the current components is 125 W and minimum power is 55 W. The thermal control for the despun section requires an additional 42 W of power with maximum power dissipated and 112 W of power with minimum power dissipated. Therefore, heaters producing 112 W will be needed in order to maintain the required temperature range for the components in the despun platform.

## 5.6 Budgets

The total mass, power, and cost budgets are presented below in Table 5.2. All costs are estimated in 1999 dollars. The power figure is representative of the BOL and will decrease as the mission lifetime increases.

**Table 5.2 Thermal System Budget**

Item	Mass (kg)	Power (watts)	Cost (M\$)
Heat Shield	79.4	0.0	1.0
Silverized Teflon	6.0	0.0	0.5
Unpolished Aluminum	4.0	0.0	0.5
Heaters	5.0	202.0	0.05
Sensors	2.6	1.0	0.01
<b>TOTAL</b>	<b>97.0</b>	<b>203</b>	<b>2.1</b>

## 5.7 Conclusion

A temperature range of 5 °C to 35 °C was defined for the despun platform and a range of 5 °C to 25 °C was selected for the spun section. To maintain these safe operating temperature ranges, ECHO will have a cold-biased thermal control system that utilizes a total of 202 W for heaters. Temperatures at BOL and EOL are the same since bare, unpolished aluminum does not degrade. Three different coatings will be employed. The despun section will use silverized teflon and unpolished aluminum, while the spun section will use unpolished aluminum and white epoxy. ECHO's truss will be coated with white epoxy to decrease thermal expansion in space and maintain structural integrity during launch. Before launch the Delta II's air conditioning unit will cool the satellite, but for five minutes during launch before separation from the fairing, a heat shield placed between the RTG's and satellite will prevent hot spots from forming on the satellite. This heat shield will consist of seven separated layers of steel and one 40 layer section of MLI. After separation from the fairing, the RTG's will be deployed on 1.6 meter long booms to separate them from the satellite during the mission.

## 5.8 References

- [5.1] Wertz, J.R. and W.J. Larsons, eds., Space Mission Analysis and Design, Kluwer Academic Publishers, Norwell, MA, 1991, p. 411.
- [5.2] Aerospace 401 Class Notes, The Pennsylvania State University, University Park, PA, Spring 1994.
- [5.3] Wertz, pp. 423-424
- [5.4] Incropera, Frank, and David Dewit, Fundamentals of Heat and Mass Transfer, John Wiley and Sons, New York, NY, 1990, p. 15, 228.
- [5.5] Van Vliet, Robert M., Passive Temperature Control in the Space Environment, Macmillan Company, New York, NY, 1965, pp. 78-79.

- [5.6] Wertz, p. 425.
- [5.7] Telephone correspondence with Brent Anderson, Sheldahl, Inc., Northfield, Minnesota.
- [5.8] Aerospace 401 Integration Notes, The Pennsylvania State University, University Park, PA, Spring 1994.
- [5.9] Fax transmission from Sheldahl, Inc., Northfield, Minnesota.

## 6.0 Propulsion Subsystem

### 6.1 Introduction

The propulsion subsystem is one of the vital components necessary for the successful completion of Project ECHO. This section will explain the various selection criteria that were used to design the propulsion system, as well as how the design will affect the mission as a whole. The subsystem has three main responsibilities: 1) completion of translunar orbit, 2) halo orbit injection upon the reaching  $L_2$  point, and 3) routine stationkeeping and attitude control duties. There are several important characteristics that are critical to the decision making process. The most important of these are power consumption, system and propellant mass, durability, and cost.

An electrical propulsion system should be selected that will require a low amount of power. A reduction in lifetime power consumption is possible by using a stationkeeping-free orbit about the  $L_2$  point. Because the main consumer of power is the electric thruster, any decrease in needed power will lower the number of radioisotope thermoelectric generators (RTG's) that are needed, thereby decreasing the mass. Also, by decreasing the number of RTG's needed, the waste heat generated will be decreased, simplifying the design of the thermal system.

Another important feature of a propulsion system is low system and propellant mass. Electric thrusters are very small and light when compared to other more conventional chemical systems. In addition, the propellant required to operate an ion thruster is dramatically smaller than the same amount that would be necessary for a chemical system, due mostly in part to the extremely high exit velocity of the ions. However, the ion thruster also produces a much lower thrust than chemical systems.

The last two characteristics of the propulsion system, durability and cost, are often seen as opposing forces in design. Most often increased durability will require an increase in cost. For Project ECHO the durability of the satellite was deemed to override the need to



keep cost down, while still remaining within the allotted total budget of \$150 million. This durability is necessary to ensure that the mission will remain productive for a minimum of ten years.

The design of the propulsion system followed a set pattern. First the type of thruster that would be used was chosen, followed by where on the satellite the thrusters should be placed to provide attitude control and stationkeeping duties. Next, the propellant that would be used to provide the thrust was selected. Once the propellant was chosen, a tank to hold the propellant had to be designed, including a type of pressurization system to keep the pressure within the tank constant. The last part of the design involved examining how the propulsion system design would affect other subsystems, and how the design could be changed to make the overall design of the satellite more efficient.

## 6.2 Propulsion System Design Overview

The following section discusses the component selection for the propulsion system of ECHO. It will also provide the reasoning behind those same selections. Trade studies were used to select the best option for a given component, resulting in the final design.

### 6.2.1 Propulsion System Determination

From the beginning of the detailed design phase for Project ECHO, it has been established that a low-thrust propulsion system would adequately meet the requirement for the mission. The most researched and flight-proven low-thrust systems are electric propulsion systems. Therefore, the following section outlines the determination of an electric propulsion system best suited for ECHO.

There are many criteria used when choosing a propulsion system for a given mission; the most important are the power required for operation, the system and propellant mass, and the overall system performance. However, reliability is a predominant trait that must be present in the final propulsion system design for ECHO. This is because the project has been

designed for a ten year operational lifetime. With this in mind, the following Equation 6.1, has been developed for use in calculating the performance index, J, for each propulsion system being considered:

$$J = (0.25)*Performance - (0.30)*Risk - (0.10)*System\ Mass - (0.20)*Propellant\ Mass - (0.15)*Power\ Required \quad (6.1)$$

Based on this relationship, the system with the greatest value for the performance index would be the best choice for the specific mission requirements. A trade study shown in Table 6.1 compares four types of electric propulsion systems: ion propulsion (electrostatic), arcjets (electrothermal), resistojets, and magnetoplasmadynamic propulsion. A trade value of one through four was assessed to each system in five different categories. A value of one was considered the lowest, or worst, value and four was considered the highest, or best, value for each respective category.

**Table 6.1 Trade Study on Electrical Propulsion Systems.**

System	Performance	Risk	System Mass	Propellant Mass	Power Required	J
Ion Propulsion	4	1	4	1	3	-0.35
Arcjet Propulsion	4	2	1	2	3	-0.55
Resistojet	4	3	2	3	3	-1.15
Magnetoplasmadynamic	4	4	3	2	3	-1.35

The above table indicates that the ion propulsion system (IPS) is the best possible choice for ECHO based on the mission specifications. The thruster chosen for ECHO is the Hughes Research Laboratories 13 cm ion thruster. This decision was based on the thruster's space proven reliability, long life expectancy, and a thrust output in the range appropriate for ECHO. Each thruster is capable of providing 17.8 mN of thrust at a peak input power of

439 W [6.1]. The  $I_{sp}$  of the thruster is 2585 sec, and the overall thruster efficiency is 51% [6.2].

To provide the power to each thruster, three power processor units (PPU) will be used. Each PPU will receive power directly from the power bus and from there transfer it to a thruster. The PPU's require an input power of 500 W and have an operational efficiency of 88% [6.3].

### 6.2.2 Thruster Positioning

Any thruster positioning scheme should provide for movement of the satellite along all three principal axes as well as provide some level of redundancy to the system as a whole. Figure 6.1 displays the thruster configuration to be used for ECHO. This scheme not only provides degrees of freedom along all three principal axes, but also allows for some level of redundancy for the propulsion system. To further explain, there are two pairs of thrusters located on the side of the spun section. These thrusters are mounted on a titanium plate (or turntable) that is in turn connected to a stepper motor. This allows the thrusters to be rotated  $360^\circ$  in a plane parallel to the spacecraft longitudinal axis. The Hughes Research Laboratory thrusters are also capable of being gimballed  $90^\circ$  in the plane perpendicular to the spacecraft longitudinal axis. This combination allows for motion of the satellite in all three principal directions. Because the thrusters can be gimballed  $90^\circ$ , as well as rotated  $360^\circ$ , each thruster can fire in the same directions, which will provide a single level of redundancy.

The PPU's are also placed in the spun section. The PPU is used to step up the voltage received from the power bus, to the amount that required by various components within the thruster. Each thruster will be directly wired to two of the PPU's by means of cross-strapping. This arrangement allows for a single level of redundancy in the event that one of the power processor units experiences difficulties.

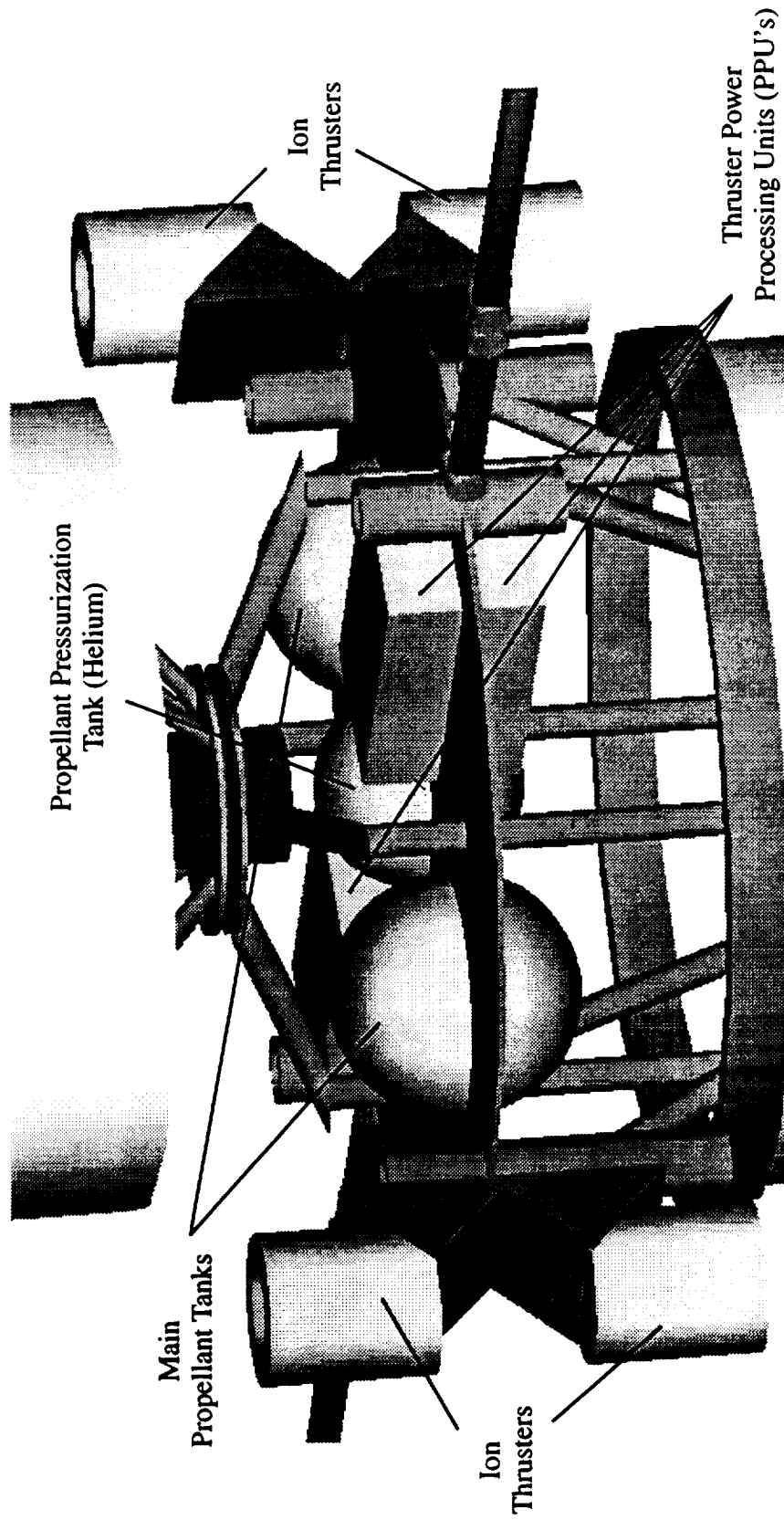


Figure 6.1 Propulsion Components Configuration.

### 6.2.3 Propellant Selection

For an electric ion thruster, the optimum propellant must have a high ion mass, high specific charge, high ionization potential and a manageable storage size and temperature. However, only certain propellants can be used with an ion thruster: argon, cesium, helium, hydrogen, hydrazine, krypton, mercury, and xenon. Cesium was immediately discarded because of the corrosive nature of the gas. Hydrazine, helium, and mercury were also eliminated from consideration because they are corrosive materials with cryogenic storage temperatures that would be too difficult to maintain.

The molecular properties of the three remaining gases are given in Table 6.2, with the relative masses and sizes of the corresponding propellant tanks given in Table 6.3.

**Table 6.2 Specification of Possible Propellants.** (Hill, Philip G., and Carl R. Peterson, Mechanics and Thermodynamics of Propulsion, Addison-Wesley Publishing Company, New York, NY, 1992, p. 659).

Propellant	Mass (10E-25 kg)	q/m (10E5 C/kg)	1st Ionization Potential (eV)
Argon	0.66	24.13	15.80
Krypton	1.39	11.50	14.00
Xenon	2.18	7.34	12.13

**Table 6.3 Tank Mass and Size for Prospective Propellants.** (Rawlin, V.K, M.J. Patterson, and R.P. Gruber, "Xenon Ion Propellant for Orbit Transfer," AIAA-90-2527, NASA Lewis Research Center, p. 22.)

Propellant	Tank Mass Fraction	Tank Radius (m) for 1041 kg
Argon	0.75	0.49
Krypton	0.27	0.62
Xenon	0.14	0.82

Using this information, and the performance index,

$$J = (0.20)*\text{Ion Mass} - (0.25)*\text{Specific Charge} + (0.10)*\text{Storage Temperature} - (0.25)*\text{Ionization Potential} + (0.20)*\text{Storage Size} \quad (6.2)$$

xenon was selected as the best propellant for this mission. This selection can be confirmed from examination of Table 6.4. A trade value between one and four was assessed to each propellant for five different characteristics. A value of one is considered the lowest value and four is considered the highest value for each category. The highest J value is the best choice for this trade study.

**Table 6.4 Trade Study of Ion Thruster Propellants.**

Propellant	Ion Mass	Specific Charge	Storage Temperature	Ionization Potential	Storage Size	J
Argon	1	4	1	2	1	-1.0
Krypton	3	3	4	3	3	0.1
Xenon	5	2	4	4	5	0.9

The selection of xenon will allow for a small tank radius to minimize space and mass. The amount of propellant that is needed for ECHO was determined based on the  $\Delta V$  requirements for the translunar orbit to the halo orbit, attitude adjustments, and stationkeeping once in the halo orbit. By knowing that after separation from the third stage the translunar orbit will require 147.52 m/s and attitude adjustment and stationkeeping require an estimated of 121.92 m/s per year [6.6], an estimation of the required propellant mass is found from

$$\Delta m = M_i \left( 1 - e^{-\Delta V/V_e} \right) \quad (6.3)$$

where  $M_i$  is the mass of the spacecraft,  $V_e$  is the exit velocity of the ion stream, and  $\Delta V$  is the velocity change required for the activity under consideration [6.7]. For these values an amount of 30 kg is needed for the insertion orbit, 80 kg for stationkeeping for 10 years, and 20 kg is included for a factor of safety. However, since a stationkeeping-free orbit will be employed only 25% of the propellant required for stationkeeping will be carried, for minute attitude adjustments and any unforeseen stationkeeping requirements. The total amount of propellant will then be 70 kg.

Lastly, the greater xenon ion mass will give a greater efficiency. And although the specific charge is slightly lower than argon and krypton, xenon's small tank mass, comparable efficiencies, and  $I_{sp}$  make it the best selection.

#### 6.2.4 Propellant Tank Design

It was decided, for purposes of limited space in the spun section, to have two smaller propellant tanks, rather than one large tank. The propellant tanks must be light as well as strong, therefore aluminum alloys were investigated because of their high strength to weight ratios. In addition, aluminum alloys can be annealed to make them less susceptible to cracks formed from microscopic stress fractures that appear during fabrication. However, some alloys are less easily machined or welded, which causes an increase in the construction costs of the tanks.

The trade study shown in Table 6.5 compares five different alloys, all of which are recommended for use as pressure vessels. The material characteristics were given a value of one through four for comparison purposes. A value of one is considered the lowest value and four is considered the highest value for each category. These values were used with Equation 6.4 to calculate the performance index of each alloy.

$$J = (0.25)*\text{Corr. Resist.} + (0.15)*\text{Machineability} + (0.20)*\text{Weldability} + (0.15)*\text{Maximum Strength} + (0.25)*\text{Annealed Strength} \quad (6.4)$$

**Table 6.5 Trade Study of Propellant Tank Materials.** (Donaldson, Bruce K., Analysis of Aircraft Structures, McGraw-Hill, Inc., New York, New York, 1993, p. 115.)

Material	Corrosion Resistance	Machine-ability	Weld-ability	Maximum Strength	Annealed Strength	Performance Index
Al-5154	4	3	4	4	4	3.85
Al-5454	4	3	4	3	2	3.20
Al-5456	2	3	1	4	2	2.25
Al-6061	4	3	4	3	3	3.45
Al-7075	4	2	4	3	3	3.30

The aluminum alloy with the highest performance index is Al-5456, with a nominal composition of 94% Al, 5.1% Mg, 0.8% Mn, and 0.10% Cr [6.9], giving high annealed strength, machinability, and weldability.

With the material chosen, the size of the propellant tanks can now be calculated. The maximum storage pressure for xenon, 7.6 MPa, was used to calculate the smallest possible volume for the propellant tanks. A compressibility factor,  $Z$ , was calculated using the Redlich-Kwong equation for compressible gas, Equation 6.5a, and from that the volume was then found, using Equation 6.6 [6.10]. Equation 6.5b and 6.5c use constants  $a$  and  $b$  which can be found from Redlich-Kwong charts, with  $P$  being the pressure and  $T$  being the absolute temperature.

$$Z = \frac{1}{1 - \frac{b^*P}{Z}} - \frac{\frac{a^{*2}b^*P}{b^*Z}}{1 + \frac{b^*P}{Z}} \quad (6.5a)$$

$$a^{*2} = \frac{a}{R^2T^{2.5}} \quad (6.5b)$$

$$b^* = \frac{b}{RT} \quad (6.5c)$$

$$V = \frac{ZRTm}{P} \quad (6.6)$$



where  $Z$  is the gas correction factor for xenon,  $R$  is the gas constant,  $T$  is the absolute temperature,  $m$  is the mass of propellant, and  $P$  is the pressure at which the gas is stored.

This volume was then used to calculate the inside diameter of the spherical propellant tanks, by using Equation 6.7. The minimum thickness of the tank was found using Equation 6.8

$$d = 2 \sqrt[3]{\frac{3V}{4\pi}} \quad (6.7)$$

$$t = \frac{Pd}{4\sigma} \quad (6.8)$$

where  $P$  is the storage pressure,  $D$  is the diameter of the spherical pressure vessel, and  $\sigma$  is the allowable stress, 310 MPa, for the annealed aluminum 5456.

The mass of the propellant tanks was calculated using the material density and thickness,

$$m = \frac{4}{3}\pi(r_o^3 - r_i^3)\rho \quad (6.9)$$

where  $r_o$  is the outside radius of the tank,  $r_i$  is the inside radius of the tank, and  $\rho$  is the density of the tank material. From this the inner diameter of the xenon propellant tanks, with 35 kg of xenon each will be 0.358 m, with a thickness of 4.39 mm. A factor of safety of 2 was taken into consideration for the tank thickness.

### 6.2.5 Pressurization System

The propellant tanks on board need to maintain constant pressure during the lifetime of the mission. This is because the xenon needs to be pressurized when it reaches the acceleration grid of the ion thrusters. A pressure regulator will be needed to reduce the

xenon from a storage pressure of 7.6 MPa to the feed pressure of 68.9 kPa upon reaching the cathode [6.1].

There are two ways to keep the propellant pressurized. The first method is installing pumps between the tank and the thruster which would pressurize the xenon. In addition to being an expensive design, these pumps are very unreliable and have a lifetime less than the ten year mission design lifetime.

The second method is using another gas, such as helium, and injecting the gas into the propellant tanks to maintain pressure. This method is very common among satellites which operate today. The complexity and cost are much lower than the first method. The xenon tanks would have a bladder inside the tank so when the helium is injected the two gases do not mix.

It was calculated that only 3 kg of helium is needed, which will be kept at a pressure of 10 MPa. This calculation came from Equation 6.6 where the volume of the helium tank was assumed to be equal to the volume of both xenon propellant tanks and a constant storage temperature. A sensor in the xenon tank will detect when pressurization in the tanks is needed. This pressurization is made possible by opening a valve which allows helium to enter the area between the propellant tank and bladder. The helium tank will have a volume of 0.0134 m<sup>3</sup>, a diameter of 0.295 m, with a thickness of 4.74 mm. This thickness is based on a factor of safety of 2. Lastly, the mass of the helium tank is 3.61 kg. All of these values were calculated in the same way that the propellant tank characteristics were, using Equations 6.5-6.8.

#### 6.2.6 Interactive Effects of Propulsion System

The propulsion subsystem effects all of the other subsystems in some way. Some of the changes that were made to the propulsion system require other subsystems to modify their design.

In the power subsystem, the propulsion subsystem requires a power input of 1000 W. This power input will enable two thrusters to be fired simultaneously at full power. The thrusters are the biggest usage of power on the spacecraft. This drives the number of RTG modules that is needed for the satellite.

After the decision to use a stationkeeping-free orbit was made, the effect on the communication subsystem had to be examined. By employing this much larger orbit, the communication coverage of the Moon is decreased about 10%. The positive side to this issue is that the amount of propellant needed for the mission decreases because the satellite does not require any stationkeeping maneuvers.

The structure subsystem is the least effected by the propulsion system. First, the thruster requires no hard points since only a low level of thrust is produced. The next effect is that the turntable requires a stepping motor to be mounted just inside the satellite, but this is not a major concern. Lastly, the structure subsystem must place the three tanks, that will be needed for holding the propellant, inside the satellite.

A subsystem that is directly related to the propulsion system is the thermal subsystem. The power requirement of the thruster is the main factor that drives the number of RTG modules that will be needed to provide power. The RTG modules will radiate heat at all times, but the close proximity of the RTG's while inside the Delta II shroud will increase the waste heat that must be dissipated. By reducing the power requirements for propulsion the RTG modules were also reduced, thereby lowering the waste heat generated in the shroud. Also, the propellant needs to be stored at a relatively constant temperature. If there is an increase or decrease in temperature the pressure of the tank could change, which could cause the tanks to fail.

The only effect on the command and data handling subsystem is the number of channels that will be needed for monitoring the propulsion system. The propulsion system requires 21 channels to monitor all propulsion system operations, with the breakdown given

in Table 6.6. These channels are used for monitoring system performance by collecting data from the sensors placed in various components.

**Table 6.6 System Monitoring Channel Breakdown.**

Component	No. of Channels
PPU	3
Thrusters	4
Tanks	3
Valves	4
Gimbal system	4
Turntable	2
Overall monitoring	1

Plume effects on the satellite is the last major area of concern. Each thruster can rotate 90 degrees from the x coordinate. Figure 6.2 illustrates that the plume from the thruster will not effect the antenna with its operation. However, the bottom thruster, when operating in the -y direction, will contact the extended skirt. The plume which is made up of ionized gas particles will react to any type of surface, which will eventually corrode the surface. A ten degree angle shift in the x-y plane will prevent the plume from affecting the skirt. Position sensors will be used to insure that the thruster will not gimbal past 80 degrees.

Another position where the plume effects the satellite can be seen from Figure 6.3. This illustrates how the plume will contact the RTG modules when the thrusters are deployed as shown. The RTG casing will be affected by the ionized gas, causing it to disintegrate, which will degrade the performance of the RTG's. A shift of ten degrees from the normal will correct this problem, achieved by using a computer code that will not gimbal the thrusters past 80 degrees. This ten degree shift will reduce the maximum effective thrust in the -y and z directions by approximately 1.0 mN.

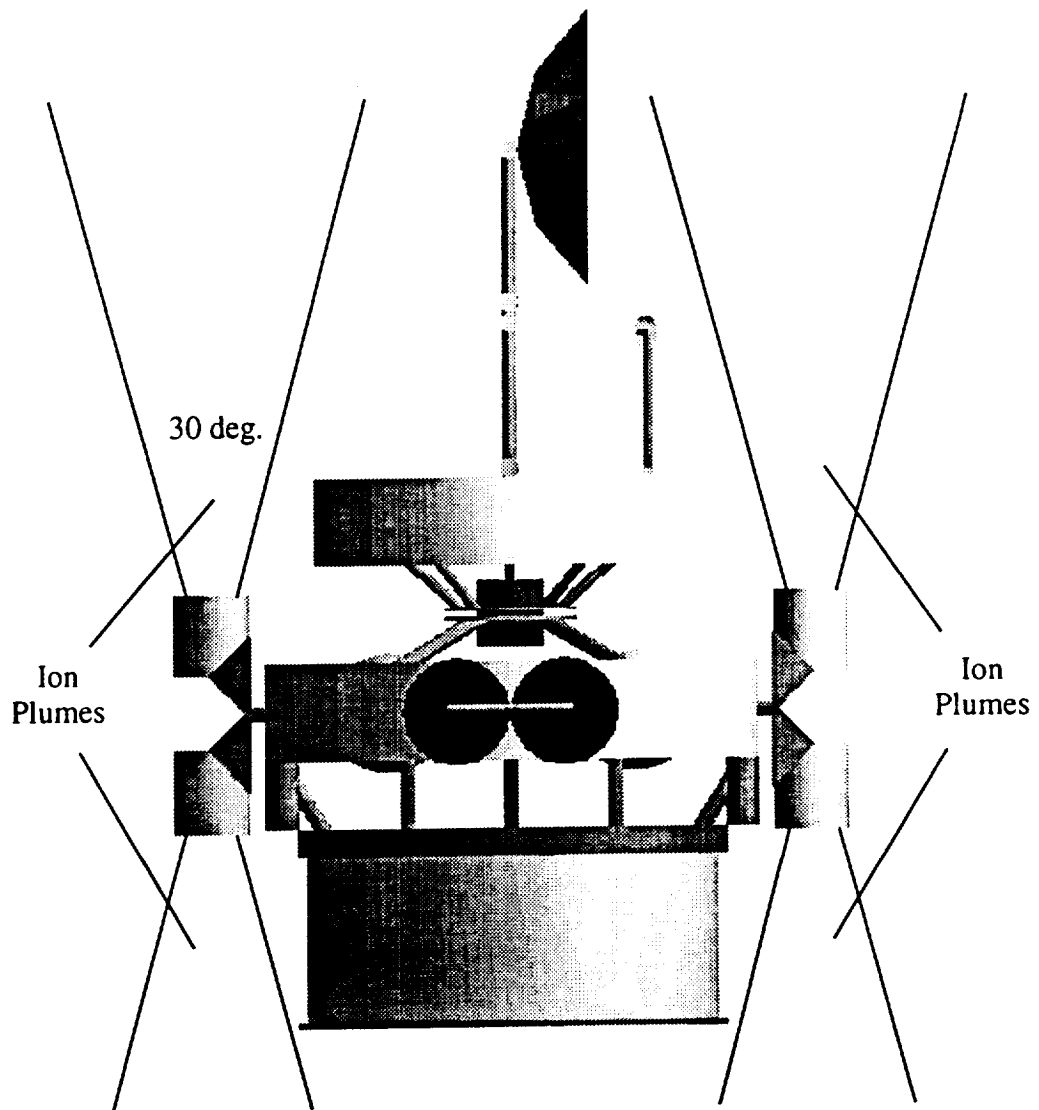


**Figure 6.2 Ion Plume Impingement on Antenna and Solar Skirt.**

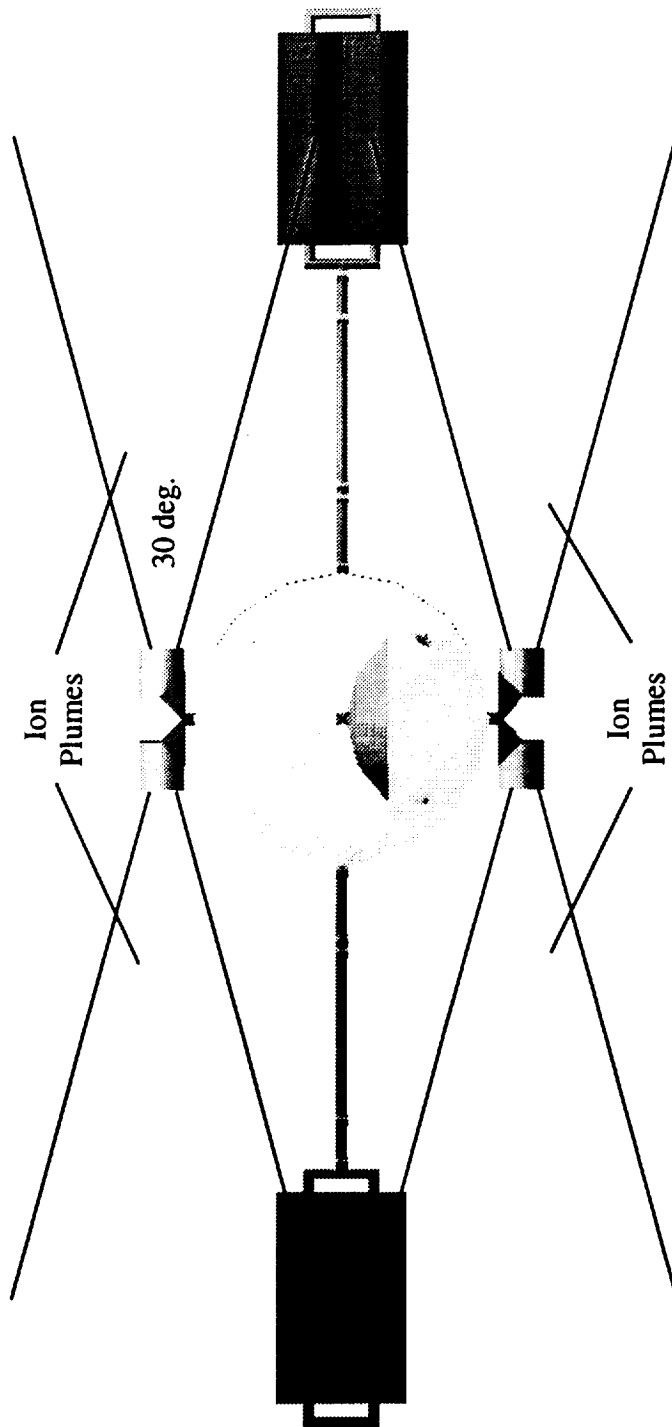


**Figure 6.3 Ion Plume Impingement on RTG Modules.**

### 6.2.7 Completion of Duties with Present Design

With the Hughes Research Lab 13 cm ion propulsion system and present configuration, the translunar orbit will be completed using two thrusters fired simultaneously. This process will require 1000 W from the power subsystem and will generate 35.6 mN of thrust. The exact trajectory and time to complete this stage of the mission is presently being investigated by the guidance, navigation, and control (GN&C) subsystem design team.

Because the thrusters are placed on a turntable that can be rotated 360°, the duty cycle of the thrusters can be decreased by a factor of two (i.e. switch thruster pairs along some point of the translunar orbit). Lessening the duty cycle decreases the chance of a thruster failing at some point during the 10 year mission duration.

The injection into the halo orbit is another matter currently being investigated by GN&C. It is apparent that this will be a slow process due to the low thrust levels attained by the ion propulsion system. Nonetheless, any trajectory proposed by GN&C based on allowable thrust levels should be feasible as the propulsion system can deliver thrust in any direction.

The use of a stationkeeping-free orbit renders the need for routine orbital stationkeeping for ECHO virtually obsolete. This orbit was computed by Dr. Kathleen Howell at Purdue University [6.11]. Employing this orbit decreases the total mass and cost of the propulsion system by limiting the amount of propellant needed for stationkeeping maneuvers. In addition, the duty cycle of the thruster is drastically reduced so that the reliability of the thruster increases.

### 6.2.8 Mass, Power, and Cost Budgets

The overall system mass, cost, and power budgets shown in Table 6.7 include each component of the propulsion subsystem. These cost figures are estimated for 1999 dollars, using an inflation rate of 3% per year. The components listed without costs were included in the purchase cost of another component. For example, the gimbal system is provided with

the purchase of the ion thrusters from Hughes Research Laboratories. Any component with an approximate cost of '0' dollars was estimated as less than 0.1 million dollars.

**Table 6.7 Mass, Power, and Cost Budgets for Propulsion Subsystem.**  
(Beattie, J.R., R.R. Robson, J.D. Williams, pp. 1-2.)

Component	Mass (kg)	Power Required (W)	Cost (\$M)
Power Processor Unit (3)	20.4	500.0	1.1
Ion Thrusters (4)	20.0	439.0	1.0
Gimbal System	8.8	~5	—
Mounting Plate Turntables	7.1	—	~0
Stepping Motors (2)	~7.0	~0	~0.1
Propellant Tanks (2)	10.0	—	~0.1
Xenon Propellant	70.0	—	~0
Pressure Regulator	1.6	~5	—
Feed Components	3.5	—	—
Pressure Feed Tank	3.61	—	~0.1
Helium Gas	3.0	—	~0
Structure	2.8	—	—
<b>TOTALS</b>	<b>197.0</b>	<b>1000.0</b>	<b>2.4</b>

### 6.3 Conclusion

The propulsive force for the satellite will be provided by four Hughes Research Laboratory 13 cm ion thrusters (2 on each side) that can be gimballed to provide thrust in any direction, as well as a single level of redundancy. The propellant for the thrusters will be xenon, and due to the decision to employ a stationkeeping-free orbit, the propellant mass will be approximately 70 kg. This propellant will be stored in two equal sized Al-5456 spherical tanks, with a diameter of 0.358 m. The pressure in the tanks must be kept at 7.6 MPa; therefore, a bladder system will be used, with helium being used to pressure the bladder in the propellant tanks. Approximately 3.0 kg of helium will be needed to maintain pressure in the propellant tanks. The helium will be stored in a smaller Al-5456 tank, with a diameter of 0.295 m.



The costs were broken down into three areas, the main propulsion system, the propellant system, and the miscellaneous components, with all costs being given in 1999 dollars. The cost of the main propulsion system, made up of the four thrusters, three PPU's, a pressure regulator, feed components, gimbal components, and mounting structure was found to be \$2.1 million. The propellant system, consisting of the xenon propellant, the helium and pressurization system, and the three tanks totaled \$0.2 million. Finally, a total of \$0.1 million was allotted for the two space-rated stepping motors and turntable system. The total cost for the propulsion subsystem will be \$2.4 million and the total mass will be 197 kg, with a power consumption of 1000 W at peak operation.

#### 6.4 References

- [6.1] Beattie, J.R., R.R. Robson, and J.D. Williams, "18-mN Xenon Ion Propulsion Subsystem," IEPC-91-010, October 14-17, 1991, Viareggio, Italy, p. 1.
- [6.2] Beattie, J.R., R.R. Robson, and J.D. Williams, p. 2.
- [6.3] Beattie, J.R., R.R. Robson, and J.D. Williams, p. 4.
- [6.4] Hill, Philip G., and Carl R. Peterson, Mechanics and Thermodynamics of Propulsion, Addison-Wesley Publishing Company, New York, NY, 1992, p. 659.
- [6.5] Rawlin, V.K, and M.J. Patterson, and R.P. Gruber, "Xenon Ion Propellant for Orbit Transfer," AIAA-90-2527, NASA Lewis Research Center, p. 22.
- [6.6] Farquhar, Robert, "A Halo Orbit Lunar Station," Astronautics and Aeronautics, June 1972, p. 59.
- [6.7] Fearn, D.G., "Ion Propulsion - A Technology for Improving the Cost-effectiveness of Large Communication Satellites," Electronics and Communication Engineering Journal, June 1992, p. 154.
- [6.8] Donaldson, Bruce K., Analysis of Aircraft Structures, McGraw-Hill, Inc., New York, NY, 1993, p. 115.
- [6.9] Donaldson, Bruce K., p. 115.

[6.10] Reid, Robert C., and John M. Prausnitz, and Bruce E. Poling, The Properties of Gases and Liquids, 4th Edition, McGraw-Hill, New York, 1987, pp. 73-76.

[6.11] Personal correspondence with Dr. Kathleen Howell, Purdue University, February 22, 1994.

## 7.0 Guidance, Navigation, and Control Subsystem

### 7.1 Introduction

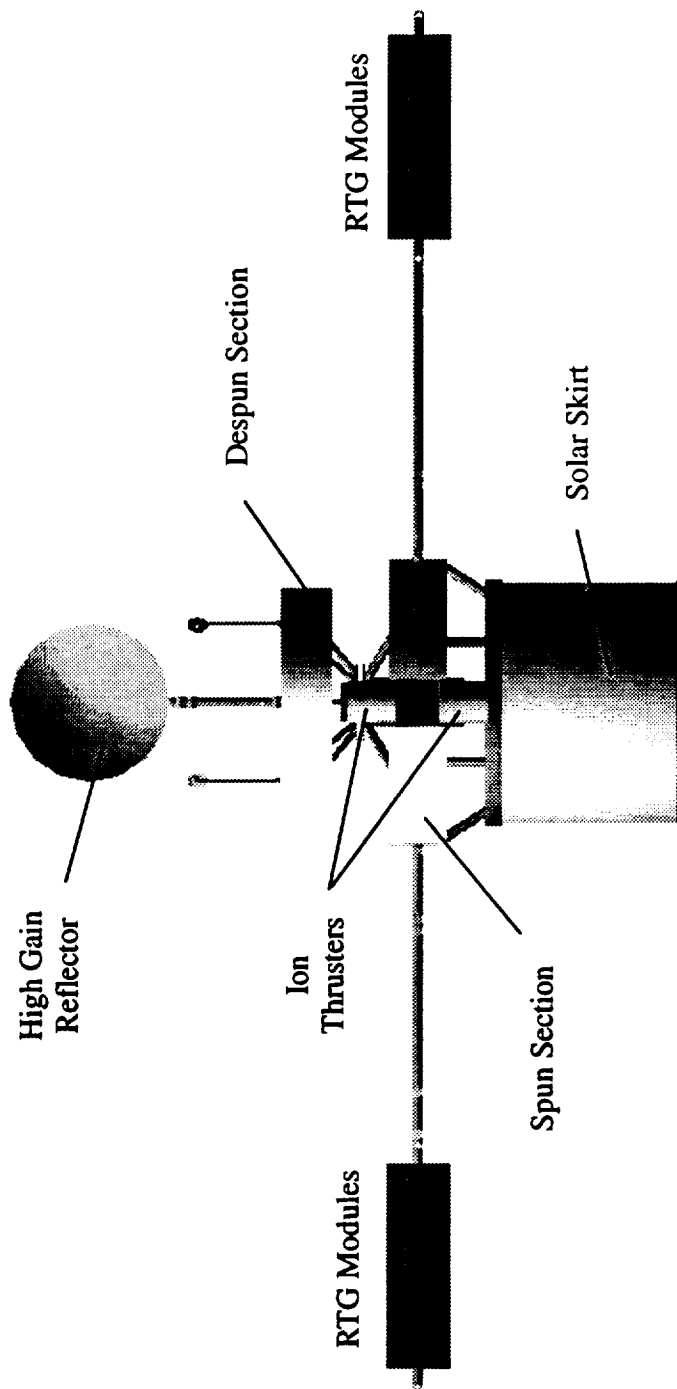
The Guidance, Navigation, and Control (GNC) subsystem will be responsible for the trajectory, stabilization, and attitude determination and control of the spacecraft. Each of these areas is constrained under specific criteria defined by the mission requirements. The trajectory is limited to using low-thrust to reach the halo orbit, and the stabilization of the satellite must be achieved via dual spin. Finally, the spacecraft must maintain semi-autonomous attitude control. To satisfy this last requirement, the Microcosm Autonomous Navigation System (MANS) was chosen.

Figure 7.1 shows the current spacecraft configuration which was used in performing all calculations. The radioisotope thermoelectric generators (RTG's) will be deployed on booms from the sides of the spacecraft. There are two RTG modules on each side of the satellite totaling 84 kg per boom. Since most of the mass of the spacecraft will be placed in the spun section to increase stability, 200 kg of mass has been approximated as being in the despun section, and 570 kg of mass has been estimated to be in the spun section. The mass distribution in each section was modeled as being homogeneous.

### 7.2 Trajectory and Halo Orbit

#### 7.2.1 Trajectory

The satellite will use a low-thrust transfer trajectory to reach the halo orbit. A computer program (see Appendix A.1) was written to determine the transfer. In order to simplify the trajectory problem, it was broken into two pieces: 1) low-thrust transfer from near-Earth to vicinity of the  $L_2$  point and 2) low-thrust transfer from  $L_2$  point to the halo orbit. Once each piece of the trajectory was found, they then could be patched together. For



**Figure 7.1 Overall Configuration of the ECHO Spacecraft.**

each portion of the trajectory the computer program integrates the set of restricted three-body equations

$$\begin{aligned}
 \ddot{x} - 2\dot{y} - x &= -\frac{(1-\mu)(x-\mu)}{\left[(x-\mu)^2 + y^2 + z^2\right]^{1.5}} - \frac{\mu(x+1-\mu)}{\left[(x+1-\mu)^2 + y^2 + z^2\right]^{1.5}} \\
 &\quad + \left(\frac{T_{s/c}}{m_{s/c}}\right) \frac{\dot{x}}{\sqrt{\dot{x}^2 + \dot{y}^2 + \dot{z}^2}} \\
 \ddot{y} + 2\dot{x} - \dot{y} &= -\frac{(1-\mu)y}{\left[(x-\mu)^2 + y^2 + z^2\right]^{1.5}} - \frac{\mu y}{\left[(x+1-\mu)^2 + y^2 + z^2\right]^{1.5}} \\
 &\quad + \left(\frac{T_{s/c}}{m_{s/c}}\right) \frac{\dot{y}}{\sqrt{\dot{x}^2 + \dot{y}^2 + \dot{z}^2}} \\
 \ddot{z} &= -\frac{(1-\mu)z}{\left[(x-\mu)^2 + y^2 + z^2\right]^{1.5}} - \frac{\mu z}{\left[(x+1-\mu)^2 + y^2 + z^2\right]^{1.5}} \\
 &\quad + \left(\frac{T_{s/c}}{m_{s/c}}\right) \frac{\dot{z}}{\sqrt{\dot{x}^2 + \dot{y}^2 + \dot{z}^2}}
 \end{aligned} \tag{7.1}$$

where the x-y coordinate system is attached at the center of mass of the Earth-Moon system with x pointing in the direction of Earth; y is perpendicular to the Earth-Moon line; and z is perpendicular to the plane in which the Earth and Moon lie and  $\mu$  is the ratio of Earth to Moon mass. The last expression in each of the equations defines the addition of thrust from the satellite tangential to the trajectory.

For the near-Earth to  $L_2$  leg of the trajectory, the motion of the satellite was assumed to occur only in the x-y plane, therefore,  $z = \dot{z} = \ddot{z} = 0$ . Since the initial conditions for the equations were unknown and the final conditions *were* known at the  $L_2$  point, the equations were integrated backward in time from the  $L_2$  point to a near-Earth point. The integration scheme used was a Runge-Kutta 5,6 method. Presented in Figure 7.2 is the resulting trajectory for the first leg with the diamond symbols representing 10 day intervals along the trajectory for time reference. There is no thrust required by the satellite during this

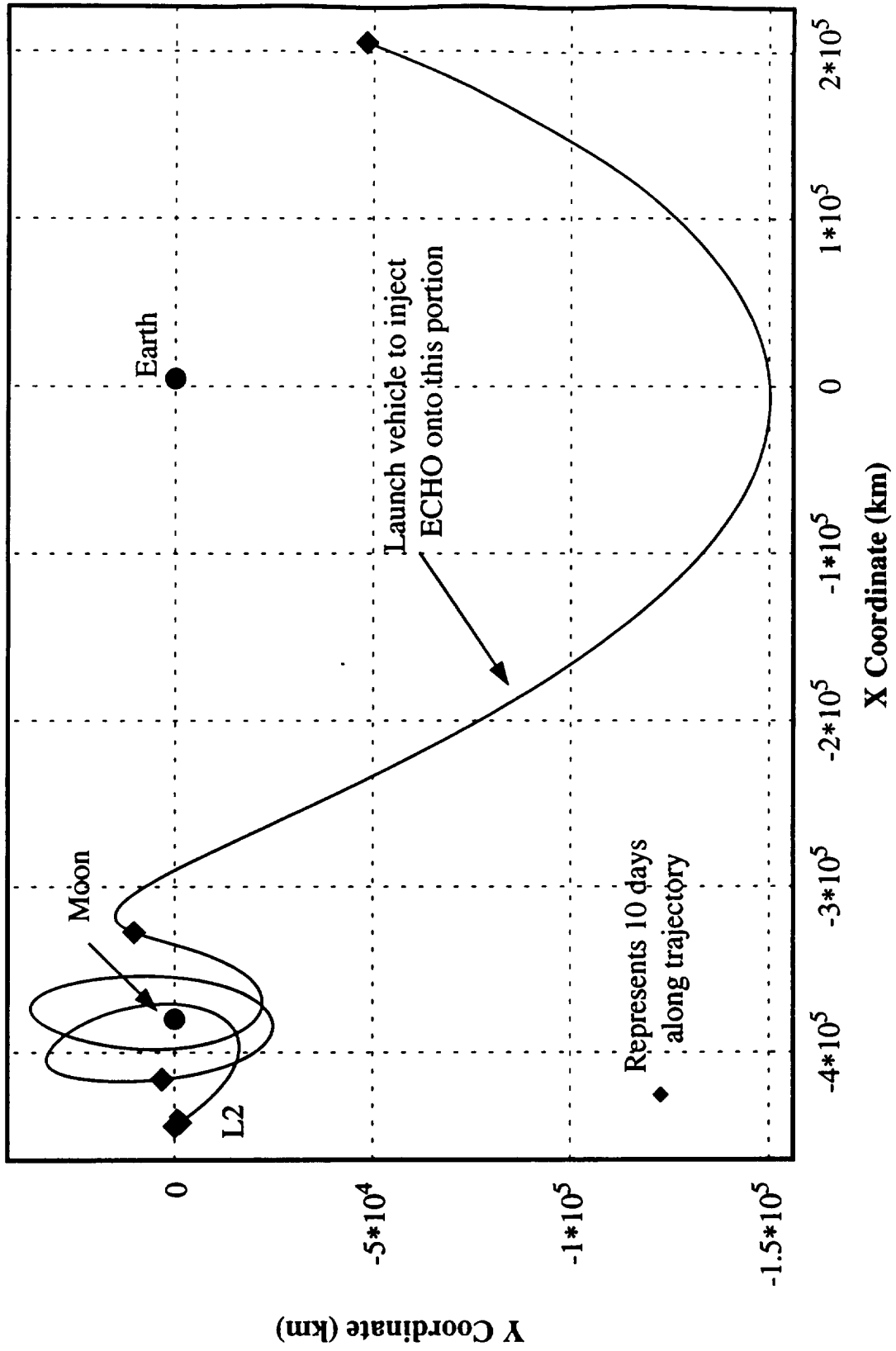


Figure 7.2 Transfer Trajectory from near-Earth Vicinity to L<sub>2</sub> Point.

trajectory. The orbital energy of the transfer is shown in Figure 7.3. A Delta 7925 launch vehicle is capable of achieving an orbital energy relative to the Earth of  $-1.0 \text{ km}^2/\text{sec}^2$  for a 1200 kg payload. So the spacecraft may be injected into the transfer trajectory between the -30 and -40 day interval shown in Figure 7.2. The orbital energy of the satellite will gradually increase as it moves further away from the Earth, and the actual orbital energy will not possess sharp 'spikes'. (These spikes are the result of the approximate integration scheme used to solve the equations of motion.)

To compute the trajectory for the second portion of the transfer, the third equation of Equation (7.1) must now be included. It is well-known that the motion of a spacecraft near any of the collinear equilibrium points is quite sensitive to initial conditions. Knowing the injection position and velocity required for the halo orbit, a transfer path was sought by integrating backwards in time from the halo injection to the  $L_2$  point. This scheme used the "velocity-to-be-gained" method described in Reference 7.1, with the assumption of a linearly increasing velocity from  $L_2$  (zero velocity) to the injection point. Because of the sensitivity to small perturbations (in this case the thrust), a transfer that matched both end-points was not found; however, families of transfers between neighborhoods of the desired end-points give confidence that an exact transfer (requiring approximately 14 days) should be possible. Determining that exact transfer would require the use of an optimal control approach.

### 7.2.2 Halo Orbit

Various halo orbits can exist around Lagrange equilibrium points, but for the purposes of this mission, two specific halo orbits were considered - a circular halo orbit with a radius of 3500 km and a stationkeeping-free orbit was considered. Originally, the circular orbit had been proposed because it allowed for constant communication between the Earth and Moon [7.2]. However, the orbit is not stable and would require a  $\Delta V$  of 400 ft/s/yr for stationkeeping. This translated into a constant thrust of approximately 7.0 mN using the ion

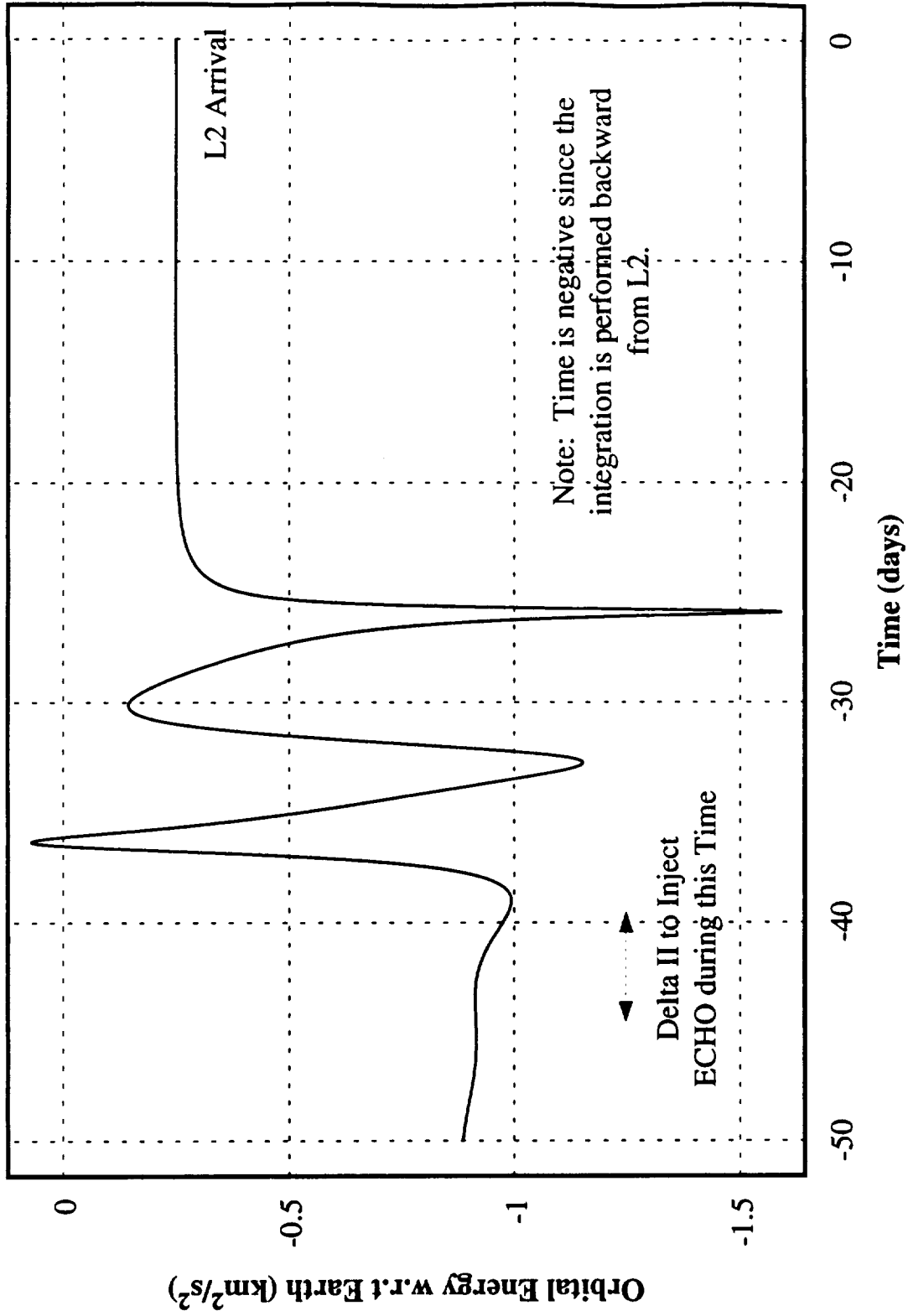
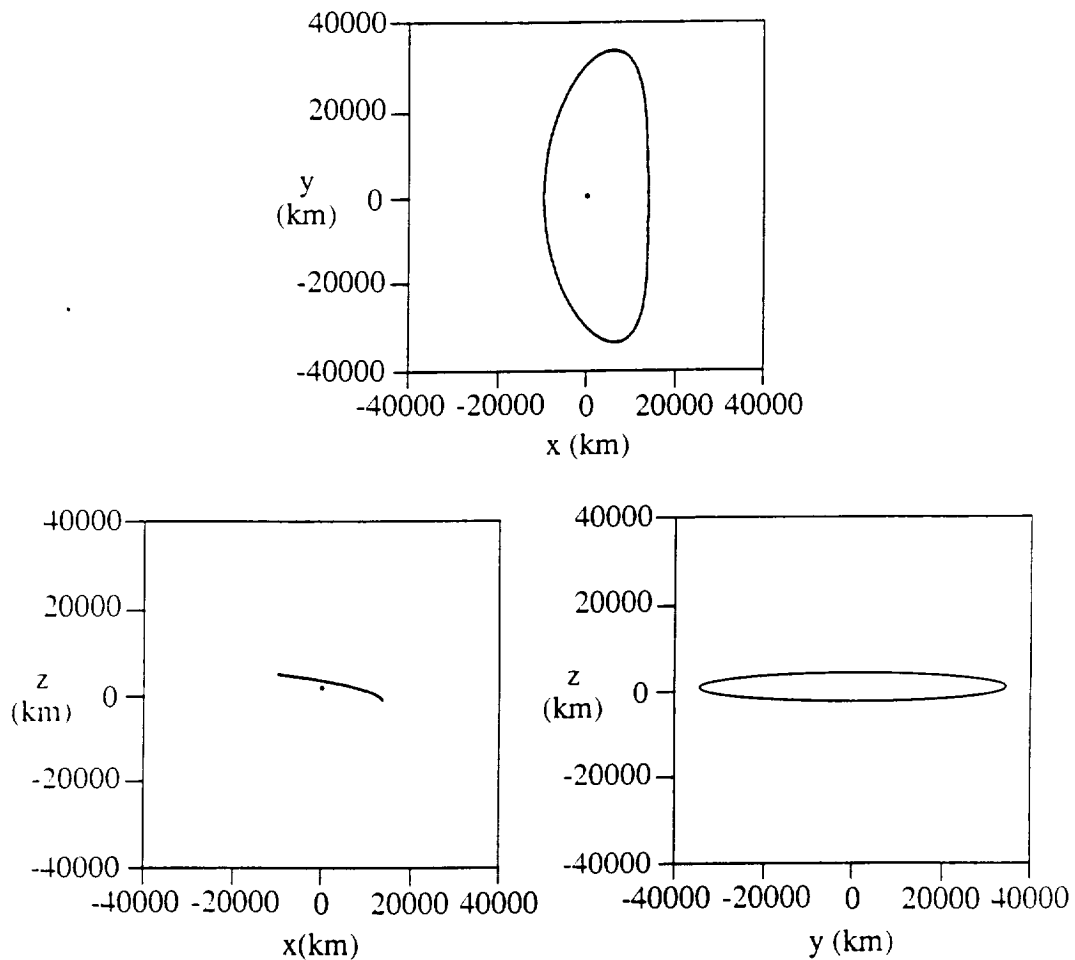


Figure 7.3 Orbital Energy w.r.t. Earth for Earth-L<sub>2</sub> Transfer.



thrusters. Since the lifetime of each thruster is on the order of 10000 hours, the circular orbit could not be maintained during the 10 year lifetime.

Recently, a new halo orbit was proposed that would require no stationkeeping [7.3, 7.4], but it is also highly elongated in the y-direction. Figure 7.4 shows three different views of this halo orbit. The semiminor axis of the orbit is 3500 km long, and the semimajor axis



**Figure 7.4 Stationkeeping-free Halo Orbit.** (Howell, K.C. and Bell, J., Private Communication with R.G. Melton, February 22, 1994)

length equals 35000 km. ECHO will use this halo orbit for its mission to conserve propellant and reduce complexity.

### 7.3 Spacecraft Stabilization

#### 7.3.1 Spin down

The spin down of the satellite will occur shortly after the third stage is deployed from the Delta launch vehicle. Figure 7.1 shows the satellite configuration that was used to calculate the mass moments of inertia. Sample calculations for the moments of inertia, angular momentum, and spin rates can be found in Appendix A.3. The spin rate of the satellite when deployed from the third stage will be approximately 45 rpm. For the duration of the mission, the despun section will have to rotate approximately once every 28 days to keep the antenna dish facing the Moon at all times, and the spun section will rotate at approximately 37 rpm to provide stability against disturbance torques. The RTG's will have to be deployed as soon as possible to reduce the amount of heat being transferred to the satellite, which will slow its spin rate. After the satellite reaches the halo orbit, it will then reconfigure itself into the dual spin mode using the BAPTA (Bearing and Power Transfer Assembly) to spin down the despun section and the thrusters to spin-up the spun section. The spin rates for each part of the mission can be found in Table 7.1.

**Table 7.1 Spin Rates.**

	Despun Section	Spun Section
Before RTG deployment	45 rpm	45 rpm
After RTG deployment (before Halo orbit)	8.6 rpm	8.6 rpm
Before final spin-up	$24.8 \times 10^{-6}$ rpm	8.76 rpm
Final spin rates	$24.8 \times 10^{-6}$ rpm	37 rpm

### 7.3.2 Disturbance Torques

Magnetic, gravity gradient, and solar pressure torques all affect a spacecraft's stability. However, the Moon has no significant magnetic field, and the halo orbit is far enough away from the Earth's magnetic field that it too has a negligible effect. Therefore, the only torques acting on the spacecraft are from the gravity gradient and the solar pressure.

The gravity gradient torque is calculated using:

$$T_g = \frac{3\mu_{Moon}}{2R^3} |I_a - I_t| \sin(2\theta) \quad (7.1)$$

where  $\mu$  = the Moon's gravitational parameter  
 $R$  = the distance from the Moon to the spacecraft  
 $\theta$  = the maximum allowable nutation angle  
 $I_a$  = the axial moment of inertia  
 $I_t$  = the transverse moment of inertia

The result for ECHO is a gravity gradient torque of  $1.4 \times 10^{-9}$  Nm.

The solar pressure force is calculated using Equation 7.2.

$$T_s = \frac{PA}{c} \quad (7.2)$$

where:  $P$  = the power flux  
 $c$  = the speed of light  
 $A$  = the surface area exposed to the sun above or below the center of mass

Once the solar pressure force is known, Equation 7.3 can be used to obtain the actual torque due to the solar pressure:

$$M_s = T_s d \quad (7.3)$$

where  $d$  is the perpendicular distance from the centroid of the exposed area to the center of mass. The total solar pressure torque is the difference between the torques acting above and below the center of mass.

The spin rate necessary for the despun section to maintain a "fixed" pointing relative to the Earth and Moon can be found by dividing the orbit of the Moon by its period and is equal to 0.5°/hr. Calculating the spin rate for the spun section involves the equation:

$$\omega = \frac{Mdt}{I_s \tan \theta} \quad (7.4)$$

where:  $M$  = the torque that needs to be stabilized  
 $dt$  = the time over which the torque is applied  
 $I_s$  = the spin moment of inertia  
 $\theta$  = the maximum nutation angle

Substituting the torques into Equation 7.4 yields an extremely high spin rate which is largely due to the solar torque since the antenna projects a greater area above the center of mass than the spun section projects below. Therefore, some method of reducing the solar torque is required.

In order to reduce the solar torque, a one meter long skirt will be extended down from the top of the tapered section of the spacecraft. The skirt would lower the total torque that needs to be stabilized against. However, the projected area of the front of the antenna is greater than that for the side. This results in different solar pressure torques acting on the satellite as the despun section rotates. To optimize the skirt area for minimum average disturbance torque, Equations 7.2 and 7.3 were used in an iterative process until the solar torque acting on the front was equal and opposite to the torque acting on the side. Equation 7.4 was then implemented to obtain the spin rate necessary to stabilize the spacecraft against the solar torque. The results of this iteration are tabulated in Appendix A.4.

Even though solar activity causes fluctuations in the solar power flux, the above process assumes that the solar torque remains constant. To maintain the pointing accuracy of

1° for two years, a spin rate of 37 rpm will be required which is high enough to allow for a margin of error in the calculations. Stationkeeping will then be needed approximately every two years to counter the effects of solar torque.

## 7.4 MANS System

### 7.4.1 Background

The Microcosm Autonomous Navigation System (MANS) provides a spacecraft with low-cost, fully autonomous navigation and attitude determination. MANS provides the position and velocity of the spacecraft every 250 milliseconds, and it can also provide the position vector of the Sun in spacecraft coordinates and the ground lookpoint [7.5]. The system uses one or more sensors to observe the Earth, Sun, and Moon [7.6], and position accuracies are expected to range from 100 meters to 3 kilometers [7.7]. MANS processes sensor data through sophisticated software consisting of over 35000 lines of Ada code. However, MANS does not possess any specific mass, power, or size requirements other than those necessary for the sensors [7.8]. The MANS system was first flight tested in 1993, but no information following that test has been made available yet [7.9].

### 7.4.2 The MANS Sensor

The MANS system has primarily been configured to receive data from the main sensor, a modified Dual Cone Scanner (DCS). The DCS is a product of the Barnes Engineering Division of EDO Corporation in Shelton, Connecticut and uses a motor driven optical scanning head that is capable of detecting the Earth's thermal radiance along with the Sun and Moon's visible light. To provide accurate and continuous data, the DCS spins at a rate of 240 rpm and must be placed outside the spacecraft's main body so that it can achieve a 70° field of view. In addition to the DCS, the MANS employs two fan sensors that detect the Sun and Moon and operate with 180 degree fields of view. The MANS sensor has a mass of

4.5 kg and requires 11 Watts of power [7.10]. The actual dimensions of the cylindrical sensor have not been found, but they have been approximated to be 0.2 meters long and 0.08 meters in diameter.

Although the sensor has not been tested for use in the halo orbit, the assumption is that it will still be effective there. Two sensors will be used in an effort to increase the accuracy of the navigation system, and they will be placed 180 degrees apart on the outside of the despun section of the satellite. This placement will provide data from at least one sensor at all times. The despun section was chosen because the DCS is primarily used for three-axis stabilized spacecraft [7.11] and because it also reduces the complexity of the processing software.

## 7.5 Budget

Table 7.2 shows the budget breakdowns for the GNC subsystem.

**Table 7.2 GNC Budgets.**

Mass (kg)	9.0
Power (W)	22.0
Cost (M\$,FY99)	14.7

The MANS sensors are the only variables in the power and mass budgets. Actual cost values were not found so the cost was approximated using a cost estimation program [7.12]. The cost value is given in terms of 1999 dollars. However, the estimation program tends to overestimate the cost, and therefore, the value given above may be higher than the actual cost.

## 7.6 Conclusion

The low-thrust trajectory for the transfer orbit was found by the course instructors using a computer code. The satellite will take approximately 70 days to reach the L<sub>2</sub> point. Once at the L<sub>2</sub> point, the spacecraft will be placed into a stationkeeping-free orbit, but the details of how the satellite will be placed into the halo orbit have not been determined.

When the RTG's are deployed immediately after the satellite leaves the third stage of the Delta launch vehicle, the spin rate of the spacecraft will be decreased from 45 rpm to 8.6 rpm, and once the satellite reaches the halo orbit, the BAPTA will slow the spin rate of the despun section to one revolution per 28 days while thrusters will be used to increase the spin rate of the spun section to approximately 37 rpm.

There are two disturbance torques significant enough to be dealt with during the mission lifetime. The solar torque has a magnitude of  $10^{-6}$  and will be more significant than the gravity gradient torque which has a magnitude of  $10^{-9}$ . While the spin rate of the satellite will create more than enough stability to compensate for the gravity gradient torque, the solar torque caused by the parabolic antenna must also be counteracted by the use of a 1.0 m long skirt extending from the top of the tapered section of the spacecraft.

The MANS system has been chosen as the best navigation system for ECHO. The decision to use MANS in the halo orbit is based on the assumption that the software and Dual Cone Sensors can be modified for use in the halo orbit. Two sensors will be used for the MANS system to increase accuracy and reliability of the system and will be placed 180° apart on the despun platform of the satellite.

## 7.7 References

- [7.1] Battin, Richard H., An Introduction to the Mathematics and Methods of Astrodynamics, American Institute of Aeronautics and Astronautics, Inc., New York, NY, 1987.
- [7.2] Farquhar, R. W., "A Halo-Orbit Lunar Station," *Astronautics and Aeronautics*, June 1972, pp. 59-63.

- [7.3] Howell, K.C. and H. J. Pernicka, "Sun-Earth Libration Point Trajectories that Avoid the Solar Exclusion Zone," *The Journal of the Astronautical Sciences*, Vol. 38, No. 3, July/September 1990, pp. 269-288.
- [7.4] Howell, K.C., Private communication with R. G. Melton, Feb. 22, 1994.
- [7.5] Wertz, James R. and E. David Skulsky, "Fully Autonomous Navigation for the NASA Cargo Transfer Vehicle," NASA Document #N93-22318. Abstract only.
- [7.6] Wertz, J.R. and W.J. Larson, eds., Space Mission Analysis and Design, Microcosm, Inc., Kluwer Academic Publishers, 1992, pp. 473, 475.
- [7.7] Tai, Frank and Peter D. Noerdlinger, "A Low Cost Autonomous Navigation System," Paper No. AAS 89-001 presented at the 12th Annual AAS Guidance and Control Conference, Keystone, Colorado, Feb. 4-8 1989.
- [7.8] Wertz and Larson, p. 484.
- [7.9] Wertz and Larson, pp. 473, 475.
- [7.10] Anthony, Jack, "Autonomous Space Navigation Experiment," Paper No. AIAA 92-1710 presented at the AIAA Space Programs and Technologies Conference, Huntsville, Alabama, March 24-26 1992.
- [7.11] Tai, p. 4.
- [7.12] Cyr, Kelley, "Cost Estimation Methods for Advance Space Systems," NASA Johnson Space Center, 1988.



## **8.0 Command and Data Handling Subsystem**

### **8.1 Introduction**

The command and data handling (C&DH) subsystem for ECHO must collect, process, and redistribute commands and data for the satellite. These commands and data may originate from several sources such as the lunar surface, a command station on Earth or other subsystems aboard the spacecraft. Essentially, the command and data handling subsystem is the brain of the satellite, serving to make decisions regarding data routing and organization.

As a preliminary requirement, it was decided to design a semi-autonomous C&DH subsystem. This would minimize ground interaction and maintenance because the satellite will be capable of monitoring its health and status while adjusting for any variation from a pre-planned guideline. Telemetry and ground communication will still be possible, allowing periodic checks and adjustments to be made if necessary.

Reliability is also a major concern; an inoperative satellite is of very little use. Therefore, redundant processing units and data paths must be designed into the C&DH subsystem to minimize the chances of failure. The central processors will have the capability of accommodating the various throughput levels of the communications and GNC subsystems with which it will communicate. In addition, should a failure occur, the remaining hardware must be capable of sustaining satellite functions at least at some minimum level.

Finally, mass and volume of this subsystem must be minimized. As launch cost is directly proportional to mass, a mass reduction will save money as well as reserve more room for propellant storage which will increase the expected mission lifetime.

What follows is a command and data handling subsystem design for ECHO. The discussion includes a detailed description of the system architecture, processors, software, and the data transfer system. An overview of the mass, power, and cost budgets is also included.

## 8.2 Architecture

The command and data handling subsystem's architecture is driven by the satellite's dual-spin configuration. Due to the need of relaying data across the spin linkage, a bus architecture was deemed the most logical as the backbone of the system. This provides the most effective method of communication between the spun and despun sections. The bus continuity across the linkage will be maintained with RF links.

In each of the two sections, the bus is combined with other architectures to achieve the most reliable and highest performing system possible. It was determined that for redundancy and increased processing speeds, two central processing units (CPU's) would be used; one in each section. Each CPU will be attached directly to the system bus. A hardware controller is also attached to the bus, in both the spun and despun sections. These devices will be small processors that will collect data from many satellite peripherals. These peripherals include all instruments in the satellite that must be controlled and/or monitored by the command and data handling subsystem. The hardware controllers' purpose is to relay data through the bus to the appropriate CPU and in turn, route commands from the CPU back to the peripherals. Sensors will be attached to the bus by means of two small ring architectures, one located in the spun and one in the despun sections. These token rings will collect data from both thermal and stress sensors and relay it to the central processing unit. The ring architecture was chosen for this application based on its speed and simplicity. A payload processor will also be attached to the bus in the despun section. The final architecture is shown in Figure 8.1.

## 8.3 Software Sizing

The size and cost of a spacecraft's computer system is directly related to the amount of software it will use and the speed, or throughput, at which it will run the software. These two factors are driven by how complex and autonomous the spacecraft in question is to be. It is desired to make ECHO a semi-autonomous spacecraft, thereby minimizing ground

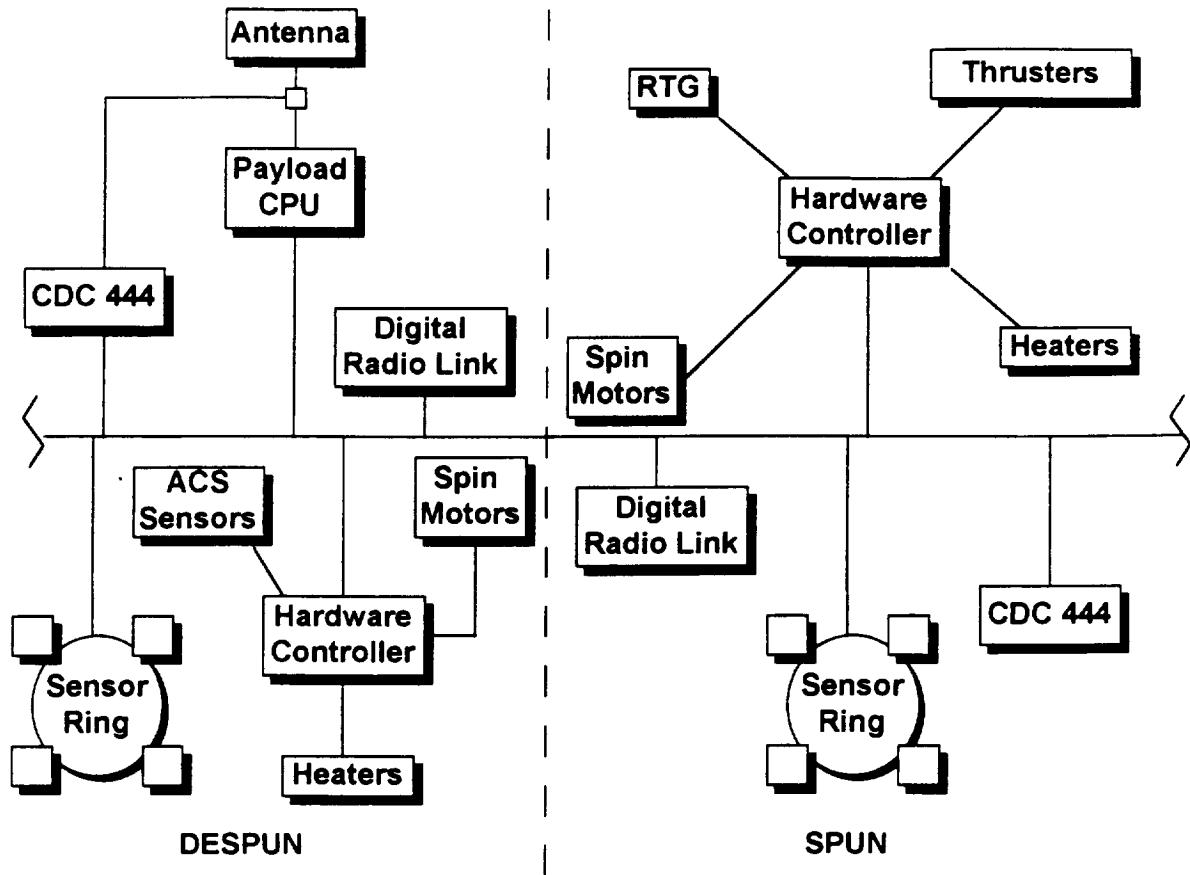


Figure 8.1 Command and Data Handling Architecture.

contact. This will increase the size and cost of the command and data handling subsystem. Two software estimates were completed. The first estimate was for a customized navigation system and the second estimate used the MANS system for guidance, navigation and control.

### 8.3.1 Customized System Estimate

Before the software and its throughput could be evaluated, a list of on-board applications was determined with their size and throughput estimates [8.1]. After the applications were determined, estimates for the computer's operating system were determined [8.2]. An overall estimate of the necessary software is given in Table 8.1. This system will require 0.64 Mbytes of memory and a throughput of 1,302.8 KIPS (kilo instructions per second). With the amount of the software known, it is relatively easy to determine that a total of 13,386 source lines of code (SLOC) will need to be written. This is assuming that the computer language of Ada is used, since this is the language in which the MANS system is written. Ada contains, on the average, seven 16-bit words of memory per SLOC. This is an important number as it reflects how long it will take to write the software.

### 8.3.2 MANS Estimate

Because the MANS software contains all guidance, navigation and control applications as well as the Kalman filter, math utilities, and other functions, it was not necessary to include them in software sizing calculations. The procedure used for the customized system estimate was repeated for the remaining functions. This estimation is shown in Table 8.2. The final data from these calculations was then added to the data obtained from the MANS system [8.5]. MANS contains 35,000 SLOC in Ada and has a throughput of at least 1 MIPS. After the MANS software is added to the custom system software, it can be seen that this system requires a total of 0.43 Mbytes of memory, 1,378 KIPS throughput, and 6,293 SLOC in Ada need to be written.

**Table 8.1 Software Requirements for ECHO.** (Wertz, James R., and Wiley, J. Larson, *Space Mission Analysis and Design*, Microcosm, 1992, p. 627)

Component	Estimation Source	Required Memory		Required Throughput (KIPS)
		Code (K words)	Data (K words)	
<b>Application Functions: [8.3]</b>	Frequency (Hz)			
• Thruster Control	2.00	0.6	0.4	2.0
• Sun Sensor (2)	2.00	1.0	0.2	6.0
• Star Tracker (2)	0.02	4.0	30.0	4.0
• Kinematic Integration	10.00	2.0	0.2	6.0
• Error Determination	10.00	1.0	0.1	4.8
• Ephemeris Propagation	1.00	2.0	0.3	2.0
• Command Processing	10.00	1.0	4.0	7.0
• Telemetry Processing	10.00	1.0	2.5	3.0
• Orbit Propagation	1.00	13.0	4.0	20.0
• Precession Control	10.00	3.3	1.5	30.0
• Complex Autonomy	10.00	15.0	10.0	20.0
• Fault Monitors	5.00	4.0	1.0	15.0
• Fault Correction	5.00	2.0	10.0	5.0
• Power Management	1.00	1.2	0.5	5.0
• Thermal Control	0.10	0.8	1.5	3.0
• Kalman Filter	0.01	8.0	1.0	80.0
<b>(a) Application Subtotal</b>	<b>77.13</b>	<b>59.9</b>	<b>67.2</b>	<b>209.2</b>
<b>Operating System: [8.4]</b>				
• Local Executive	n=240 (1)	3.5	2.0	72.0
• Runtime Kernel (COTS)*		8.0	4.0	N/A
• Input/Output Handlers	m=880 (2)	10.0	3.5	44.0
• Bit/Diagnostics		0.7	0.4	0.5
• Math Utilities		1.2	0.2	N/A
(b) Subtotal: COTS		8.0	4.0	N/A
(c) Subtotal: Non-COTS		15.4	6.1	116.5
(d) Operating System Subtotal	(b) + (c)	<b>23.4</b>	<b>10.1</b>	<b>116.5</b>
(e) Total Software Size and Throughput Estimate	(a) + (d)	83.3	77.3	325.7
<b>Margin Calculations:</b>				
(f) Needed to compensate for requirements uncertainty	100% of non-COTS: 1.0*[(a) + (c)]	75.3	73.3	325.7
(g) On-orbit spare	100% spare: 1.0*[(e) + (f)]	158.6	150.6	651.4
Estimate of computer requirements	(e) + (f) + (g)	<b>317.2</b>	<b>301.2</b>	<b>1,302.8</b>

- \* COTS — commercial-off-the-shelf
- (1) n = number of scheduled tasks per second.  
n = 3 \* 77.13 Hz = 231.39 ~ 240
- (2) m = number of data words handled per second.  
m = 67.2 K words / 77.13 Hz = 871.26 words/sec ~ 880 words/sec

**Table 8.2 Software Requirements for MANS System.** (Wertz, James R., and Wiley, J. Larson, Space Mission Analysis and Design, Microcosm, 1992, p. 627)

Component	Estimation Source	Required Memory		Required Throughput (KIPS)
		Code (K words)	Data (K words)	
<b>Application Functions:</b> [8.3]	Frequency (Hz)			
• Command Processing	10.00	1.0	4.0	7.0
• Telemetry Processing	10.00	1.0	2.5	3.0
• Complex Autonomy	10.00	15.0	10.0	20.0
• Fault Monitors	5.00	4.0	1.0	15.0
• Fault Correction	5.00	2.0	10.0	5.0
• Power Management	1.00	1.2	0.5	5.0
• Thermal Control	0.10	0.8	1.5	3.0
<b>(a) Application Subtotal</b>	<b>41.10</b>	<b>25.0</b>	<b>29.5</b>	<b>58.0</b>
<b>Operating System:</b> [8.4]				
• Input/Output Handlers	m=720 (1)	10.0	3.5	36.0
• BIT and Diagnostics		0.7	0.4	0.5
<b>(b) Subtotal: COTS</b>		<b>0.0</b>	<b>0.0</b>	<b>N/A</b>
<b>(c) Subtotal: Non-COTS</b>		<b>10.7</b>	<b>3.9</b>	<b>36.5</b>
<b>(d) Operating System Subtotal</b>	<b>(b) + (c)</b>	<b>10.7</b>	<b>3.9</b>	<b>36.5</b>
<b>(e) Total Software Size and Throughput Estimate</b>	<b>(a) + (d)</b>	<b>35.7</b>	<b>33.4</b>	<b>94.5</b>
<b>Margin Calculations:</b>				
<b>(f) Needed to compensate for requirements uncertainty</b>	100% of non-COTS: 1.0*[(a) + (c)]	35.7	33.4	94.5
<b>(g) On-orbit spare</b>	100% spare: 1.0*[(e) + (f)]	71.4	66.8	189.0
<b>Estimate of computer requirements</b>	<b>(e) + (f) + (g)</b>	<b>142.8</b>	<b>133.6</b>	<b>378.0</b>

- \* COTS — commercial-off-the-shelf
- (1) m = number of data words handled per second.  
m = 29.5 K words / 41.10 Hz = 717.76 words/sec ~ 720 words/sec

### 8.3.3 Comparison

The software requirements contain three important drivers: required memory, required throughput, and SLOC to be written. These values are compared in Table 8.3. Although the MANS system requires a greater throughput, it should be easier to implement. To eliminate the possibility of an error in computations, the larger values will be used for hardware sizing. This is because the MANS system and the customized system should have approximately the same software.

**Table 8.3 MANS versus Customized System.**

Function	MANS	Customized
SLOC to be written	6,293	13,386
Required Memory (Mbytes)	0.43	0.64
Required Throughput (KIPS)	1,378	1,302.8

#### 8.3.4 Payload Software

Since the throughput for the communication system is expected to be very high, all communications will be sorted with a separate processor. ECHO will receive 7-byte packets at 90 Mbytes/second. This data will arrive at the payload processor where it will be checked for errors by convolutional coding. This code is designed to be run in the background and therefore is very fast and efficient. If the data is error free, the payload processor will then determine its destination. There are three possible destinations: the Moon, the Earth, or one of the satellite's processors. If the data has an error the code will correct it if possible, request retransmission, or if necessary, ignore it. The software requirements for the payload processor are shown in Table 8.4. Here, the number of data words handled per second,  $m$ , has twice the transmission rate, 90 Mbytes/second, added to it. The payload processor will require 0.183 Mbytes of memory, a throughput of 344 KIPS, and a total of 3,756 SLOC in Ada.

#### 8.4 Hardware Selection

With the selection and sizing of the software complete, a decision on system hardware, mainly the CPU's, can be made. Although MANS will most likely be used, the larger software estimate will be used to size the hardware. This is because the MANS system must incorporate all the software in the non-MANS estimate.

**Table 8.4 Payload Software Requirements.** (Wertz, James R., and Wiley, J. Larson, *Space Mission Analysis and Design*, Microcosm, 1992, p. 627)

Component	Estimation Source	Required Memory		Required Throughput (KIPS)
		Code (K words)	Data (K words)	
<b>Application Functions:</b> [8.3]	Frequency (Hz)			
• Fault Monitors	5.00	4.0	1.0	15.0
• Fault Correction	5.00	2.0	10.0	5.0
<b>(a) Application Subtotal</b>	<b>10.00</b>	<b>6.0</b>	<b>11.0</b>	<b>20.0</b>
<b>Operating System:</b> [8.4]				
• Local Executive	n=30 (1)	3.5	2.0	9.0
• Runtime Kernel (COTS)	m=1130 (2)	8.0	4.0	N/A
• Input/Output Handlers		10.0	3.5	56.5
• Bit/Diagnostics		0.7	0.4	0.5
• Math Utilities		1.2	0.2	N/A
<b>(b) Subtotal: COTS</b>	<b>(b) + (c)</b>	<b>8.0</b>	<b>4.0</b>	<b>N/A</b>
<b>(c) Subtotal: Non-COTS</b>		<b>15.4</b>	<b>6.1</b>	<b>66.0</b>
<b>(d) Operating System Subtotal</b>		<b>23.4</b>	<b>10.1</b>	<b>66.0</b>
<b>(e) Total Software Size and Throughput Estimate</b>	<b>(a) + (d)</b>	<b>29.4</b>	<b>21.1</b>	<b>86.0</b>
<b>Margin Calculations:</b>				
<b>(f) Needed to compensate for requirements uncertainty</b>	100% of non-COTS: 1.0*[(a) + (c)]	21.4	17.1	86.0
<b>(g) On-orbit spare</b>	100% spare: 1.0*[(e) + (f)]	50.8	38.2	172.0
<b>Estimate of computer requirements</b>	<b>(e) + (f) + (g)</b>	<b>101.6</b>	<b>76.4</b>	<b>344.0</b>

\* COTS — commercial-off-the-shelf

(1) n = number of scheduled tasks per second.

$$n = 3 * 10.0 \text{ Hz} = 30$$

(2) m = number of data words handled per second.

$$m = 11,261.26 \text{ K words} / 10.00 \text{ Hz} = 1126.13 \text{ words/sec} \sim 1130 \text{ words/sec}$$

This number is high because of the enormous amount of data being transmitted through the processor.

#### 8.4.1 CPU Selection

Since the MANS system requires the Mil-Std 1750A architecture and is written in Ada [8.5], the choices of hardware selection were greatly reduced. The available off-the-shelf technology which had a large enough throughput for the appropriate software is summarized in Table 8.5.



**Table 8.5 Space Qualified Computers.** (Wertz, James R., and Wiley, J. Larson, *Space Mission Analysis and Design*, Microcosm, 1992, p. 626)

Manufacturer	Computer	Word Size (Bits)	Size (cm <sup>3</sup> )	Mass (kg)	Power (W)	Thru-put (MIPS)	Memory (Mbyte)
CDC	444	16	1048	3.2	12	2	3.906
Honeywell	AST III	16	4921	5.2	30	2.5	3
Honeywell	ASCM-CPM	16	5899	8.98	25.3	3	1 to 5
Honeywell	ASCM-ATIM	32	5899	7.8	25	35	2 to 6
Honeywell	ASC/PAM	16	595	0.95	5.1	1.6	0.5
Honeywell	HSC	16	3700	4.5	7.0	1.7	1
IBM	GVSC	16	1280	8.2	23	4.5	3.906
Rockwell	RI-1750A/B	16	2050	2.5	6.6	1.8	3.906

A trade-study was performed to determine which computer best fit the satellite's needs. The equation was determined by ranking size, mass, power, and throughput as the important elements for the computer. Because all computers selected for the trade-study are capable of handling the processing chores adequately, mass was deemed the most important factor and given a weight of 0.4. Mass was determined most important because of the need to minimize it and because of the cost approximation method available. The cost of the CPU's will be directly proportional to mass. Therefore minimizing mass will also minimize cost. The throughput was selected as the second most important factor, since as throughput is increased, processing speed is also increased. Throughput was given a weight of -0.3 and size, being the third most important factor, was given a weight of 0.2. Power was deemed the least important factor because even the worst of the selected CPU's fits well within the power budget for this subsystem. The computer trade study equation is

$$J = 0.2 * (\text{size}) + 0.4 * (\text{mass}) + 0.1 * (\text{power}) - 0.3 * (\text{throughput}) \quad (8.1)$$

Values of one to six were assigned to each attribute (six is high and one is low). Table 8.6 shows the computers considered and their computed trade values.

**Table 8.6 CPU Trade Study.**

Manufacturer	Computer	Size	Mass	Power	Thru-put	J
CDC	444	2	2	4	2	1
Honeywell	AST III	5	3	6	2	2.2
Honeywell	ASCM-CPM	6	6	5	2	3.5
Honeywell	ASCM-ATIM	6	5	5	6	1.9
Honeywell	ASC/PAM	1	1	1	1	0.4
Honeywell	HSC	4	3	2	1	1.9
IBM	GVSC	2	5	5	3	2
Rockwell	RI-1750A/B	3	2	1	1	1.2

Although the Honeywell ASC/PAM is the best computer as determined by the trade-study, its low memory capacity may require a data storage unit (DSU). Because of this, the Control Data Corporation (CDC) 444 was chosen in an effort to keep the system simple and keep the mass and volume low. Although two main computers will be used, one CDC 444 alone can perform the tasks necessary.

#### 8.4.2 Payload Processor Selection

To increase spacecraft autonomy and reliability, an on-board payload processor was added. The payload processor in the despun section will process all incoming data from the antenna to determine its correct destination. Data will have one of three destinations or sources: the lunar surface, an Earth station, or an on-board CPU. In any case, the payload processor will have the responsibility of routing the data to its proper destination. To provide a single level of redundancy, a one-time-only data switch will be installed between the antenna and the payload processor (see Figure 8.1). The payload processor will be monitored by the watchdog timer and if a failure has been detected, the data pathway will be redirected from the payload processor to the despun central processing unit. The CPU will take over the data processing responsibilities with minimal loss to overall station processing rates.

To ensure compatibility with the CDC 444 processors, the payload processor must have a Mil-Std 1750 architecture and an Ada compiler. Table 8.7 shows the available off-the-shelf processors with ample throughput and memory necessary to accomplish the goals of the payload processor.

**Table 8.7 Space Qualified Computers for Role of Payload Processor.**  
(Wertz, James R., and Wiley, J. Larson, *Space Mission Analysis and Design*, Microcosm, 1992, p. 626)

Manufacturer	Computer	Word Size (Bits)	Size (cm <sup>3</sup> )	Mass (kg)	Power (W)	Thru-put (MIPS)	Memory (Mbyte)
CDC	444	16	1048	3.2	12	2	3.906
Honeywell	AST III	16	4921	5.2	30	2.5	3
Honeywell	ASCM-CPM	16	5899	8.98	25.3	3	1 to 5
Honeywell	ASCM-ATIM	32	5899	7.8	25	35	2 to 6
Honeywell	ASC/PAM	16	595	0.95	5.1	1.6	0.5
Honeywell	HSC	16	3700	4.5	7.0	1.7	1
Honeywell	DSBC	16	1200	1.2	4	1.2	0.256
IBM	GVSC	16	1280	8.2	23	4.5	3.906
Rockwell	RI-1750A/B	16	2050	2.5	6.6	1.8	3.906

Because of concern for excess memory to store data sent and received, the same trade study equation used to select the main processors was not used. Although memory was a concern, it was not an overpowering driver. Equation 8.2 shows the payload trade study equation

$$J = 0.1 (\text{size}) + 0.4 (\text{mass}) + 0.1 (\text{power}) - 0.3 (\text{throughput}) - 0.1 (\text{memory}) \quad (8.2)$$

Values of one through six were assigned to each of the above attributes. The best trade-off value will be the lowest. The results of the trade study is presented in Table 8.8.

**Table 8.8 Payload Processor Trade Study.**

Manufacturer	Computer	Size	Mass	Power	Thru-put	Memory	J
CDC	444	2	2	4	2	5	0.3
Honeywell	AST III	5	3	6	2	4	1.3
Honeywell	ASCM-CPM	6	6	5	2	6	2.3
Honeywell	ASCM-ATIM	6	5	5	6	6	0.7
Honeywell	ASC/PAM	1	1	1	1	1	0.2
Honeywell	HSC	4	3	2	1	2	1.3
Honeywell	DSBC	2	1	1	1	1	0.3
IBM	GVSC	2	5	5	3	5	1.3
Rockwell	RI-1750A/B	3	2	1	1	5	0.4

Based on the above results, the best processor for the task is the Honeywell, ASC/PAM. It will have approximately 0.3 Mbytes of excess memory for data storage. If necessary, the CDC 444 can also do the payload processing with no losses to the payload. The only losses will occur in housekeeping.

#### 8.4.3 Hardware Controllers

The hardware controllers are simple devices that route data from the central processors to various subsystem components and back. These controllers are small, lightweight components that are common in satellite system architectures.

The spun section hardware controller will be responsible for the BAPTA and the heater(s). This hardware controller is also connected to the RTG's and thrusters. The hardware controller in the despun section has less responsibility. It will interface with the attitude control sensors and heaters.

#### 8.5 Data Transfer Across the Spin Linkage

Transferring data across the spin linkage is a major concern for the command and data handling subsystem. It will require a system that provides high performance with low risk and low channel noise. The number of channels across the spin linkage has been set at

fourteen. This was determined by assuming that each component linked to the data bus will need to transmit data across the spin linkage at the same time with a single level of redundancy.

To increase the efficiency of the data transfer system, each channel will pass through digital multiplexing equipment before transmission across the spin linkage. This equipment will collect data bit streams from a central processing unit and assign each one a time division. Multiple time divisions can then be transmitted on the same channel across the spin linkage. After transmission, the data bit streams are then passed through digital multiplexing equipment again, where it is decoded for a second central processor. In addition to the transmission of many sources over a single channel, multiplexing provides the additional benefit of processing every source so that they have almost identical formats [8.6]. This permits the transmission equipment, which will carry different types of traffic, to be of a single design type. Data transmission can be accomplished by the use of either the traditional slip ring system or a digital radio link.

### 8.5.1 Slip Ring

The traditional slip ring data transfer utilizes metal rings embedded in the spinning shaft that connects the spun and despun platforms. Spring-loaded brushes in the despun compartment contact the rings and complete the circuit for data transfer. Figure 8.2 shows different views of this type of data transfer system.

A disadvantage to using this system is the high possibility of failure over a long period of time. The first major mode of system failure occurs when the brushes have worn out. Brush lifetime is determined by the amount of conductive material that is mounted to the spring. Friction between the spinning shaft and the contact brush causes the brush material to wear. The faster the spin rate, the faster the brush will wear. Once all of the conductive material has worn off of the brush, there is no electrical contact and the channel is no longer usable.

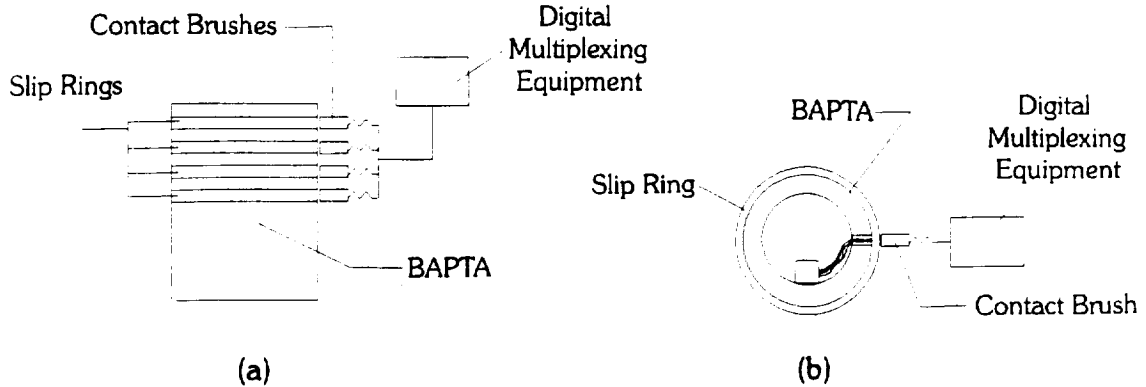


**Figure 8.2 Slip Ring Data Transfer: (a) internal view, (b) cross-sectional view.**

This failure is directly related to a second mode of failure; short circuits due to metallic deposits. As the metallic brushes wear, dust collects in the despun compartment. As this dust deposits on the slip rings, a conductive link will form between the channels. Once enough dust has been deposited, the effected channels will be disabled from the resulting short circuit. An advantage to slip ring data transfer is low system noise. Any white noise that is introduced into the system, because of the metal on metal contact, can be filtered out in the receiver and digital multiplexer.

### 8.5.2 Digital Radio Link

The elements of a generalized digital radio link are shown in Figure 8.3. Note that this system consists of an information source, an encoder and a decoder, and an information receiver, all connected by a data transmission system. This transmission system will consist of a transmitter and receiver on both sides of the spin linkage to provide a two-way transmission path.

Two major advantages of using a digital radio link is first, its high reliability and second, its performance. The solid state hardware is durable and will not physically wear

out. Failures can occur however, because of severe power spikes and overheating. As with all electronics, it will be very important for the power and thermal subsystems to regulate voltage and temperature on-board the satellite.

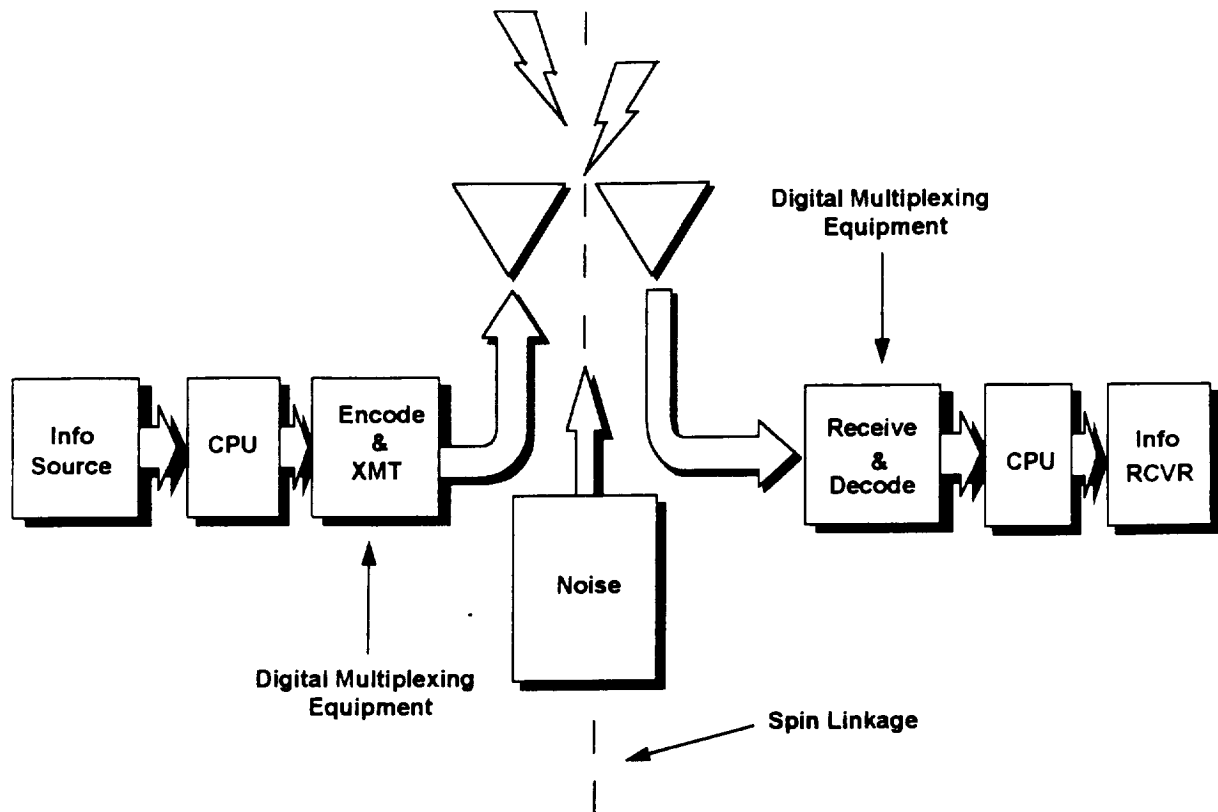


**Figure 8.3 Generalized Digital Radio Link System.**

A major disadvantage to a digital radio link is the noise that can be introduced into the system. Radio frequency propagation is affected by absorption, reflection, refraction, thermal, and intermodulation noise. Thermal noise is caused by a resistance and intermodulation noise is caused by system non-linearities and signal losses [8.7].

### 8.5.3 Data Transfer System Trade Study

Data transfer on ECHO will be accomplished using the digital radio link system. This selection was based on a trade study of the slip ring and radio link systems. A specific trade

value equation was formed to rate the systems. High performance was considered an advantage, while high risk, cost, and noise were considered disadvantages. These areas of concern were then rated on a scale of 1.0 to 2.0, one being the lowest and two being the highest. The system with the highest trade value would be considered the best selection for ECHO. Equation 8.3 was used for this trade study. The results are shown in Table 8.9.

$$J = 0.3 * (\text{performance}) - 0.3 * (\text{risk}) - 0.25 * (\text{cost}) - 0.15 * (\text{noise}) \quad (8.3)$$

**Table 8.9 Data Transfer System Trade Study.**

System	Performance	Risk	Noise	Cost	J
Radio Link	2	1	2	2	-0.5
Slip Ring	1	2	1	1	-0.7

The digital radio link system has a trade study value of -0.5, making it the best choice for this mission. This system, however, must be designed to overcome the problem of noise before it can be used on ECHO.

## 8.6 Operational Lifetime

In an effort to increase the operational lifetime of ECHO, a watchdog timer will be integrated into the command and data handling subsystem. This timer will provide a method of determining a computer failure independent of the processor itself by checking hardware and software alike. In addition, a class 'S' parts program will be implemented over the less reliable class 'B' parts program. This decision will increase the operational lifetime of the satellite without an increase in the amount of hardware; however, material cost will increase.



## 8.7 Channel Sizing

An important consideration in hardware sizing and selection is the number of signal channels throughout the satellite. This was determined by a consistent method of assigning channels to each device on the satellite. It was assumed that each channel could carry one data stream for a given device. The numbers of channels was determined as follows: one channel was assigned to each sensor in order to monitor sensor input, a second channel was provided for redundancy; two channels are assigned to each device that must be activated, one channel to activate the device and another to monitor the device, and again two redundant channels are provided for a total of four. Following this standard, channel totals were estimated for the entire satellite.

Attached to the despun hardware controller are the spin motors. Exact details about these motors are unavailable at this time. The conservative estimate is for two motors. Following the above convention, this would require eight channels. Also attached to this controller may be heaters necessary for thermal control. A conservative estimate was to allow for twelve channels accommodating up to three devices. Another eight channels will be required by the two Attitude Control System (ACS) sensors. The total number of channels for the despun hardware controller is therefore twenty-eight.

The support function, or sensor ring will be attached to twenty-five thermal sensors. This then gives a total of fifty channels to monitor temperature gradients in the despun section and fifty channels in the spun section as these two rings will be identical. An actual number of strain gauges to monitor structural integrity has not been supplied. Therefore, twenty-five such sensors were assumed for another fifty channels in each section. This brings the ring channel totals to one-hundred.

The hardware controller in the spun section will support the majority of the on-board devices. Among these devices are the four control thrusters. Four channels per thruster were assigned to the propulsion subsystem as requested which is consistent with the established channel sizing method for a total of sixteen channels. The two spin motors for thruster

pointing will require another eight channels. In addition, fifty channels will be assigned to the RTG's (this includes any channels necessary to accommodate the deployable booms). Heaters are also located in the spun section. As with the despun section, twelve channels are assumed sufficient to handle these functions. The propulsion subsystem requires a constant pressure in the propellant tanks. Valves and inflatable bladders in the tanks will be used to accomplish this task. Channels have been assigned to control the propellant flow and bladder volume. Therefore, at this point, it will be assumed the spun section hardware controller will need to handle 108 input channels.

The only remaining channel requirements to consider are for the payload processor and the antenna. It was specified by mission requirements that there are to be six communication channels. For redundancy the payload processor will need to handle twelve communication channels. Additionally, two channels are assigned to monitor the antenna itself to determine if it is functioning properly.

## 8.8 Budgets

The cost, mass, and power budgets have all been determined. Mass for the command and data handling system is broken into individual component masses and is detailed in Section 8.8.1. The power budget, located in Section 8.8.2, consists of peak operating power requirements for individual system components. Finally, the cost of the command and data handling subsystem was determined using the Cyr Cost Estimation Method [8.8]. The cost budget is detailed in Section 8.8.3.

### 8.8.1 Mass Budget

Conservative mass requirements for the command and data handling subsystem on-board the satellite are presented in Table 8.10. The figures include a contingency factor of 10% to account for wiring and harness masses.

**Table 8.10 Mass Budget for C&DH.**

Component	Mass (kg)
CDC 444 Processors (2)	7.1
Honeywell ACS/PAM Payload Processor	1.1
Data Transfer System	4.2
Hardware Controllers (2)	2.2
Data Switch	0.1
<b>Total Mass</b>	<b>14.7</b>

### 8.8.2 Power Budget

Table 8.11 presents the power budget for the command and data handling subsystem. These values have a 10% built-in contingency for power loss and system efficiency.

**Table 8.11 Power Budget for C&DH.**

Component	Power (W)
CDC 444 Processors (2)	26.8
Honeywell ACS/PAM Payload Processor	6.3
Data Transfer System	16.9
Hardware Controllers (2)	8.2
<b>TOTAL</b>	<b>58.2</b>

### 8.8.3 Cost Budget

Cost figures were estimated using the Cyr cost modeling program and it should be noted that the figures given here are very liberal estimates. The total cost for the design, testing, and production of the command and data handling subsystem is approximately \$14.1 million FY99 (as the expected launch date is set for 1999). Although this value is rather

high, it should be noted that, for the Cyr model, the cost of a component increases with its mass. This may be true in most cases, but this is not so for computers. Three sets of each component are needed for testing, production and backup purposes. See Table 8.12 for a break down of individual component costs.

**Table 8.12 Cost Budget for C&DH.**

Component	Cost (M\$, FY99)
CDC 444 Processors (6)	7.1
Honeywell ACS/PAM Payload Processor (3)	2.2
Hardware Controllers (6)	1
Data Switches (6)	0.01
Digital Radio Link System (3)	3.8
<b>TOTAL</b>	<b>14.1</b>

A generation factor of 5 was used for the components. This is due to their space rated nature of the components.

### 8.9 Conclusion

A pair of CDC 444 computers have been chosen to manage the processing and data routing needs of ECHO's command and data handling system. A single Honeywell ACS/PAM payload processor will have the responsibility of controlling the uplink and downlink functions. For an added level of redundancy, a one-time data switch is positioned between the payload processor and the antenna. In the event of a payload processor failure, uplink and downlink functions will be transferred to the despun CDC 444 processor.

A bus architecture will be used as the primary architecture type and will be combined with both smaller centralized and ring type architectures to efficiently transfer the data between components and subsystems. Two hardware controllers will interface between the

data bus and spacecraft hardware. In addition, data bus continuity across the spin linkage will be accomplished using a digital radio link system.

#### 8.10 References

- [8.1] Wertz, J.R. and Larson, W.J., eds, Space Mission Analysis and Design, 2nd ed., Microcosm, Inc., Kluwer Academic Publishers, 1992, p. 621.
- [8.2] Wertz, p. 623.
- [8.3] Wertz, p. 621.
- [8.4] Wertz, p. 623.
- [8.5] Hansen, Jane L., "A Scalable Architecture for an Operational Spaceborn Autonav System," Advances in the Astronautical Sciences, Guidance and Control 1991, pp. 39-52,
- [8.6] Townsend, A. R., Digital Line of Sight Radio Links, Prentice Hall International, 1988, p. 133.
- [8.7] Killen, Harold B., Digital Communications with Fiber Optics and Satellite Applications, Prentice Hall International, 1988, p. 219.
- [8.8] Cyr, Kelley, "Cost Estimation Methods for Advanced Space Systems," NASA Johnson Space Center, 1988.

## **9.0 Communications Subsystem**

### **9.1 Introduction**

The purpose of Project ECHO (Electronic Communications from Halo Orbit) is to provide communication and data relay services from the far side of the Moon to an Earth ground station. In the halo orbit, the satellite will maintain line-of-sight contact with the Moon's far side and with the Earth. This section contains a detailed summary of the investigation and design of the communications subsystem.

The communications subsystem is to provide a minimum of six channels allocated in the following manner: two voice, one color video, one telemetry, one command, and one scientific. In order to increase reliability, reduce cost, and reduce complexity in the guidance, navigation, and control subsystem, one fixed antenna with two offset feed arrays will be used to point the surfaces of both the Moon and the Earth. A multiplexer must be used to combine the channels, since one antenna will be used. The NASA Deep Space Network (DSN) will maintain the ground support for the communications satellite.

### **9.2 Ground Support**

The ground system's main function is to support the space segment and to relay mission data from the spacecraft to the user. The NASA Deep Space Network (NASA DSN) will be used to support the communications satellite of Project ECHO. The NASA DSN has a state-of-the-art telecommunications system that can be upgraded to meet the requirements of new missions, such as Project ECHO, while maintaining support for current missions [9.1].

### 9.2.1 NASA DSN

The NASA Deep Space Network is the largest and most sensitive scientific telecommunications and radio navigation network in the world [9.1]. The network consists of the three Deep Space Communications Complexes, each positioned on a different continent. These three complexes are located at Goldstone in Southern California's Mojave Desert; Madrid, Spain; and Canberra, Australia. The Deep Space Facilities are approximately 120 degrees apart in longitude, which will ensure continuous observation and suitable overlap for transferring the radio link from one complex to the next [9.2]. The communication link between the ground stations are via land lines, submarine cable, terrestrial microwaves, and communication satellites. Spacecraft data sent over these lines are automatically checked for transmission error [9.3]. The Operations Control Center is located at the Jet Propulsion Laboratory in Pasadena, California.

Each Deep Space Communications Complex contains four stations equipped with four steerable, high-gain parabolic antennas: one 26-meter diameter, two 34-meter diameter, and one 70-meter diameter [9.4]. One of the 34-meter diameter antennas will be used for the deep space mission of ECHO. This antenna will transmit and receive the command and telemetry frequencies.

### 9.2.2 Frequency Ranges

The NASA Deep Space Network uses the S (2.025-2.120 GHz) and X (7.145-7.190 GHz) band frequency ranges to transmit the command (uplink) data to satellites. To receive information from satellites, the DSN uses the 2.2-2.3 GHz and 8.4-8.5 GHz frequency ranges. In addition, the DSN has specific data rate ranges for the telemetry [9.5]. The frequency and data rate ranges for the command (uplink) and telemetry (downlink) must be similar to the data rates and frequencies chosen by the Command and Data Handling subsystem and required by the various channels.

ECHO will use an 8.4 GHz frequency to transmit the telemetry and scientific data to the Earth ground stations. This frequency was based on the following equation

$$\phi = \frac{2l}{fd} \quad (9.1)$$

The antenna diameter,  $d$ , was desired to be as near to 1 m as possible, and the beam width,  $\phi$ , was fixed at 3 degrees. Therefore, the downlink frequency,  $f$ , was determined to be 8.4 GHz. The uplink frequency from Earth will be 7.185 GHz. The uplink and downlink frequencies must be applied for and approved by the NASA Deep Space Network before ECHO is launched [9.6]. The downlink frequency from the communications satellite to the Moon will be in the S-band frequency range (2.8 GHz). The command frequency from the Moon to the satellite will depend on the antenna facilities on the Moon.

### 9.2.3 Ground Segment and Operations Costs

The costs for the various elements of the ground stations are based upon a typical distribution of costs between software, equipment, facilities, logistics, and several system levels [9.7]. These costs are based upon a percentage of the total software development costs: flight software and ground software. The software development costs are based on thousand-lines-of source code, KLOC. The flight and ground software cost equations (in K\$, FY92) are shown below [9.7]:

$$\text{Flight Software Cost} = 375 \times \text{KLOC} \quad (9.2)$$

$$\text{Ground Software Cost} = 190 \times \text{KLOC} \quad (9.3)$$

KLOC is a function of the memory capacity of the computer being used by ECHO. The computer chosen by the C&DH subsystem group is the CDC 444, which has a memory of



3,906 Mbytes, can supply words at a length of 16 bits, and uses the high order language Ada [9.8]. The conversion from bytes to KLOC is shown below:

$$3.906 \times 10^6 \text{ bytes} = 70 \text{ KLOC} \quad (9.4)$$

The conversion also includes a 25% factor because developing a data word takes about one quarter of the effort for developing a word of executable code [9.9].

The 70 KLOC is used to find the total software development costs from Equations 9.2 and 9.3. Then, the total software cost is distributed by a certain percentage to the ground station elements shown in Table 9.1. The total cost of the ground segment and operations, shown in Table 9.1, is approximately \$50.7 million. This cost is assumed to include approximately \$4.0 million in 1999 dollars, since ECHO only requires ground support for one month.

**Table 9.1 Ground Segment and Operations Costs (M\$,FY99).** (Larson, W.J. and Wertz, J.R., Space Mission Analysis and Design, 2nd edition, Kluwer Academic Publisher, 1992, pp. 730,737.)

Element	Cost Distribution (%)	Cost (M\$,FY99)
Software (Ada)	33	16.6
Equipment	27	13.7
Facilities	6	3.0
Management	6	3.0
Systems Engineering	10	5.1
Product Assurance	5	2.6
Integration and Test	8	4.1
Logistics	5	2.6
<b>TOTAL</b>		<b>50.7</b>

### 9.3 Channels

In order to maximize the efficiency and future applicability of this satellite, a minimum of six transmission channels is required in the communications system design. These include one color video channel, two voice channels, one telemetry channel for scientific payloads on the lunar surface, one telemetry channel for the housekeeping of the satellite, and one channel for uplinked commands.

#### 9.3.1 Data Rates

The data rates were selected to fulfill the various channel requirements and for compatibility with the Command and Data Handling system. For ECHO, the channel data rates are 44 Mbps (bits per second) for the color video channel, 64 kbps for each voice channel [9.11], and 1000 bps for uplinked commands [9.5]. A study of various scientific instruments, including mappers, dust counters, and samplers used on a comet sample recovery satellite yielded a projected data rate of 40.35 Mbps for the scientific data [9.12]. This number allows for a wide range of scientific payloads that can be used on the lunar surface.

#### 9.3.2 Channel Design

A rotating schedule will be used to transmit the data from the color video channel and some of the scientific payloads since the data rates for the color video channel and some of the scientific instruments are in the 40 Mbps range. Since ECHO is designed to be semi-autonomous, the housekeeping channel was incorporated into the communications system design primarily to check pointing accuracy on a predetermined schedule. A data rate of 1000 bps was chosen to cover this transmission.

#### 9.4 Modulation and Coding

Several modulation schemes were investigated including amplitude, phase, frequency, and polarization. In order to determine which method was most suitable, a trade study equation (Equation 9.5), where 1 is a low value and 4 is high, was developed to quantify objectives and decisions.

$$J = -0.4(\text{Bit error rate}) - 0.3(\text{Spectrum utility}) - 0.15(\text{Performance}) + 0.15(\text{Complexity}) \quad (9.5)$$

One of the major objectives in choosing the modulation scheme was to keep the frequency spectrum small to avoid interference. Other driving factors include limiting power requirements and transmitter size, and reducing antenna mass. Amplitude modulation requires larger transmitters that cannot operate at saturation for maximum power efficiency [9.13]. Therefore, amplitude modulation was excluded from the possibilities. Although polarization modulation allows for frequency reuse, it requires expensive antennas, and was not chosen. Since frequency modulation increases the frequency spectrum and has poor spectrum utilization, it too was removed from consideration. Thus, phase shift keying will be used.

Several types of phase shift keying are available; however, many compromises must be made. Phase shift keying is susceptible to phase disturbances. The effect of this distortion can be reduced using differential phase shift keying (DPSK) [9.14]. Although DPSK decreases the phase disturbances, it requires a higher signal-to-noise ratio to maintain the same bit error rate. One way to overcome this problem is to introduce forward error correction coding [9.15]. Unfortunately, the extra error correction bits increase the bit rate and hence the transmission bandwidth. For example, the binary phase shift keying (BPSK) modulation scheme plus a rate 1/2 convolutional coding scheme would result in half the spectrum utilization of stand-alone BPSK modulation. Since the data rates are already high and the bandwidth is already wide, a modulation scheme with a more efficient spectrum

utilization is desirable. Quadriphased phase shift keying (QPSK) is one such scheme for reducing the spectrum width. In fact, QPSK reduces the spectrum by one half. Thus, a signal rate doubled by R-1/2 convolutional coding could be made to fit in the same spectrum by using QPSK. Since QPSK provides excellent use of the spectrum and R-1/2 convolutional coding decreases the signal-to-noise ratio required, both will be used. A trade study illustrated in Table 9.2 leads to the same conclusion.

**Table 9.2 Trade Study on Modulation and Coding.**

Modulation	BER (C1)	Spec. Ut. (C2)	Perform. (C3)	Complex. (C4)	Trade Value (J)
BPSK	2	3	2	2	-1.7
DPSK	1	3	1.5	2	-1.225
QPSK	2	4	3	2	-2.15
FSK	1	1	1	2	-0.55
8FSK	2	2	1	1	-1.4
BPSK,R-1/2	3	2	3	3	-1.8
QPSK,R-1/2	3	3	4	3	-2.25
8FSK,R-1/2	4	1	3	3	-1.9
BPSK,RS	4	2	4	4	-2.2

Since the coded information will be corrected before retransmission, a decoder is necessary. The optimum decoding of convolutionally coded sequences can be carried out using the Viterbi algorithm [9.16]. A soft-decision decoder offers an additional coding gain of about 2 dB over hard-decision decoding [9.17]. In addition, information is generally forwarded in quantized packets; typically, a packet contains 7 code words (K=7, in this case, means 28 bits). Thus the modulation and coding scheme can be summed up as QPSK plus R-1/2, K=7, Viterbi soft decoding.

## 9.5 Link Design for ECHO

The link equation was used in order to quantify many of the communications subsystem parameters. These calculations were done for each of the six channels used on ECHO. The basic equation used for link design was

$$\frac{E_b}{N_o} = \frac{PL_tG_tL_sL_aG_r}{kT_sR} \quad (9.6)$$

In this equation,  $E_b/N_o$  is the received energy-per-bit to noise density,  $P$  is the transmitter power,  $L_t$  is line loss,  $G_t$  is transmitter gain,  $L_s$  is space loss,  $L_a$  is path loss,  $G_r$  is receiver gain,  $k$  is Boltzmann's constant,  $T_s$  is system noise temperature,  $R$  is the data rate [9.18]. Since the modulation and coding scheme is QPSK plus R-1/2, K=7, Viterbi soft decoding, the data rates of each channel must be twice the information rate [9.19].

### 9.5.1 Satellite Downlinks

Since ECHO will be using the NASA Deep Space Network (NASA DSN) for transmissions from the satellite to Earth, downlink frequencies are restricted to X- or S-band frequencies. In order to keep the diameter of the satellite antenna at 1.0 m or less while decreasing the beamwidth, the satellite to Earth frequency will be set to the X-band (7.145-7.190 GHz). Transmissions between the satellite and the Moon will use the S-band (2.025-2.120 GHz). All transmissions from the satellite to the Earth will be received on the NASA DSN 34 m antenna. Table 9.3 contains the link equation results for all of the satellite downlinks [9.19]:

Video Channel — The video channel has an information rate of 44 Mbps (a data rate of 88 Mbps) and has to be transmitted 450262 km. As shown in the table, transmissions of this channel will require the system to operate at the peak power of 20 W output, requiring 85 W input.

Scientific Payloads — The channel for scientific equipment on the lunar surface has a data rate of 75 kbps and will use 5 W output (30 W input) for transmission.

**Table 9.3 Downlink Budgets for ECHO.** (Wertz, J.R. and Larson, W.J., *Space Mission Analysis and Design*, 2nd Edition, Kluwer Academic Publishers, 1993, p. 536.)

Item	Symbol	Video ECHO-Earth	Voice ECHO-Earth	Voice ECHO-Moon	Scientific ECHO-Earth	Telemetry ECHO-Earth
Beamwidth	Q (deg)	3	3	9	3	3
Antenna Diameter	$D_t$ (m)	0.83	0.83	0.83	0.83	0.83
Peak Gain	$G_{pt}$ (dB)	34.8	34.8	25.2	34.8	34.8
Gain	$G_t$ (dB)	34.4	34.4	25.2	34.4	34.4
Frequency	f (GHz)	8.4	8.4	2.8	8.4	8.4
Pointing Error	$e_t$ (deg)	0.5	0.5	0.5	0.5	0.5
Pointing Loss	$L_{pt}$ (dB)	-0.33	-0.33	-0.04	-0.33	-0.33
Line Loss	$L_l$ (dB)	-1	-1	-1	-1	-1
Propagation Loss	$L_a$ (dB)	-0.5	-0.5	0	-0.5	-0.5
Equivalent Isotropic Radiated Power	EIRP (dBW)	46.4	40.4	31.2	40.4	33.4
Received energy/bit noise density	$E_b/N_o$ (dB)	10.5	32.9	31.2	29.2	43.9
Carrier to Noise	$C/N_o$ (dB-Hz)	89.9	83.9	82.3	83.9	76.9
Implementation Loss	Imp Loss (dB)	-2	-2	-2	-2	-2
Margin	M (dB)	3.0	25.4	23.7	21.7	36.4
Received energy/bit to noise density	$E_b/N_o$ req (dB)	5.5	5.5	5.5	5.5	5.5
Bit error rate	BER	10e-7	10e-7	10e-7	10e-7	10e-7
Transmitter Power	P(W)	20	5	5	5	1
Transmitter Power	P(dB)	13.0	6.9	6.9	6.9	0
System Temp.	$T_s$ (K)	552	552	552	552	552
Gain	$G_r$ (dB)	66.8	66.8	26.7	66.8	66.8
Peak Gain	$G_{pr}$ (dB)	66.9	66.9	26.7	66.9	66.9
Pointing Loss	$L_{pr}$ (dB)	-0.12	-0.12	-0.12	-0.12	-0.12
Beamwidth	Q (deg)	0.07	0.07	7.5	0.07	0.07
Pointing Error	$e_r$ (deg)	0.007	0.007	0.75	0.007	0.007
Antenna Diameter	$D_r$ (m)	34	34	1	34	34
Space Loss	$L_s$ (dB)	-223	-223	-176	-223	-223
Data Rate	R (bps)	88000000	128000	128000	300000	2000
Path Length	S (km)	450262	450262	73384	450262	450262

High Data Rate Scientific Payloads — Some lunar scientific payload equipment may have high information rates, such as an IR spectral mapper (40 Mbps), and will require higher power to be transmitted from the satellite to Earth. Any scientific equipment with a data rate larger than 75 kbps will be transmitted through the color video channel to avoid having to open two high data rate channels.

Two Voice Channels — Each of the pulse code modulated voice channels will have an information rate of 64 kbps and will use 5 W output for transmission. Transmissions from the satellite to the lunar surface will require receiving antenna of 1.0 m or larger.

Telemetry Channel — The telemetry channel has an information rate of only 1000 bps (a data rate of 2000 bps) and will require only minimal power (1 W output, 15 W input) to be transmitted to the NASA DSN 34 m antenna. The data rate for telemetry was kept low since the satellite is designed to be fully autonomous and frequent contact will not be necessary.

## 9.5.2 Satellite Uplinks

As stated in Section 9.5.1, ECHO will be using the X-band of frequencies for transmissions between the satellite and the Earth and the S-band of frequencies for transmissions between the satellite and the Moon. Since power and antenna size are not as important for Earth stations as for lunar stations, the uplink section focuses on the uplinks from the Moon to the satellite [9.20].

Video Channel - In order to transmit the video channel from the Moon to the satellite at an excursion, the Moon station will need a 3.26 m antenna and 280 W output power (700 W input power) as shown in Table 9.4. If the video channel is only transmitted while the satellite is within 3500 km of the L<sub>2</sub> point, the output power and input power are reduced to 200 W and 450 W respectively. Therefore, any lunar mission wanting to transmit color video will need to develop a video transmission schedule tailored to its power capabilities.

Remaining Moon-Satellite Uplinks - As shown in Table 9.4, the voice, scientific, and telemetry channels can be transmitted from the Moon to the satellite with a 1.25 m antenna and 10 W output power, 30 W input power. Therefore, if the lunar station does not need to transmit color video or scientific data with an information greater than 150 kbps, it can be equipped with a smaller antenna and use less power.

**Table 9.4 Uplink Budgets for ECHO.** (Wertz, J.R. and Larson, W.J., *Space Mission Analysis and Design*, 2nd Edition, Kluwer Academic Publishers, 1993, p. 536.)

Item	Symbol	Video Moon-ECHO	Voice Moon-ECHO	Scientific Moon-ECHO	Telemetry Moon-ECHO
Beamwidth	Q (deg)	2.3	6	6	6
Antenna Diameter	$D_t$ (m)	3.26	1.25	1.25	1.25
Peak Gain	$G_{pt}$ (dB)	37.0	28.7	28.7	28.7
Gain	$G_t$ (dB)	36.97	28.72	28.65	28.65
Frequency	f (GHz)	2.8	2.8	2.8	2.8
Pointing Error	$e_t$ (deg)	0.2	0.2	0.5	0.5
Pointing Loss	$L_{pt}$ (dB)	-0.09	-0.01	-0.08	-0.08
Line Loss	$L_l$ (dB)	-1	-1	-1	-1
Propagation Loss	$L_a$ (dB)	0	0	0	-0.5
Equivalent Isotropic Radiated Power	EIRP (dBW)	60.45	37.72	27.65	27.65
Received energy/bit noise density	$E_b/N_o$ (dB)	8.58	14.23	10.46	31.72
Carrier to Noise	$C/N_o$ (dB-Hz)	88.02	65.30	65.23	64.73
Implementation Loss	Imp Loss (dB)	-2	-2	-2	-2
Margin	M (dB)	1.08	6.73	2.96	24.22
Received energy/bit to noise density	$E_b/N_o$ req (dB)	5.5	5.5	5.5	5.5
Bit error rate	BER	10e-7	10e-7	10e-7	10e-7
Transmitter Power	P(W)	280	10	10	10
Transmitter Power	P(dB)	24	10	10	10
System Temp.	$T_s$ (K)	552	552	552	552
Gain	$G_r$ (dB)	25.10	25.10	25.10	25.10
Peak Gain	$G_{pr}$ (dB)	25.22	25.22	25.22	25.22
Pointing Loss	$L_{pr}$ (dB)	-0.12	-0.12	-0.12	-0.12
Beamwidth	Q (deg)	9	9	9	9
Pointing Error	$e_r$ (deg)	0.9	0.9	0.9	0.9
Antenna Diameter	$D_r$ (m)	0.83	0.83	0.83	0.83
Space Loss	$L_s$ (dB)	-199	-199	-199	-199
Data Rate	R (bps)	88000000	128000	300000	2000
Path Length	S (km)	73384	73384	73384	73384



## 9.6 Antenna

For communications between the satellite and Earth, the satellite for Project ECHO needs to have high-gain capabilities due to the distances involved in the stationkeeping-free orbit (35,000 km at the farthest point of the elliptical halo orbit). The purpose for choosing a high-gain antenna as opposed to a low-gain antenna is due to the mission constraints, most notably the cost of the project.

### 9.6.1 Antenna for Communications in Halo Orbit

Through an antenna trade study (shown in Table 9.5), the antenna that will be used on the mission for high-gain transmission is the parabolic reflector offset shaped sub-reflector with feed array (The highest trade value gave the appropriate antenna to use for the mission). Equation 9.7 shows the performance index equation for the antenna trade study. The parameters for the trade study were set at Aperture Blockage (0.40), Weight (0.30) and Risk (0.30). Note - the higher the  $K_i$  value for a specific parameter, the better that parameter is for that antenna [9.21].

$$J = K_1(\text{Aperture Blockage}) + K_2(\text{Weight}) + K_3(\text{Risk}) \quad (9.7)$$

**Table 9.5 Antenna Trade Study for High-Gain Communication Between the Satellite and Earth.**

Antenna	Aperture Blockage, $K_1$	Weight, $K_2$	Risk, $K_3$	J
Parabola Offset Feed	4	3	4	3.7
Parabola w/ Feed Array	3	4	2	3.0
Parabola Center Feed	1	2	1	1.3
Parabola Cassegrain	2	2	4	2.6

### 9.6.2 Beam Coverage

Multibeam beam coverage is a requirement for this mission because of the distances involved; full coverage of the Earth and the Moon is not possible with a single beam of any antenna type, but smaller losses of coverage are incurred with the use of a parabolic reflector offset shaped sub-reflector with feed array. Phased arrays were investigated for this subsystem design, but were not used because of their high cost and mass (to fulfill mission requirements, the phased array would weigh approximately 300 kg and have a cost far exceeding that of the offset feed array).

Figures 9.1 and 9.2 illustrate how the beams for each of the links will cover the required surfaces. The beamwidths for the Earth and Moon links will be three degrees and nine degrees, respectively. These wide beamwidths will enable the beams to maintain coverage from any point in the orbit without being steered along the minor axis of the orbit. From the top view, as shown in Figure 9.2, it is evident that the beams must be steered, or scanned, along the major axis of the orbit in order to maintain suitable coverage. Since, a feed array can only steer a beam by a maximum scan angle of ten degrees, the Bearing and Power Transfer Assembly (BAPTA) will have to point the antenna to a position between the Earth and the Moon where the scan angles required for the beams to paint the Earth and Moon are less than ten degrees. At each orbit excursion, the satellite will not be able to cover 15% of the far side of the Moon.

### 9.6.3 Antenna Usage for Halo Orbit Insertion

The coverage area and the gain of the communications transmission were the deciding factors in determining which antenna would be used for the transfer orbit (after deployment from the third stage of the Delta rocket). The choices were limited to a few small low-gain antennas (a low-gain antenna system was chosen because of its small size and mass, as opposed to the high-gain antenna) because of the distance involved (approximately 450000 km). Furthermore, the antenna chosen for the orbit insertion communications could act as a

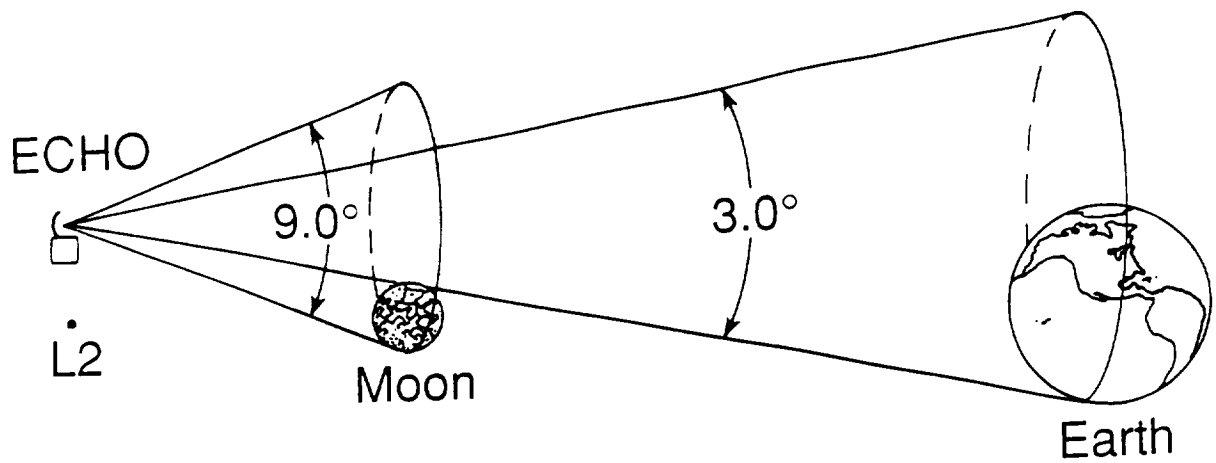


Figure 9.1 Side View of Beam Coverage for Moon and Earth Links.

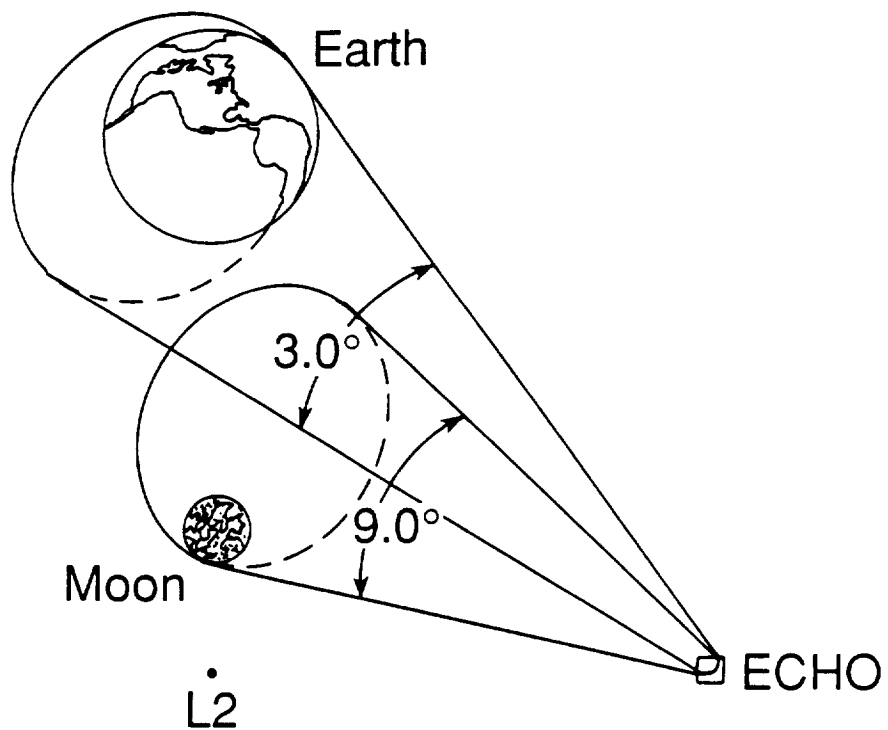


Figure 9.2 Top View of Beam Coverage for Moon and Earth Links.

back-up, in case of failure by the high-gain antenna. A trade study, shown in Table 9.6, was performed to appropriately choose the antenna that would be used on the satellite. The weighting factors for the performance index equation, Equation 9.8, were set for Gain (0.35), Beamwidth (0.20), Mass (0.25) and Reliability (0.20). As seen from the trade study, the antenna that will be used is the dipole for low-gain transmission during transfer orbit (the antenna with the highest trade value was the one chosen). Note - the higher the  $K_i$  value for a specific parameter, the better that parameter is for that antenna [9.22].

$$J = K_1(\text{Gain}) + K_2(\text{Beamwidth}) - K_3(\text{Mass}) + K_4(\text{Reliability}) \quad (9.8)$$

**Table 9.6 Trade Study for Low-Gain Antenna Communications During the Transfer Orbit.**

Antenna	Gain	Beamwidth	Mass	Reliability	J
Quad Helix	2	2	2	3	1.2
Conical Log Spiral	1	4	3	4	1.2
Horn	4	2	1	2	1.95
Dipole	3	3	1	4	2.2

## 9.7 Multiplexer

The same high-gain antennas that were used for communications between the satellite and the Earth will also be used for the communications between the Moon and the satellite with the use of a multiplexer. The two most common multiplexers are the Frequency Division Multiple Access (FDMA) in which a fraction of the frequency bandwidth is allocated to every user all the time, and the Time Division Multiple Access (TDMA) in which the entire bandwidth is used by each user for a fraction of the time [9.23]. A trade study, shown in Table 9.7, was performed to determine which multiplexer was appropriate for the mission. The parameters for the trade study were set at Performance (0.35), Cost (0.35) and Transmitter Power (0.30). Note, the higher the  $K_i$  value for a specific parameter,

the better that parameter is for that antenna). Equation 9.9 shows the performance index equation used for the trade study. The multiplexer that will be used on the mission for communications transmission is the Frequency Division Multiple Access (The highest trade value gave the appropriate multiplexer to use for the mission).

$$J = K_1(\text{Performance}) + K_2(\text{Cost}) + K_3(\text{Transmitter Power}) \quad (9.9)$$

**Table 9.7 Multiplexer Trade Study.**

Multiplexer	Performance K <sub>1</sub>	Cost, K <sub>2</sub>	Transmitter Power, K <sub>3</sub>	J
Frequency Division Multiple Access	1	2	2	1.65
Time Division Multiple Access	2	1	1	1.35

## 9.8 Amplifiers

ECHO's communication system will require the use of an amplifier. Two types of amplifiers under consideration are a solid-state amplifier and a traveling wave tube amplifier (TWTA). A trade study was conducted between these two amplifiers to determine the best type for use by ECHO.

The elements that will determine the best amplifier type are mass, input power, output power, power efficiency, and reliability. The performance index equation including the weighting factors is shown below.

$$J = 0.3(\text{Mass}) + 0.2(\text{In. Power}) - 0.2(\text{Out. Power}) - 0.2(\text{Power Eff.}) - 0.1(\text{Relbty.}) \quad (9.10)$$

The mass element received the highest weighting factor, because ECHO has a mass budget constraint. Each of the power elements received the same weighting factors, because they are

a function of each other. Figure 9.3 shows the relationship between a solid-state amplifier and a TWTA based on the elements listed above.

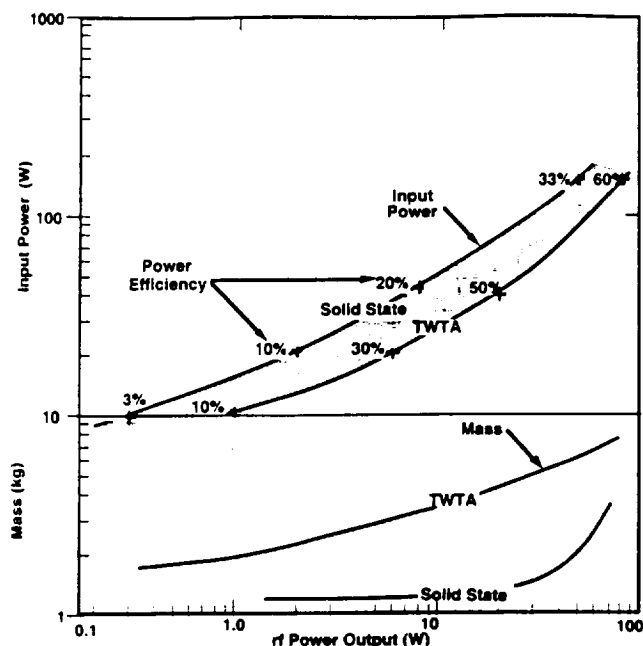


**Figure 9.3 Satellite Transmitter Power and Mass Versus rf Power Output.** (Wertz, J.R. and Larson, W.J., *Space Mission Analysis and Design*, 2nd edition, Kluwer Academic Publisher, 1992, p. 543.)

The values for each element in Equation 9.10 ranged from 1 to 2. A two indicated a "high" value while a one indicated a "low" value. Figure 9.3 supports the reasoning for the value selections for each element in Table 9.8. A 'two' was given to the solid-state amplifier for reliability, because solid-state amplifiers are more reliable than the TWTA, mostly because they require lower voltages [9.24].

**Table 9.8 Trade Study of Amplifiers.**

Amplifier	Mass	Input Power	Output Power	Power Efficiency	Reliability	J
Solid-State	2	1	2	1	2	-0.3
TWTA	1	2	1	2	1	0

Table 9.8 shows that the solid-state amplifier is the type to be used for ECHO. The lowest performance index, J, indicates the most desirable amplifier.

Two solid-state amplifiers will be used by ECHO, and they will be manufactured by the SSPA Microwave Corporation. The dimensions and mass of the amplifiers are based on the input and output power requirements. The solid-state amplifiers will operate at an input power of 85 W and an output power of 20 W. According to Figure 9.3, these two power values correspond to an amplifier mass of approximately 1.3 kg for each one. Even though the TWTA would have a better power efficiency value than the solid-state, the mass of the TWTA would be about 5 times greater than the solid-state amplifier.

## 9.9 Budget

The budget constraints set on the communications subsystem were 22.2 kg, 85 W of power, and \$13.1 million (FY99) [9.25]. The break down of these constraints is concluded in this subsection.

### 9.9.1 Components

As with all communication subsystems, components within the satellite must be compatible with the existing Telemetry, Tracking, & Command (TT&C) system to be used on the mission. Therefore, off-the-shelf technology was the standard of choice for the components used. The subsystem contains two transponders (for redundancy); a low-pass filter; band-reject filter; a double-pole, a double-throw rf switch; a diplexer; and finally, the antenna [9.26].

### 9.9.2 Component Mass and Power

Table 9.9 gives the parameters for the individual components within the communications subsystem. All of the values were determined by cross checking the values found for the X and S Band communication subsystems [9.27].

### 9.9.3 Component Costs

As stated in Section 9.2, the cost for one month of ground support will be approximately four million dollars. The remaining \$9.1 million covers all subsystem components. This cost was based on subsystem mass using Cyr's Cost Estimating Methods For Advanced Space Systems [9.28].

**Table 9.9 Parameters for Communications Subsystem.**

Component	Quantity	Total Mass (kg)	Power (W)	Dimensions (cm)
Transponder Receiver Transmitter	2	9.5	20 65	14x30x9
Filters/switch diplexers	1	1.5		10x22x4
Antennas Parabolic Reflector	1	9		83 dia x 21
Sub-Reflector	2	1		10 dia x 2.5
Dipole	1	1.2		
<b>TOTAL</b>		<b>22.2</b>	<b>85</b>	

### 9.10 Conclusion

The six channels and corresponding data rates for this communications system satisfy the requirements set for the system design. These rates are compatible with the C&DH system and the NASA Deep Space Network. The NASA DSN is able to support Project ECHO because of the selected frequencies for the various channels. Transmission of both the command and scientific data is achieved by the use of multiplexing and a 0.83 m parabolic, dual offset feed antenna mounted on the despun section of the spacecraft.



## 9.11 References

- [9.1] "The Deep Space Network," Microfiche N88-20524, Jet Propulsion Laboratory, California Institute of Technology, Pasadena, CA, January 1988, p. 2.
- [9.2] "The Deep Space Network," p. 4.
- [9.3] "The Deep Space Network," p. 8.
- [9.4] "Space Propulsion Laboratory/Deep Space Network fact sheet," Jet Propulsion Laboratory, Monday, February 28, 1994.
- [9.5] Wertz, J.R. and W.J. Larson, Space Mission Analysis and Design, 2nd Edition, Microcosm, Inc., Kluwer Academic Publishers, 1992, p. 516.
- [9.6] Wertz, p. 534.
- [9.7] Wertz, p. 729.
- [9.8] Wertz, p. 622.
- [9.9] Wertz, p. 629.
- [9.10] Wertz, pp. 730, 737.
- [9.11] Wertz, p. 515.
- [9.12] Schwehm, G. H. and Y. Langevin, A Comet-Nucleus Sample-Return Mission, ESA Publications Division, 1991, pp. 60-61.
- [9.13] Wertz, p. 527.
- [9.14] Wertz, p. 530.
- [9.15] Wertz, p. 531.
- [9.16] Mazda, Fraidoon, Telecommunications Engineer's Reference Book, Butterworth-Heinemann Ltd., Linacre House, Jordan Hill, Oxford, 1993, p. 123.

- [9.17] Ha, Tri T., Digital Satellite Communications, Second edition, McGraw-Hill, Inc., New York, NY, 1990.
- [9.18] Wertz, p. 520.
- [9.19] Wilson, Andrew, Interavia Space Directory 1992-1993, Jane's Informational Group, Inc., Alexandria, VA, p. 548.
- [9.20] Wertz, pp. 516, 535.
- [9.21] Wertz, p. 480.
- [9.22] Wertz, p. 482.
- [9.23] Rom, Raphael and Moshe Sidi, Multiple Access Protocols, Performance and Analysis, Springer-Verlag, New York, NY, 1990, p. 120.
- [9.24] Wertz, p. 543.
- [9.25] Cyr, Kelley, "Cost Estimating Methods For Advanced Space Systems," Presentation at the 47th Annual Conference of The Society of Allied Weight Engineering, Inc., Plymouth, Michigan, 23-24 May, 1988.
- [9.26] Wertz, p. 579.
- [9.27] Wertz, p. 370.

## 10.0 Conclusion

A preliminary mission design that provides continuous communication services between the far side of the Moon and the Earth has been completed. The design fulfills the modified Discovery-class criteria: 1) total cost must not exceed \$150 million (excluding launch vehicle), 2) launch must be achieved by a Delta-class vehicle, and 3) the design lifetime must exceed 10 years.

There are some design issues that still need to be addressed. First, the thermal effects in the launch vehicle payload fairing due to the four RTG's are a major concern. A detailed thermal analysis is required to determine if the heat shield will provide adequate protection during the time interval between loss of ground-support air conditioning and ejection of the fairing. A reduction in the number of RTG modules may be possible with refinements to the L<sub>2</sub>-Halo transfer trajectory. At this time, the thrust history required to inject ECHO into the halo orbit has not been determined. If the ion thrusters do not need to operate at full power, it would be possible to reduce the number of RTG modules. Lastly, the communications system for the data relay between the Earth and the far side of the Moon is general in design. Once the types of missions to be sent to the Moon's far side are defined (such as the Artemis robotic payload lander), the communications system design could become more specialized.

## Appendix — Guidance, Navigation, and Control

### A.1 Computer Source Code for Computing Low-Thrust Trajectory

```
program halo
c
c *****
c
c The following program integrates the equations of motion for a
c spacecraft to find *a* trajectory from low Earth orbit to a halo
c orbit around the Earth-Moon L2 point. The equations of motion
c are listed in a canonical set of units with the following
c conversions:
c
c     1 Mass Unit = Earth mass + Moon mass (kilograms)
c     1 Time Unit = Earth-Moon system period (seconds)
c     1 Dist Unit = Earth-Moon distance (kilometers)
c
c
c Variable directory:
c
c     alpha      : angle of initial velocity vector measured
c                 : CCW from the +s2 axis direction (deg.)
c     counter,_2 : iteration counters
c     earthmass  : Earth mass (kg)
c     emdist     : Earth-Moon distance (km)
c     energy     : orbital energy (km2/s2)
c     epos       : position of Earth in coordinate system
c                 : centered at E-M system c.m. (km)
c     g1,g2,g3,g4 : temporary arrays for RK4
c     idir       : RK4 integration direction
c                 : (-1 = backward, +1 = forward)
c     ier        : error flag for RK4
c     istep      : integration step size (min.)
c     mpos       : position of Moon in coordinate system
c                 : centered at E-M system c.m. (km)
c     moonmass   : Moon mass (kg)
c     mu         : ratio of Earth mass to Moon mass (non-dim)
c     ndim       : dimension of the problem (# eqns.)
c     nvar       : number of problem variables
c     pi         : value of pi
c     r1         : s/c distance from the Earth (km)
c     r2         : s/c distance from the Moon (km)
c     rcm        : position of E-M system center of mass from
c                 : Earth (km)
c                 : the vector centered at Earth (km)
c     scmass     : spacecraft mass (kg)
c     scthrst    : current thrust produced by s/c engines (N)
c     t          : time counter (sec)
c     temp       : temporary array for RK4
c     tf         : end time of simulation (days)
c     thrust     : thrust level (N)
c     toff       : turn thrust off a period of time after
c                 : initial start (days)
c     tunit      : time unit
```

```

c          univgrav      : universal gravitation constant (N m^2/kg^2)
c          v             : s/c velocity in non-inertial frame (km/s)
c          v0            : initial velocity magnitude of s/c (km/s)
c          vi            : current s/c velocity (inertial) in i direction
c                       : (km/s)
c          vj            : current s/c velocity (inertial) in j direction
c                       : (km/s)
c          x             : first-order d.e. variables [x xdot y ydot]
c          x0            : initial position of s/c in s1 direction
c                       : measured from Earth center (km)
c          xdot          : first-order d.e.'s [xdot x2dot ydot y2dot]
c          y0            : initial position of s/c in s2 direction
c                       : measured from Earth center (km)

```

```

c          (Note that variables including a "_cd" indicate they are in the
c          canonical set of dimensions)

```

```

c          Required subroutines:  RK4, DERIVS

```

```

c          I/O Files:

```

```

c          energy.out    : orbital energy at each time step
c          daypos.out    : s/c position every ?? days
c          halo.dat      : input data
c          thrust.out    : thrust-level at each time step
c          traj.out      : computed position at each time step
c          velocity.out  : computed velocity at each time step

```

```

c          T. F. Starchville, Jr., R. G. Melton, and R. C. Thompson
c          February-March 1994

```

```

c          *****

```

```

c          implicit real*16 (a-z)
c          common mu, scthrst_cd, scmass_cd
c          dimension x_cd(4), xdot_cd(4), temp(4), k1(4), k2(4), k3(4), k4(4)
c          dimension k5(4), k6(4)
c          integer ndim, nvar, idir, ier, counter, counter2
c          logical switch
c          external derivs
c          pi=atan(1.0q0)*4.0q0
c          ndim=4
c          nvar=4

```

```

c          Open the input and output files

```

```

c          open(unit=7, file='halo.dat', status='old')
c          open(unit=8, file='traj.out', status='new')
c          open(unit=9, file='thrust.out', status='new')
c          open(unit=11, file='velocity.out', status='new')
c          open(unit=12, file='daypos.out', status='new')
c          open(unit=13, file='energy.out', status='new')
c          open(unit=14, file='empos.out', status='new')

```

```

c
c   Set up the Earth-Moon system physical constants
c
mu = 0.012150572q0
univgrav = 6.673q-11
earthmass = 5.973343324q24
moonmass = (mu / (1 - mu)) * earthmass
earthmu = (univgrav / 1000**3) * earthmass
moonmu = (univgrav / 1000**3) * moonmass
soimoon = 66100.q0
earthradius = 6378.145q0
emdist = 3.8439906q5
period = (2.q0 * pi) * sqrt(emdist**3 / ((univgrav / 1000**3) *
&      (earthmass + moonmass)))
c
c   Compute the center of mass for the E-M system
c
rcm = (1.0q0 / (earthmass + moonmass)) * (moonmass * emdist)
epos = rcm
mpos = -(emdist - rcm)
write(14,9010) epos,0.q0
write(14,9010) mpos,0.q0
c
c   Compute the velocity of the Earth
c
vearthi = 0.q0
vearthj = ((2.q0 * pi) / period) * epos
c
c   Setup the conversion factors to canonical units
c
distunit = 1 / emdist
massunit = 1 / (earthmass + moonmass)
timeunit = 1 / (period / (2.q0 * pi))
c
c   Enter the input data for the problem from the data file
c
read (7,*) x0, y0, v0, thrust, toff, scmass, alpha, istep, tf
c
c   Convert all SI inputs to the canonical set of distance unit (DU),
c   time unit (TU), and mass unit (MU) and correct for Earth-Moon
c   center of mass
c
epos_cd = epos * distunit
mpos_cd = mpos * distunit
soimoon_cd = soimoon * distunit
x0_cd = (x0 + rcm) * distunit
y0_cd = y0 * distunit
vearthi_cd = vearthi * (distunit / timeunit)
vearthj_cd = vearthj * (distunit / timeunit)
v0_cd = v0 * (distunit / timeunit)
thrust_cd = (thrust / 1000.q0) * (massunit * distunit /
&      timeunit**2)
toff_cd = toff * 86400.q0 * timeunit
scmass_cd = scmass * massunit
istep_cd = istep * 60.0q0 * timeunit
tf_cd = tf * 86400.q0 * timeunit

```

```

x_cd(1) = x0_cd
x_cd(2) = -v0_cd * sin(alpha * pi / 180.0q0)
x_cd(3) = y0_cd
x_cd(4) = v0_cd * cos(alpha * pi / 180.0q0)

xdot_cd(1) = 0.q0
xdot_cd(2) = 0.q0
xdot_cd(3) = 0.q0
xdot_cd(4) = 0.q0

t_cd = 0.0q0
scthrst_cd = 0.q0 * thrust_cd
c
c
c
Write initial conditions to files

write (8, 9010) x_cd(1)/distunit, x_cd(3)/distunit
write (12, 9010) x_cd(1)/distunit, x_cd(3)/distunit

scthrst = (scthrst_cd * 1000.q0) / (massunit * distunit /
&      timeunit**2)

write (9, 9010) t_cd/timeunit/86400.q0, scthrst
write (11, 9010) x_cd(2)*(timeunit/distunit),
&      x_cd(4)*(timeunit/distunit)
write (6, 9020) 'Halo orbit simulation in progress...'
write (6, 9010) t_cd/timeunit/86400.0q0
idir = -1
switch = .false.
counter = 1
do while (abs(t_cd) .lt. tf_cd)
  call rk56 (x_cd,xdot_cd,derivs,t_cd,istep_cd,idir,ndim,nvar,
&      temp,k1,k2,k3,k4,k5,k6,ier)
  write (8, 9010) x_cd(1)/distunit,x_cd(3)/distunit
c
c
c
Compute the Jacobi constant for the problem

jacobi_cd = (x_cd(2)**2 + x_cd(4)**2) / 2 - 0.5q0 * (x_cd(1)**2
&      + x_cd(3)**2) - (1 - mu) / sqrt((x_cd(1) - epos_cd)**2
&      + x_cd(3)**2) - mu / sqrt((x_cd(1) - mpos)**2
&      + x_cd(3)**2)
scthrst = (scthrst_cd * 1000.q0) / (massunit * distunit /
&      timeunit**2)
write (9, 9010) t_cd/timeunit/86400.q0, scthrst
write (11, 9010) x_cd(2)*(timeunit/distunit),
&      x_cd(4)*(timeunit/distunit)
c
c
c
Establish positive thrust when s/c passes appropriate position

if (.not. switch) then
  if (sqrt((x_cd(1)-mpos_cd)**2+x_cd(3)**2) .gt.
&      soimoon_cd) then
    scthrst_cd = 1.q0 * thrust_cd
    switch = .true.
  end if
end if

```

```

C
C      Compute the transfer orbital energy.  First transform the velocity
C      vector computed from rotating 's'-frame to inertial frame
C
vi = x_cd(2) * (timeunit / distunit) - ((2.q0 * pi) / period) *
&      x_cd(3) / distunit
vj = x_cd(4) * (timeunit / distunit) + ((2.q0 * pi) / period) *
&      x_cd(1) / distunit
v = sqrt((vi - vearthj)**2 + (vj - vearthj)**2)

r1 = sqrt((x_cd(1) - epos_cd)**2 + x_cd(3)**2) / distunit
r2 = sqrt((x_cd(1) - mpos_cd)**2 + x_cd(3)**2) / distunit

energy = v**2 / 2.q0 - earthmu / r1 - moonmu / r2
write(13, 9010) t_cd/timeunit/86400.q0, energy

C
C      Update time and thrust information to screen and marker data file
C
if ((energy .gt. -0.900005q0) .and. (energy .lt. -8.99999)) then
  write(12, 9010) x_cd(1)/distunit,x_cd(3)/distunit
endif
if (counter .eq. 1440) then
  print *, ' '
  write(6, 9010) t_cd/timeunit/86400.0q0, energy
  write(6, 9010) x_cd(1)/distunit,x_cd(3)/distunit
  write(6, 9010) scthrst
  write(12, 9010) x_cd(1)/distunit,x_cd(3)/distunit
  counter = 1
else
  counter = counter + 1
end if
end do
9010 format (3(1pe32.24, 2x))
9020 format (/1x,50a,//1x)
end

subroutine derivs (x, xdot, t, ndim, nvar)
C
C *****
C *      Set of first-order differential equations derived from      *
C *      the restricted, three-body equations.                      *
C *                                                                  *
C *      Author:  Thomas F. Starchville, Jr.                       *
C *****
C
implicit real*16 (a-z)
integer ndim, nvar
common mu, scthrst_cd, scmass_cd
dimension x(ndim), xdot(ndim)
xdot(1) = x(2)
xdot(2) = 2.0q0 * x(4) + x(1) - (1.0q0 - mu) * (x(1) - mu) /
&      ((x(1) - mu)**2
&      + x(3)**2)**1.5 - mu * (x(1) + 1.0q0 - mu) /
&      ((x(1) + 1.0q0 - mu)**2 + x(3)**2)**1.5
&      + (scthrst_cd / scmass_cd) * x(2) / (x(2)**2 + x(4)**2)**0.5
xdot(3) = x(4)

```



```

      xdot(4) = -2.0q0 * x(2) + x(3) - (1.0q0 - mu) * x(3) /
& ((x(1) - mu)**2 + x(3)**2)**1.5 -
& mu * x(3) / ((x(1) + 1.0q0 - mu)**2 + x(3)**2)**1.5
& + (scthrst_cd / scmass_cd) * x(4) / (x(2)**2 + x(4)**2)**0.5
      return
      end

      subroutine rk56 (x,xdot,f,t,h,idir,ndim,nvar,temp,k1,k2,k3,k4,
&                    k5,k6,ier)
C
C *****
C *      Integrates a set of first-order differential equations      *
C *      using a Runge-Kutta (5,6) method.                          *
C *                                                                 *
C *      Author: Thomas F. Starchville, Jr.                         *
C *****
C
      implicit real*16 (a-z)
      integer ndim, nvar, ier, idir, tfs
      dimension x(ndim),xdot(ndim),temp(ndim)
      dimension k1(ndim),k2(ndim),k3(ndim),k4(ndim),k5(ndim),k6(ndim)
      external f
      if (nvar .gt. ndim) then
         ier = 1
         return
      else
         ier = 0
      end if
      call f(x,xdot,t,ndim,nvar)
      do 100 tfs = 1,nvar
         k1(tfs) = h * xdot(tfs)
         temp(tfs) = x(tfs) + k1(tfs) / 4.0q0
100 continue
      call f (temp,xdot,t+idir*h/4.0q0,ndim,nvar)
      do 200 tfs = 1,nvar
         k2(tfs) = h * xdot(tfs)
         temp(tfs) = x(tfs) + k1(tfs) / 8.q0 + k2(tfs) / 8.0q0
200 continue
      call f (temp,xdot,t+idir*h/4.0q0,ndim,nvar)
      do 300 tfs = 1,nvar
         k3(tfs) = h * xdot(tfs)
         temp(tfs) = x(tfs) - k2(tfs) / 2.q0 + k3(tfs)
300 continue
      call f (temp,xdot,t+idir*h/2.q0,ndim,nvar)
      do 400 tfs = 1,nvar
         k4(tfs) = h * xdot(tfs)
         temp(tfs) = x(tfs) + (3.q0 / 16.q0) * k1(tfs) +
& (9.q0 / 16.q0) * k4(tfs)
400 continue
      call f (temp,xdot,t+idir*3.q0*h/4.q0,ndim,nvar)
      do 500 tfs = 1,nvar
         k5(tfs) = h * xdot(tfs)
         temp(tfs) = x(tfs) - (3.q0 / 7.q0) * k1(tfs) + (2.q0 / 7.q0) *
& k2(tfs) + (12.q0 / 7.q0) * k3(tfs) - (12.q0 / 7.q0) *
& k4(tfs) + (8.q0 / 7.q0) * k5(tfs)
500 continue
      call f (temp,xdot,t+idir*h,ndim,nvar)

```



#### A.4 Calculation of Solar Skirt Size

All calculations assume that the tapered section, antennas, and skirt masses are negligible and that the RTG's are located at the center of mass.

The spin moment of inertia, which consist of the axial moment of inertia for the even section of the spun section plus the transverse moment of inertia of the RTGs, is calculated as follows:

$$I_s = mr^2/2 + m(3r^2 + L^2)/12 + md^2$$

$$I_s = (442 \text{ kg})(1.5/2 \text{ m})^2(0.5) + (4 \cdot 42 \text{ kg})(3(0.33 \text{ m})^2 + (1.08 \text{ m})^2)/12 + (4 \cdot 42 \text{ kg})(1.08/2 \text{ m} + 1.6 \text{ m} + 1.5/2 \text{ m})^2$$

$$I_s = 1546.036 \text{ kg} \cdot \text{m}^2$$

The axial moment of inertia is calculated as follows:

$$I_a = I_s + mr^2/2$$

$$I_a = 1546.036 \text{ kg} \cdot \text{m}^2 + (10 \text{ kg})(0.2 \text{ m})^2(0.5) + (155 \text{ kg})(1.2/2 \text{ m})^2(0.5)$$

$$I_a = 1573.986 \text{ kg} \cdot \text{m}^2$$

The transverse moment of inertia is calculated in a similar fashion.  $I_t$  is equal to the transverse moment of inertia of the spun section plus the transverse moment of inertia of the despun section. However, since the transverse moment of inertia only affects the gravity gradient torque and this torque is small compared to the solar torque, the RTG's were modeled as point masses for this calculation only.

$$I_t = m(3r^2 + h^2)/12 + 2md^2$$

$$I_t = (442 \text{ kg})(3(1.5/2 \text{ m})^2 + (0.3 \text{ m})^2)/12 + (10 \text{ kg})(3(0.2/2 \text{ m})^2 + (0.3 \text{ m})^2)/12 + (155 \text{ kg})(3(1.2/2 \text{ m})^2 + (0.25 \text{ m})^2)/12 + 2(4)(42 \text{ kg})(0.4 \text{ m} + 0.3/2 \text{ m} - 0.60346333 \text{ m})^2 + (442 \text{ kg})(0.4 \text{ m} + 0.3/2 \text{ m} - 0.60346333 \text{ m})^2 + (10 \text{ kg})(0.4 \text{ m} + 0.3/2 \text{ m} - 0.60346333 \text{ m})^2 + (155 \text{ kg})(0.4 \text{ m} + 0.3 \text{ m} + 0.3 \text{ m} + 0.25/2 \text{ m} - 0.60346333 \text{ m})^2$$

$$I_t = 125.320201 \text{ kg} \cdot \text{m}^2$$

The gravity gradient torque is calculated as follows:

$$M_{gg} = (3\mu/(2R^3))(I_a - I_t)\sin(2\theta)$$

$$M_{gg} = (3(4903 \text{ km}^3/\text{s}^2)/(2(64600 \text{ km})^3))(1573.986 \text{ kg} \cdot \text{m}^2 - 125.320201 \text{ kg} \cdot \text{m}^2) \cdot \sin(2(1 \text{ deg}))$$

$$M_{gg} = 1.379 \times 10^{-9} \text{ N} \cdot \text{m}$$

The center of mass from the bottom of the satellite is calculated as follows:

$$cm = (\Sigma(md))/(\Sigma m)$$

$$cm = [(442 \text{ kg})(0.3/2 \text{ m} + 0.4 \text{ m}) + (10 \text{ kg})(0.3/2 \text{ m} + 0.3 \text{ m} + 0.4 \text{ m}) + (155 \text{ kg})(0.25/2 \text{ m} + 0.3 \text{ m} + 0.3 \text{ m} + 0.4 \text{ m})]/[442 \text{ kg} + 10 \text{ kg} + 155 \text{ kg}]$$

$$cm = 0.60346333 \text{ m}$$

The solar pressure force for the area below the center of mass is calculated as follows:

$$T_s = PA/c$$

$$T_s = (1358 \text{ W/m}^2)(1.5 \text{ m})(0.60346333 \text{ m} - 0.4 \text{ m} + 0.564 \text{ m}) / (3 \times 10^8 \text{ m/s})$$

$$T_s = 5.3537 \times 10^{-6} \text{ N}$$

The solar pressure force for the area above the center of mass in the front configuration is calculated as follows:

$$T_s = PA/c$$

$$T_s = (1358 \text{ W/m}^2)[(0.4 \text{ m} + 0.3 \text{ m} - 0.60346333 \text{ m})(1.5 \text{ m}) + (0.3 \text{ m})(0.2 \text{ m}) + (0.25 \text{ m})(1.2 \text{ m}) + (3.14159)(0.415 \text{ m})^2] / (3 \times 10^8 \text{ m/s})$$

$$T_s = 4.7343 \times 10^{-6} \text{ N}$$

The projected area of the dish in the side configuration was calculated by integrating the equation:

$$y = 9.41x^2$$

(which was obtained from the dimensions of the dish) with respect to x. This was then doubled to obtain the total area above and below the centerline of the antenna.

$$A = \int (9.41x^2) dx$$

$$A = 0.0581 \text{ m}^2 \text{ when integrated from } 0.0 \text{ m to } 0.21 \text{ m}$$

The solar pressure force for the area above the center of mass in the side configuration is calculated as follows:

$$T_s = PA/c$$

$$T_s = (1358 \text{ W/m}^2)[(0.4 \text{ m} + 0.3 \text{ m} - 0.60346333 \text{ m})(1.5 \text{ m}) + (0.3 \text{ m})(0.2 \text{ m}) + (0.25 \text{ m})(1.2 \text{ m}) + 0.0581 \text{ m}^2] / (3 \times 10^8 \text{ m/s})$$

$$T_s = 2.5481 \times 10^{-6} \text{ N}$$

The solar torque for the area below the center of mass is calculated as follows:

$$M_s = T_s d$$

$$M_s = (5.3537 \times 10^{-6} \text{ N})[(1.5 \text{ m})(0.564 \text{ m})(0.564/2 \text{ m} + 0.60346333 \text{ m} - 0.4 \text{ m} + 0.15 \text{ m}) + (1.5 \text{ m}) * (0.60346333 \text{ m} - 0.4 \text{ m})(0.60346333 \text{ m} - 0.4 \text{ m})/2] / [(1.5 \text{ m})(0.564 \text{ m}) + (1.5 \text{ m}) * (0.60346333 \text{ m} - 0.4 \text{ m})]$$

$$M_s = 2.7064 \times 10^{-6} \text{ N*m}$$

The solar torque for the area above the center of mass in the front configuration is calculated as follows:

$$M_s = T_s d$$

$$M_s = (4.7343 \times 10^{-6} \text{ N})[(1.5 \text{ m})(0.7 \text{ m} - 0.60346333 \text{ m})(0.7 \text{ m} - 0.60346333 \text{ m})/2 + (0.3 \text{ m})(0.2 \text{ m})(0.3/2 \text{ m} + 0.7 \text{ m} - 0.60346333 \text{ m}) + (0.25 \text{ m})(1.2 \text{ m})(0.25/2 \text{ m} + 0.3 \text{ m} + 0.7 \text{ m} - 0.60346333 \text{ m}) + (3.14159)(0.415 \text{ m})^2(0.8 \text{ m} + 0.25 \text{ m} + 0.3 \text{ m} + 0.7 \text{ m} - 0.60346333 \text{ m})] / [(1.5 \text{ m})(0.7 \text{ m} - 0.60346333 \text{ m}) + (0.3 \text{ m})(0.2 \text{ m}) + (0.25 \text{ m}) * (1.2 \text{ m}) + (3.14159)(0.415 \text{ m})^2]$$

$$M_s = 4.3497 \times 10^{-6} \text{ N*m}$$

The solar torque for the area above the center of mass in the side configuration is calculated as follows:

$$M_s = T_s d$$

$$M_s = (2.5481 \times 10^{-6} \text{ N}) [(1.5 \text{ m})(0.7 \text{ m} - 0.60346333 \text{ m})(0.7 \text{ m} - 0.60346333 \text{ m})/2 + (0.3 \text{ m})(0.2 \text{ m})(0.3/2 \text{ m} + 0.7 \text{ m} - 0.60346333 \text{ m}) + (0.25 \text{ m})(1.2 \text{ m})(0.25/2 \text{ m} + 0.3 \text{ m} + 0.7 \text{ m} - 0.60346333 \text{ m}) + (0.0581 \text{ m}^2)(0.8 \text{ m} + 0.25 \text{ m} + 0.3 \text{ m} + 0.7 \text{ m} - 0.60346333 \text{ m})] / [(1.5 \text{ m})(0.7 \text{ m} - 0.60346333 \text{ m}) + (0.3 \text{ m})(0.2 \text{ m}) + (0.25 \text{ m})(1.2 \text{ m}) + (0.1162 \text{ m}^2)]$$

$$M_s = 1.0762 \times 10^{-6} \text{ N} \cdot \text{m}$$

The spin rate need for stabilization is calculated as follows:

$$\omega = Mdt / (I_s \tan \theta)$$

$$\omega = \{ (4.3497 \times 10^{-6} \text{ N} \cdot \text{m} - 2.7064 \times 10^{-6} \text{ N} \cdot \text{m} + 1.379 \times 10^{-9} \text{ N} \cdot \text{m}) (2 \cdot 365 \cdot 24 \cdot 60 \cdot 60 \text{ s}) / [(1546.036 \text{ kg} \cdot \text{m}^2) \tan(1 \text{ deg})] \} (60 / 3.14159 / 2 \text{ rad/s/rpm})$$

$$\omega = 36.713786 \text{ rpm}$$